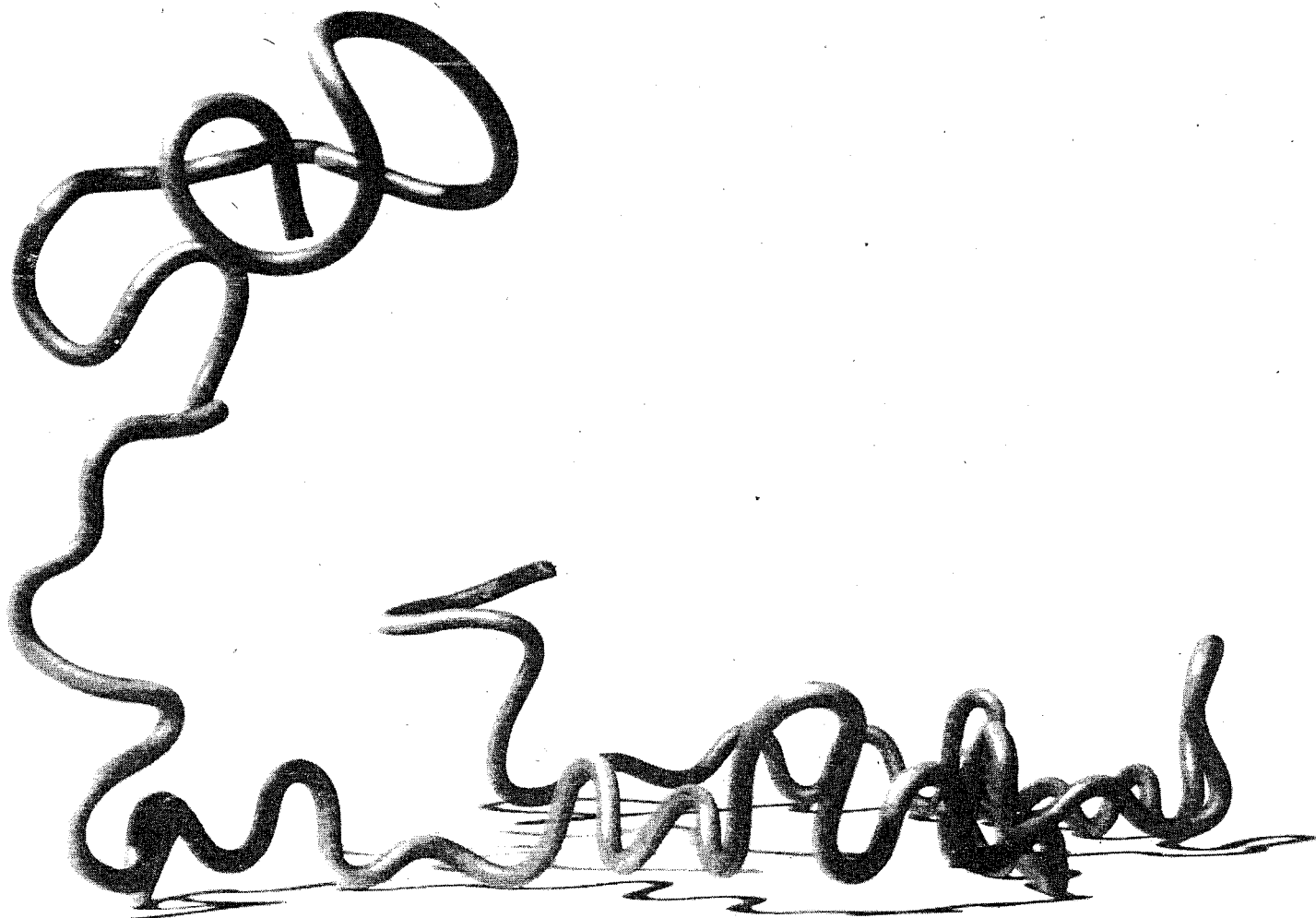# FLEXIBLE POLYMERS

AT A SOLID-LIQUID INTERFACE

THE ADSORPTION OF POLYVINYL PYRROLIDONE ONTO SILICA

M.A. COHEN STUART

FLEXIBLE POLYMERS AT A SOLID-LIQUID INTERFACE

The adsorption of polyvinyl pyrrolidone onto silica

Voor mijn ouders
Voor Marina

Promotor: dr. B.H. Bijsterbosch, hoogleraar in de fysische- en kolloïdchemie

Co-referent: dr. G.J. Fleer, wetenschappelijk hoofdmedewerker

M.A. Cohen Stuart

FLEXIBLE POLYMERS AT A SOLID-LIQUID INTERFACE

The adsorption of polyvinyl pyrrolidone onto silica.

Proefschrift
ter verkrijging van de graad van
doctor in de landbouwwetenschappen,
op gezag van de rector magnificus,
dr. H.C. van der Plas,
hoogleraar in de organische scheikunde,
in het openbaar te verdedigen
op woensdag 23 april 1980
des namiddags te vier uur in de aula
van de landbouwhogeschool te Wageningen

Voorwoord

Dit proefschrift is het topje van een ijsberg: het dankt zijn verschijnen aan de opwaartse kracht die velen eraan meegegeven hebben. Gedurende de ruim vier jaar die het onderzoek in beslag nam heb ik in de vakgroep Fysische- en Kolloidchemie steeds een bijzonder plezierige werkkring gevonden; de stimulans die uitging van de goede sfeer die er heerst is voor dit proefschrift van grote betekenis geweest. Mijn dank gaat dan ook uit naar ieder die daartoe bijdroeg.

Bert Bijsterbosch, in de jaren waarin het onderzoek op gang kwam heb je je als promotor steeds bescheiden opgesteld en de vorderingen van enige afstand, maar met veel belangstelling, gevolgd. Ik ben daardoor zeer vrij geweest in de keuze van de richting die het onderzoek nam en ik realiseer me dat die vrijheid voor mij van grote waarde is geweest. Toen de resultaten vastere vorm kregen heb ik vaak van je kritische vermogen en je nauwgezetheid mogen profiteren. Voor het voortdurende vertrouwen dat je in mij hebt gesteld ben ik je zeer erkentelijk.

Gerard Fleer, jij hebt in de totstandkoming van dit werkstuk een groot aandeel gehad. Je grote kennis van het vakgebied is voor mij vooral in het begin van het onderzoek onmisbaar geweest terwijl je onstuitbaar enthousiasme me niet weinig heeft aangemoedigd. Met genoegen denk ik terug aan de vele uren dat ik met je als collega, en als vriend, mocht samenwerken.

Jan Scheutjens, jouw naam is ten nauwste met dit proefschrift verbonden. Niet alleen ben ik blij dat ik het uitgroeien van de Scheutjens-Fleer theorie tot een rijp werkstuk van zo nabij heb meegemaakt, maar ook bewaar ik een prettige herinnering aan je belangstelling voor het experiment en aan de vele geestdriftige discussies die we over tal van zaken gevoerd hebben. Ik prijs me gelukkig dat de samenwerking tussen ons in de komende jaren wordt voortgezet.

Een belangrijk deel van het in de hoofdstukken 3 t/m 5 beschreven experimentele werk is op bekwame wijze verricht door Peggy Bosman en Joop Nuysink. De diversiteit aan toegepaste technieken die ik nastreefde bracht tal van lastige problemen met zich mee. Peggy en Joop, ik dank jullie van harte voor de manier waarop jullie die problemen met veel inventiviteit en doorzettingsvermogen het hoofd hebben geboden. Jullie bijdragen vormen pijlers waarop dit proefschrift rust.

Van de calorimetrische gegevens werd een deel vergaard door H.W. Postma, in het kader van zijn ingenieursstudie. M. Weststraten en Th. Kooyers - beide stagiares van een laboratoriumschool - zijn beide behulpzaam geweest bij de adsorptiemetingen.

Contents   p.

Chapter 1

Introduction

1.1 GENERAL BACKGROUND AND AIM OF THIS WORK

Flexible polymers have a large number of internal degrees of freedom, and this property is reflected in their typical behaviour in solution and in the solid state. Since the days of Staudinger they have, therefore, attracted much attention. Most of the compounds under investigation owe their mere existence to the skill of organic chemists, but this is not to say that such investigations have no bearing upon the behaviour of a variety of flexible *biopolymers*.

A systematic study of the behaviour of long chain molecules at interfaces could only be fruitful after some insight in the solution properties had been obtained. Some 30 years ago the random coil picture of a flexible polymer in solution became firmly established and the adsorption problem could be formulated. Since then numerous experimental and theoretical studies have been published.

A characteristic feature of polymer adsorption is that the adsorbed amount as a rule exceeds what is calculated for a dense monolayer of monomer units. Furthermore, adsorbed polymers frequently have a dramatic effect on the stability of colloidal dispersions, either stabilizing or destabilizing them. Both observations can be accounted for when at least parts of the adsorbed molecule extent far into the solution. In 1951, Jenkel and Rumbach proposed the now generally accepted model in which some of the polymer segments are in contact with the surface (*trains*), the remaining ones dangling in the solution as *loops* or *tails*. On the basis of this picture, a number of polymer adsorption theories has been formulated. Because of the large number of conformations that polymers can assume, these treatments involve complicated statistics. Some theories circumvent the mathematical complications by means of suitable approximations. It was not until recently, that an elegant matrix procedure was devised to deal with the conformational probability distribution (*DiMarzio* and *Rubin*, 1971).

The subject of polymer adsorption is, however, not only of academic interest. The use of adsorbed polymers for technical and practical purposes dates back to early history (see *Stillman*, 1924) and is nowadays very wide. For instance, the stabilizing effect on dispersions is operative in products as diverse as inks, paints and coatings, pesticides, foods, pharmaceuticals, and magnetic tapes, whereas destabilization is helpful in water purification, improvement of soil structure, mineral processing, etc. Polymer adsorption phenomena are important

in lubricants, detergents,and foams and they play a major role in biological adhesion.

In studying polymer adsorption from a fundamental point of view it is mandatory to have available reliable experimental information on well-defined model systems. Here, the investigator is faced with the problem to experimentally assess the conformational properties of the molecules at the interface. Of the various techniques that have been proposed to do this, neutron scattering is probably the most powerful one. With this technique chain conformations can be studied directly provided the molecules can be labeled by isotopic substitution of hydrogen by deuterium. For polymers in solution, this was already done (Daoud et al., 1975) and for adsorbed polymers there is some hope that the density of monomer units as a function of the distance from the adsorbing wall can be measured.

Other methods give more limited information about the conformational state of adsorbed molecules. Trains can often be detected owing to their interaction with the surface, which gives rise to an enthalpy change or a change in spectroscopic and electrical properties upon adsorption. Infrared spectroscopy, electron spin resonance (ESR) and nuclear magnetic relaxation (NMR) as well as micro-calorimetry and an electrochemical method all have been used to estimate the amount of polymer in trains.

Experimentally, loops and tails can hardly be distinghuished from each other. Perhaps they differ somewhat in segmental mobility. Both may be detected by virtue of their hydrodynamic interactions with the solvent, or by the change in refractive index they bring about in the neighbourhood of the interface. Measurements of layer thicknesses by hydrodynamic (electrophoresis, viscometry) or optical (ellipsometry) techniques are based on these properties. A drawback of all these methods is, however, that none of them is generally applicable and that the information obtained is related to conformational quantities in a rather indirect way, involving disputable assumptions.

In view of the difficulties listed above it is not surprising that polymer adsorption theories have, at best, been verified only semiquantitatively. Only some trends, observed in some systems agree with some theories, but a choice between different theories could not yet be made. Preferably, several different techniques should be combined in order to obtain a firm basis for interpretations. It is therefore our aim to study the adsorption of a well-defined polymer on a single adsorbent with as many techniques as possible. Moreover, we want to relate the results to the parameters that govern the adsorption equilibrium, particularly the chain length, and the free energies of polymer solvent and polymer surface interactions. The determination of these parameters involves

another set of measurements, each with its inherent interpretational difficulties.

1.2 SYSTEM USED AND OUTLINE OF THE STUDY

For the present study we selected polyvinyl pyrrolidone (PVP) as the polymer. This substance is soluble in water and in a number of apolar organic solvents. This property is both unusual and interesting enabling us to make a comparison between adsorptions from solvents of widely different character. The solubility in water is important, since in aqueous systems the stabilization and destabilization phenomena mentioned above are particularly relevant so that these have been studied most extensively. The spectroscopic properties of PVP allow an easy concentration determination, as well as infrared and NMR studies. Also, PVP can be obtained in a wide range of molecular weights and the distribution of molecular weights in a sample can be modified by means of fractionation techniques. The fact that PVP is a homopolymer simplifies interpretation of the results.

As the adsorbent we choose a pyrogenic silica. Particular advantages are that it is non-porous, has a high specific surface area and is chemically very pure. It allows measurement of adsorption isotherms with good precision, and because of its low light scattering and its capability to form strong hydrogen bonds with proton accepting substances it is suitable for infrared studies. Stable sols with high surface area can be prepared, which is important for calorimetric and NMR investigations.

The solvents used were water and dioxane. Water was chosen for the reasons mentioned above. Dioxane is a virtually apolar, aprotic solvent which is transparant in the relevant infrared wavelength range. Moreover, the solution properties of PVP in water and in dioxane are fairly well known.

In chapter 2 we deal with general and theoretical concepts, and we briefly review some theories. It turns out that a recent theory by *Scheutjens* and *Fleer* (1979), based on the already mentioned matrix formalism, offers the best and the most complete description of the adsorption phenomenon. We also concern ourselves with the physical meaning of theoretical concepts, leading to our proposing a simple modification of this Scheutjens-Fleer theory. In chapter 3 we collect data about those properties of the adsorbent, the polymer, and the solvent which are relevant to adsorption. The adsorbed amount as a function of chain length, heterodispersity, surface properties, and solvent quality is discussed in chapter 4. Here, we also consider desorption (displacement) brought about by some additives and we demonstrate how, in principle, the adsorption energy can be derived from such displacement studies. Chapter 5 deals with the conformation of the adsorbed polymers as measured by means of infrared, NMR,

ESR and microcalorimetry. The principles and assumptions underlying the application of these techniques are discussed here.

In our last chapter we compare all experimental results with numerical results obtained from the Scheutjens-Fleer theory and we discuss to what extent this theory is supported by experiment. We also review the possibilities and limitations of each of the experimental techniques in the light of this comparison. Finally, we roughly sketch the conformation of adsorbed polyvinyl pyrrolidone as it emerges from this study.

Chapter 2

General features and theoretical aspects of polymer adsorption

2.1 GENERAL FEATURES

Flexible, linear polymers adsorb far more readily than their low molecular weight counterparts. For long chains the adsorbed amount A (generally expressed as the *adsorbed weight* per unit of surface area) may already be considerable at extremely low equilibrium concentrations c, while at higher concentrations the adsorbed amount becomes nearly constant. The adsorption isotherm, A(c), is then of the high-affinity type.

In many cases the plateau value of A for high molecular weight polymers is of the order of 1 or 2 mg m^{-2}. Estimates for a close-packed monolayer of monomer units show that it is impossible to accomodate such amounts of material in direct contact with the surface. This has led early investigators (*Jenkel and Rumbach*, 1951) to postulate that only part of the adsorbed chain molecules is directly bound to the adsorbing interface. A sequence of such bound monomer units is called a *train*. The remaining units must find a place in sequences with both ends on the surface (*loops*) or sequences with only one end on the surface (*tails*). This is schematically pictured in fig. 2.1.
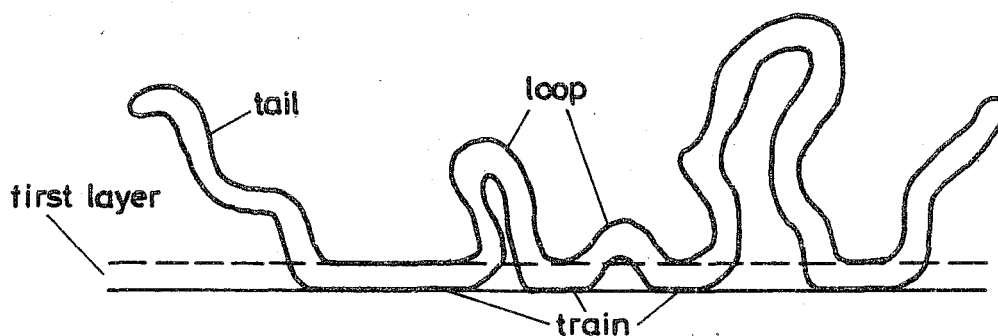
Fig. 2.1. Model representation of an adsorbed chain molecule.

Clearly, adsorption implies a drastic change in the conformation of the molecules. A measure of the conformation of adsorbed chains is the bound fraction p, the fraction of monomer units adsorbed in trains, defined as:

$$p = A_{tr} /A \qquad\qquad (2.1)$$

Here A_{tr} is the contribution of the trains to A. If p is close to 1, the molecules are nearly two-dimensional flat structures whereas for molecules retaining much of their three-dimensional coiled shape, p will be close to zero. The loop, train and tail model implies that the adsorbed molecules extend a considerable distance into the solution. Various experiments reveal the existence of thick adsorbed layers (*Lipatov*, 1974, Ch. 4), although the relia- bility of the reported values for the layer thickness is often questionable.

The driving force for adsorption is the reduction in free energy arising from the binding of train units to the surface. The binding process including the removal of solvent molecules from the surface can be described by a suitable *adsorption energy parameter*. The reduction in free energy upon binding is counteracted by the changes in conformation from a wholely three dimensional coil to an (at least partially) two-dimensional structure. This rearrangement process is accompanied by a considerable loss of entropy per molecule which depends on chain length and chain flexibility.

Not only will the conformation change upon adsorption but also the inter- action of the polymer with the solvent. In the interpenetrating distorted coils near the surface a high density of monomer units and, therefore, a reduced polymer-solvent interaction is likely to occur. So we also expect a free energy contribution due to the mixing of polymer chains and solvent. Here, the rele- vant quantity is the *polymer-solvent interaction parameter*.

We conclude that at least five independent variables determine the equilibrium number and the conformations of macromolecules on a given surface: concentration in the solution, chain length, flexibility, adsorption energy parameter and polymer-solvent interaction parameter. Other variables may some- times also play an important role in experimental situations; we mention the effects of temperature, time (kinetics) and polydispersity of the polymer.

Below we discuss the main trends found in polymer adsorption in terms of the variables listed above. The reader is referred to reviews of *Lipatov* (1974) and *Silberberg* (1962) for more experimental details. A discussion about the effects of chain flexibility and polydispersity must be omitted here, because these variables have never been studied systematically. In sections 2.6 and 2.7 we consider them from a theoretical viewpoint.

Adsorption energy parameter

To our knowledge, values of the adsorption energy parameter have never been determined experimentally, but the way in which adsorption depends on this parameter may be qualitatively estimated from the fact that macromolecules do not always adsorb. There are combinations of solvent, adsorbent and polymer that do not give rise to adsorption, whereas high affinity adsorption occurs in many other cases. Surprisingly, intermediate cases (high molecular weight, but low affinity) are extremely rare. This suggests that the adsorbed amount is not a very smooth function of the adsorption energy. Instead, it indicates that there exists a critical value for the adsorption energy which sharply separates regions where adsorption does occur from regions where it is absent.

Concentration

Appreciable adsorption may already occur at concentrations far below experimental detection levels. On the other hand, the determination of adsorbed amounts from concentrated solutions (by the depletion method) is also difficult from an experimental point of view. Therefore, in most cases only a part of the adsorption isotherm, usually in the concentration range from 1 up to 1000 mg dm^{-3} can be measured with sufficient accuracy. A steep initial rise and a (semi-) plateau are general features, although adsorbed amounts of strongly polydisperse samples often rise continuously with increasing concentration (see section 2.6.2). The concentrations at which the plateau seems to be reached differ from one experimental system to another.

It is generally assumed that at low adsorbed weight A, i.e. in the initial steep part of the isotherm, the conformation of the adsorbed molecules is flatter than at high A. Correspondingly, the bound fraction p decreases with increasing A. This has been confirmed by various measurement of p (e.g. *Fontana et al.*, 1961, *Thies et al.*, 1967 and *Fox et al.*, 1974). Values of p between 0.8 and 0.2 have been reported.

Molecular weight

At a given equilibrium concentration the weight of polymer adsorbed on a nonporous surface is nearly always an increasing function of the molecular weight M. Lipatov (1974, Ch. 3) gives a number of examples. However, the functional behaviour A(M) is difficult to establish because in many cases the molecular weight of the polymer samples under investigation is poorly defined. Moreover, it has been shown (*Stromberg*, 1967; *Felter et al.*, 1969; *Vander Linden et al.*, 1978) that high molecular weight polymers adsorb preferentially

over lower ones, so that any heterogeneity (polydispersity) of the polymer
sample is an additional complicating variable. Although we devised a method to
deal with polydisperse samples (sections 2.7 and 4.1.2) the complications can
be avoided if narrow, well defined fractions are used. Very good results have
recently been obtained by Vander Linden et al. (1978a), which indicate that
the shape of A(M) depends on the solvent quality.

A high adsorbed amount is only obtained if each of the adsorbed chains
occupies only a few sites on the surface. Therefore, p will probably decrease
with increasing A and M. Vander Linden found that A_{tr} is constant for high
molecular weights while A still increases with M. Thus at the plateau of the
adsorption isotherm p was inversely proportional to A in this case.

Polymer-solvent interaction parameter

The solvent quality - expressed in the interaction parameter - has a
pronounced effect. Generally the adsorbed weights and the thickness of the ad-
sorbed layer are lower from good solvents than from poor solvents. The data
of Vander Linden (1978a) indicate that, in a good solvent, A(M) increases
initially but levels off at high M. In a theta-solvent A(M) keeps rising,
approaching a linear dependency on log M.

Temperature

The adsorbed amount can be expected to depend upon temperature, since both
energy-parameters may depend on T. These changes may be of either sign.
Experimentally, however, the temperature dependency has been found to be small,
and no general trend is observed.

Time effects

Long times are often required to establish equilibrium, especially if the
molecular weight is very high. Slow reconformation processes and/or diffusion
must be the main reasons for such time effects. In polydisperse samples dis-
placement of short molecules by longer ones may have an additional effect.
It is generally accepted that steric barriers against conformation changes
(dynamic stiffness) play an important role in all these kinetic phenomena
(*Schurz*, 1974, p. 52). The question of whether frozen non-equilibrium states
occur in polymer adsorption has been the subject of some dispute. Experimental
evidence is inconclusive however (*Botham and Thies*, 1969), see also section 2.7 .

Desorption

Desorption is often studied in connnection with adsorption, because it is believed to shed some light on the question of reversibility. Low molecular weight substances are often readily desorbed by diluting the equilibrium solution with enough solvent. As a rule, polymers cannot or only to a very limited extent be removed by washing with the solvent from which they were adsorbed (*Grant*, 1975). However, the adsorbed layer can sometimes be (partly) removed by switching to a different solvent. Obviously, this involves changes in the energy parameters. In chapter 4 we describe a method to desorb the polymer completely by means of low molecular weight additives. In this way a quantitative estimate for the magnitude of the adsorption energy parameter becomes possible.

2.2 THE DESCRIPTION OF CONFORMATIONS OF FREE AND ADSORBED CHAINS

For an understanding of the behaviour of flexible chain molecules infor-mation on the (average) conformation of the molecules is indispensable. A full description of the shape of a molecule requires knowledge of the relative position of each of its atoms (the *configuration*, see *Flory*, 1969, p. 1), but in theoretical treatments it is common to consider the chain as consisting of a number of connected chain *segments*. The *conformation* of the chain is then specified in terms of the relative positions of the endpoints of these segments. Such a definition was adopted by *Kuhn* (1934). For the moment, we leave open the problem of a precise definition of a segment; it should not be confused with the monomer unit.

Due to the thermal motion in solutions the conformation is generally time dependent and we may assign a probability to every possible conformation. Then, a time (or ensemble) average over the conformational probability distribution gives us an idea of what a typical molecule looks like. It is known that flexible polymers in solution adopt a coiled shape and occupy a spherical or ellipsoidal volume. Many parameters are used to describe the conformation. We mention the mean square *end-to-end distance* $< h^2 >$, the *segment density distribution*, $\phi (d_g)$ (where d_g is the distance from the center of gravity) and the mean square radius of gyration $< s^2 >$.

In the neighbourhood of an adsorbing interface, the polymer molecule experiences short range, attractive forces. As a result of these forces, every segment which is bound to the interface lowers the free energy of the system. At the same time the whole molecule is distorted from its three-dimensional coiled shape, which entails a considerable entropy loss. As a result of these

opposing free energy contributions only a fraction of the segments is bound to the surface (see fig. 2.1). We are interested in the conformational probability distribution for the adsorbed chains, and look for useful averages to describe typical adsorbed molecules.

Due to the presence of the wall, the molecules lose the spherical (or ellipsoidal) symmetry characteristic of free chains in solution and becomes anisotropic. Properties in a direction parallel to the wall will be different from those in a direction perpendicular to the wall. If many molecules find a place on the surface, they will strongly interpenetrate and the segment density in a layer parallel to the wall becomes nearly constant. Therefore, individual chain properties like the end-to-end distance, or the radius of gyration are uninteresting. It is more relevant to characterize the adsorbed layer as a whole, e.g. in terms of the total segment density distribution ϕ (z) along the z-axis perpendicular to the wall, and the loop, train and tail contributions to ϕ (z), designated by ϕ_1 (z), ϕ_{tr} (z) and ϕ_t (z), respectively.

If ϕ (z) is the volume fraction of segments due to adsorbed chains at a distance z from the wall, ϕ (z) dz is the volume of segments per unit of surface area between z and z + dz. Hence, integrating the segment density we obtain the total volume of segments in adsorbed chains per unit surface area. Dividing this by the specific volume V_2 of the polymer, we obtain the *adsorbed weight* per unit area

$$A = \frac{1}{V_2} \int_o^\infty \phi \ (z) \ dz \quad . \tag{2.2}$$

For the separate contributions of loops, trains, and tails we write:

$$A = A_1 + A_{tr} + A_t = \frac{1}{V_2} \int_o^\infty \{\phi_1 \ (z) + \phi_{tr} \ (z) + \phi_t \ (z)\} \ dz \tag{2.3}$$

The bound fraction has been introduced as a measure of the conformation (eqn. 2.1). Another useful quantity is the root mean square layer thickness δ, which can also be derived from ϕ (z):

$$\delta^2 = \int_o^\infty z^2 \ \phi \ (z) \ dz \ / \ \int_o^\infty \phi(z) \ dz \tag{2.4}$$

2.3 GENERAL THEORETICAL FRAMEWORK

In section 2.4 and 2.5 we compare the theoretical approaches and their results as given by Hoeve, Silberberg, Roe, and Scheutjens and Fleer. (*Hoeve*, 1965a, 1966, 1970, 1971; *Silberberg* 1962, 1967, 1968; *Roe* 1974; *Scheutjens* and *Fleer* 1979, 1980). Many more authors have paid attention to polymer adsorption theory but their treatments are either obsolete or fail to elaborate relevant cases (which can be compared with experiment). In this section, we first review some general concepts.

All theories are based upon the methods of statistical thermodynamics. First, the partition function, from which thermodynamic quantities can be derived, is formulated. For instance, the canonical partition function Q is related to the (Helmholtz) free energy F:

$$F = - k T \ln Q \qquad (2.5)$$

where k is Boltzmann's constant and T the absolute temperature. Next, this partition function must be maximized which is usually done by collecting terms of equal energy E_j with multiplicity Ω_j and subsequent maximization of the product Ω_j exp. $(- E_j/kT)$. Differences between the theories are mainly present in the model underlying the partition function and in the mathematical approximations applied in the deduction of results. In polymer adsorption theories concepts which were originally developed for the description of polymer solutions are frequently used. Let us first discuss a few of these basic ideas.

In all theories the polymer chain is represented by a sequence of r segments, all of the same size and chemical properties, and connected to each other by some flexible bond. The flexibility of this bond may be subject to some constraint (e.g. the chain must fit into a lattice) or it is 'freely jointed' so that every segment may assume an arbitrary orientation with respect to its neighbours. Of course, the model chain of segments must adequately represent the statistical properties of the real chain of monomer units it replaces. This requirement determines the size of these segments, and their number per chain.

To illustrate this let us compare properties of a model chain and a real chain with respect to their dimensions. For an isolated model chain in three dimensional space, consisting of r segments of length l_s, Kuhn (1934) calculated the undisturbed mean square end-to-end distance $<h_o^2>$ by means of random flight statistics:

$$< h_o^2 > = r l_s^2 \qquad (2.6)$$

For real chains, with a polymethylene backbone containing $m + 1$ carbon atoms, the bond length between them being l, $< h_o^2 >$ is found to be:

$$< h_o^2 > = C \, m \, l^2 \qquad (2.7)$$

where the *characteristic ratio* C is a constant for a given polymer solvent combination (*Flory*, 1969, ch. 2).

Now the real chain can be represented by many model chains with different r and l_s, provided that r and l_s are chosen such that $<h_o^2>$ has the value calculated by (2.7). However we can fix the values of r and l_s by another requirement, namely that both the real and the model chain have the same length when fully stretched. For the model chain this leads to:

$$L = r l_s \qquad (2.8)$$

and for the real polymethylene chain, assuming planar zig-zag conformation (*Morawetz* 1965, p. 120) the result is:

$$L = 0.253 \, m/2 \quad (nm) \qquad (2.9)$$

Eleminating L and $<h_o^2>$ from these equations and using $l = 0.154$ nm for the carbon-carbon bond length we find:

$$r = m/1.48 \, C \qquad (2.10)$$

$$l_s = 0.188 \, C \quad (nm) \qquad (2.11)$$

It is seen that r is proportional to m and hence proportional to the molecular weight M. We assume that in other cases (for instance for chains in a lattice) a model chain can also be defined for which such a proportionality holds.

With only a few exceptions, theories of polymer adsorption make use of the widely accepted thermodynamical theory of Flory and Huggins (Flory, 1941, 1942; Huggins, 1941, 1942). In this approach the conformation probability of a chain molecule, alone or in the presence of other molecules is calculated by placing the segments one by one in adjacent lattice sites. The sequence of steps, each from one lattice site to the next, constitutes a three dimensional random walk. A step in such a walk is only possible if the lattice site towards which it was directed is unoccupied. Therefore the probability of each step is proportional to the probability of finding a vacant lattice site.

In Flory's theory all the previously placed segments are considered to be

uniformly distributed so that the solution is a completely random mixture. This means that at every point the local concentration is assumed to be equal to the average concentration of the whole solution. Therefore all segments in the solution reduce the probabilities for the next step in the random walk in the same way. Such a walk in which all steps are assigned equal weights will be denoted as a *purely random walk.* Theories where such an average segment concentration replaces the real local concentration are known as 'mean field' theories.

Physically, it is impossible that connected segments distribute themselves completely at random. But when the concentration of segments is sufficiently high the segment density distribution does not differ too much from the uniform distribution and a mean field approach makes sense. The Flory-Huggins theory is therefore valid for relatively high concentrations where the polymer coils extensively overlap.

At low concentrations where the assumption of a homogeneous segment distribution does not hold, the conformation probability can be found from a *self-avoiding walk.* In such a walk a step from one lattice site to a neighbouring one is only allowed if the latter is not occupied by a segment of the same chain. This reduces the effective coordination number for the walk and shifts the probability distribution towards more expanded conformations. At intermediate concentrations short sequences of segments may behave as self avoiding walks, whereas at longer distances the random walk behaviour predominates.

These notions also apply for adsorbed macromolecules. If the adsorbing wall attracts segments strongly, it is reasonable to expect high segment densities close to the surface, although the equilibrium solution may be very dilute. Moreover, we expect a constant segment density parallel to the surface (see section 2.2) and a varying segment density perpendicular to the surface. Therefore a step in the random walk from one lattice site to a neighbouring one situated at a distance z from the interface has to be weighted according to the segment density at z. In this way the Flory-Huggins theory for concentrated polymer solutions can be applied to adsorbed chains, provided that the statistics of the chain molecules are described as walks in a mean field density gradient of segments such that the density is only a function of the distance z from the interface. We will call this type of walk, in which steps are weighted according to local (average) segment densities, a step-weighted random walk. At large distances from the surface the segment density must some-how drop to the usually very low bulk solution value, and in this region the mean field assumptions do not hold any longer.

In the Flory-Huggins theory solvent effects are accounted for by means of

the well known polymer solvent interaction parameter χ. 2χ is the free energy (in units of kT) associated with the exchange of one solvent molecule in pure solvent with an equal volume of polymer in pure (disoriented) polymer. Obviously, this parameter occurs also in adsorption theory, because changes in the solvation of chains contribute considerably to the free energy change. As χ increases the solvent becomes poorer, the repulsion between polymer segments decreases and the adsorbance increases (see section 2.1).

The interaction between a segment and the surface may be included in an analogous way by defining the parameter χ_s as the difference in free energy (in units of kT) associated with two simultaneous 'processes':

1) the transfer of a polymer segment from a site completely surrounded by other polymer segments (i.e. in pure polymer) to a site also in pure polymer but in contact with the surface;

2) a similar transition for a corresponding volume of solvent in pure solvent. This definition, due to *Silberberg* (1968), relates χ and χ_s to the same reference state of pure components. It has the advantage that χ_s is independent of χ, because the definition of χ_s does not incorporate the energy of the polymer-solvent contact. As shown by Silberberg, $-\chi_s kT$ is the energy associated with the exchange of a polymer segment in the solution with a corresponding solvent volume at the surface, if the volume fraction of segments ϕ equals 0.5 both in the solution and in the surface layer.

All polymer adsorption theories assume that the adsorbing surface can be divided into a number of identical adsorption sites, each of which can bind one segment. If all sites are occupied, the segments in direct contact with the surface form a *complete monolayer*. It is common to define a dimensionless adsorbed amount or *adsorbance* Γ as the number of adsorbed segments per surface site, in other words: the number of (equivalent) complete monolayers that can be formed from the adsorbed segments. This means that Γ is the ratio between the adsorbed weight and the weight adsorbed in a complete monolayer, A^{mon}:

$$\Gamma = A / A^{mon} \tag{2.12}$$

In the same way we relate the *surface occupancy* θ to the weight adsorbed in trains

$$\theta = A_{tr} / A^{mon} \tag{2.13}$$

From the definition of the bound fraction p (2.1) we see that

$$\Gamma = \theta / p \tag{2.14}$$

The number of adsorbed segments can be defined in two different ways: either as a surface excess with respect to the bulk solution, taking the surface as the Gibbs dividing plane (Γ_{ex}, *IUPAC* (1972)) or as the number of segments belonging to chains which have at least one segment directly on the surface (Γ). When the bulk solution is dilute the difference heteen Γ and Γ_{ex} is negligible.

2.4 COMPARISON OF THEORETICAL APPROACHES

2.4.1 *Chain models*

Hoeve's model chain consists of the freely jointed statistical segments which were earlier defined by Kuhn. These segments are allowed to assume every orientation in space; they are not placed on a lattice. A clear advantage of this approach is that the results do not contain a lattice parameter. However, Hoeve introduces a *flexibility parameter* the value of which may be estimated from a lattice model.

Silberberg, Roe, and Scheutjens et al. place the polymer chains on a lattice. They assume that each lattice site can be occupied either by a segment or by a solvent molecule. The distinct advantage of a lattice theory is that the number of conformations can, in principle, be enumerated exactly, although even for short chains the computational problems are enormous (*Ash* et al., 1969). A disadvantage is that, if the results depend strongly on the lattice type, the outcome is obviously not very reliable.

As has been pointed out in the previous section, a conformation of an adsorbed polymer chain can be described as a walk in a density gradient of polymer segments and solvent molecules. Each step in such a walk has Z^* *a priori* possibilities where Z^* is the coordination number of the lattice. The exception is a step starting in the first layer adjacent to the surface. For a step from this surface layer, the number of possibilities is Z_{tr}, where Z_{tr} is the coordination number in the first layer. Clearly $Z_{tr} < Z^*$. As discussed before not every step is equally probable. Each step must be weighted by taking into account the segment density at the location towards which it is directed (step weighted random walk). According to the mean field concept this segment density can be averaged in a layer parallel to the surface. If the segment density profile is given, the weighting factor depends only on the distance from the surface. However, since the conformation probability from which the segment density profile must be found is also a function of that density profile, a solution can only be found by an iteration procedure, or on the basis of some reasonable assumption for the general shape of the profile. The theories diverge strongly in this respect.

2.4.2 *The theory of Hoeve*

Hoeve (1966, 1970) assumed that the most probable type of conformation consists of loops and trains (in alternating order) only, and that end effects (tails) may be neglected. This assumption can be shown to be justified in the limit of infinitely long chains. Hoeve calculated partition functions for the loops, treating them as purely random walks 'restricted by an adsorbing barrier, starting at and returning to the surface. For these loops the Gaussian approximation which is only valid for long walks, was used. To every train segment he assigned the partition function σ_H, irrespective of the length of the train in which such a segment finds itself. This parameter σ_H, expressing the preference of a segment for a surface site over the solution is related to the adsorption energy. The partition function Q^{ca} (due to the conformation in loops and trains and the adsorption of train segments) for one isolated adsorbed chain consisting of a number of loops and trains of variable lengths is then

$$Q^{ca} (T, V, r) = \Sigma \quad (\sum_\lambda n_\lambda) \ ! \ \Pi_\lambda \frac{\omega_\lambda^{n_\lambda}}{n_\lambda !} \quad (\sum_\tau m_\tau) \ ! \ \Pi_\tau \frac{\nu_\tau^{m_\tau}}{m_\tau !} \tag{2.15}$$

where the summation is over all possible distributions.

Here, n_λ is the number of loops consisting of λ segments and m_τ is the number of trains of τ segments. Since loops and trains alternate, $\sum_\lambda n_\lambda = \sum_\tau m_\tau$ for long chains. Furthermore $\nu_\tau = \sigma_H^\tau$ in the partition function for a train of τ segments and $\omega_\lambda = c_H \lambda^{-3/2}$ is the partition function for a loop of λ segments. The constant c_H is a flexibility parameter which is related to the transition probability from a loop into a train and back.

From the maximization of Q^{ca}, it was found that for non-interacting chains the segment density decays exponentially with the distance from the surface. For interacting chains the free energy contains not only ΔF^{ca} ($- kT \ln Q^{ca}$ per adsorbed molecule) but also a mixing term ΔF^m depending on the segment density and on χ:

$$\Delta F = \Delta F^{ca} + \Delta F^m \tag{2.16}$$

This ΔF^m was calculated assuming random mixing in each layer parallel to the surface and retaining the exponential segment density profile also for interacting chains.

Here, the assumption is made that polymer-solvent interactions have a negligible effect on the shape of the density profile.

Thus, before minimizing the free energy Hoeve restricted the conformation probability distribution by two requirements:

1)   the segment density profile is exponential

2)   the contribution of tails is negligible.

Hoeve was able to formulate the results in a number of relatively simple analytical expressions.

2.4.3 *The theory of Silberberg*

Silberberg (1968) started also by making a reasonable assumption about the most probable type of conformation. Like Hoeve, he neglected tails. He distinguished two types of conformations:for good (athermal) solvents the conformations correspond to self-avoiding walks and for theta-solvents the purely random walk model was chosen. Silberberg's partition function Q^{ca} can be rewritten in a form suitable for comparison with Hoeve's result, eqn. (2.15). If we make use of the relation $\sum_\lambda n_\lambda = \sum_\tau m_\tau$ and if we assume that the coordination number in the bulk, z^*, applies also to the loops, Silberberg's result becomes identical to eqn. (2.15) provided the following relations are satisfied:

for an athermal solvent:

$$\omega_\lambda = \gamma_1 \gamma_{tr} \lambda^{-4/3}$$

$$\nu_\tau = \tau^{1/3} \left\{ (Z_{tr}/z^*) \exp \chi_s \right\}^\tau$$

(2.17)

and for a theta-solvent:

$$\omega_\lambda = \gamma_1 \gamma_{tr} \lambda^{-3/2}$$

$$\nu_\tau = \left\{ (Z_{tr}/z^*) \exp \chi_s \right\}^\tau$$

(2.18)

Here Z_{tr} is the coordination number at the surface and γ_1 and γ_{tr} are constants related to the probability that a loop ends and a train starts, or the reverse, respectively. (For the athermal case, Silberberg has an extra (small) factor in the denominator of the partition function. For the sake of simplicity, it is omitted here).

It is interesting to note that for the theta solvent, eqn. (2.18), Hoeve's partition functions for loops and trains are obtained with $c_H = \gamma_1 \gamma_{tr}$ and $\sigma_H = (Z_{tr}/z^*) \exp \chi_s$. Furthermore we can compare the athermal solvent with the

theta solvent. It can be seen from the above equations that for loops in the athermal solvent the dependence on the sequence length (λ and τ, respectively is weaker than in the theta solvent. Therefore a loop of a given length contributes less entropy in an athermal solvent than in a theta solvent. For trains, the reverse is true, provided that $(z_{tr}/z^* \exp \chi_s) > 1$.

In the same way as Hoeve, Silberberg added a mixing term to the free energy. This term was calculated by means of placing polymer and solvent on a lattice and assuming a *constant* segment densing between the surface and a plane at a distance of half the average loop length from the surface. Beyond this plane, the segment density drops discontinuously to the bulk solution value. This step function is to be contrasted with Hoeve's choice of an exponential distribution. Thus, Silberberg restricts the conformation probability distribution prior to the minimization of the free energy by the following requirements:

1)   the density profile is a step function

2)   tails do not contribute

Silberberg's results could not be expressed analytically. Numerical methods are needed to solve the equations. Comparing Hoeve's and Silberberg's treatments, we arrive at the following conclusions. Both adopt a *configuration factor* for *isolated* chains (i.e. walks in which steps are not weighted according to the segment density) and both make assumptions about the segment density profile. Hoeve's purely random walk approach underestimates the expansion effects due to self-exclusion, which may become important at low segment densities and in good solvents. Self avoiding walks should then be considered as done by Silberberg. However, the assumption of a constant segment density throughout the adsorbed layer is probably an overestimation of these expansion effects so that it is not very probable that the theory of Silberberg gives considerably better results than Hoeve's. With a few exceptions the results of the two theories give similar trends with respect to the effect of the chain length, the solvent power and the polymer concentration on the adsorbed amount. These trends are the same as those found experimentally, as discussed in section 2.1.

2.4.4 *The theory of Roe*

In order to enumerate conformations Roe employed a lattice of W layers parallel to the surface, labeled (starting from the surface) 1, 2, ..., i, ..., W, with L_w lattice sites each. The partition function was derived for random walks on this lattice, in which each step towards layer i is weighted with the average expectancy of finding a vacant lattice site in i (step weighted random

walk). In this respect Roe's consistent application of the mean field concept is an improvement on the theories of Hoeve and Silberberg where such weighting factors are absent.

In the derivation of results, Roe uses the simplifying assumption that each segment of an r-mer gives the same contribution ϕ_i/r to the total volume fraction ϕ_i in i, regardless of its ranking number in the chain. One of the consequences of this assumption is that inversion symmetry with respect to the ranking number is lost. This has been criticized by *Helfand* (1976). As a result of the simplification Roe was able to maximize his partition function with respect to the number n_i of segments in each layer. He obtained W implicit equations for the W segment densities ϕ_i at equilibrium. Solving all the equations by an iteration procedure yields the segment densing profile. From this, the (excess) adsorbed amount Γ_{ex}, the surface occupancy θ and other observable quantities can be derived. However, details about the conformation are lost so that contributions of loops, trains, and tails cannot be distinguished.

2.4.5 *The theory of Scheutjens and Fleer*

In the most recent theoretical development, presented by Scheutjens and Fleer (1979) major simplifications could be rigorously avoided. These authors employed a lattice identical to that of Roe and wrote the canonical partition function for a set $\{n_c\}$ of specified conformations. To avoid confusion we should point out here that the conformations defined by us (see 2.2) are denoted as *arrangements* by Scheutjens et al. They define a conformation as being completely specified by giving not the *position* for each segment but only the *layer number* in which each segment finds itself. Thus several arrangements can be grouped together to give a conformation.

Free molecules in bulk solution can attain a number of arrangements of the order of $z^{*(r-1)}$ (see 2.6.1) where z^* is the coordination number in the bulk. The presence of a surface imposes restrictions and reduces this number of arrangements by a factor of ω_c; ($\omega_c < 1$). Obviously, this reduction factor ω_c is different for different conformations.

Scheutjens and Fleer find for the configurational part Ω_n^c of the partition function for the mixture of n polymer molecules and $WL_w - rn$ solvent molecules

$$\Omega_n^c \left(W,\ L_w,\ T,\ \{n_c\}\ \right) = \sum_c \frac{(L_w!)\ \dfrac{Z}{L_w}^{(r-1)n}\ \Pi_c\ \dfrac{\omega_c}{n_c!}^{n_c}\ \Pi_{i=1}^{W}\ \dfrac{1}{n_i^o!}}{\dfrac{rn!}{n!}\ \dfrac{Z}{rn}^{(r-1)n}} \qquad (2.19)$$

Here, n_c is the number of chains in conformation c, $n = \sum_c n_c$ is the total number of polymer chains and n_i^o is the number of solvent molecules in layer i. Note that the partition function contains the factor

$$\Pi_c\ \frac{\omega_c}{n_c!}^{n_c}$$

which takes into account all the allowed conformations, i.e. conformations of free and adsorbed chains and conformations with not only trains and loops, but also tails. Hoeve and Silberberg incorporated only factors

$$\Pi_\lambda\ \frac{\omega_\lambda}{n_\lambda!}^{n_\lambda} \quad \text{and} \quad \Pi_\tau\ \frac{\nu_\tau}{m_\tau!}^{m_\tau}$$

for loops and trains. The denominator in (2.19) is Flory's expression for a chain in pure bulk polymer, which serves here as the reference state.

The energy part of the partition function contains a contribution for polymer-solvent interactions in every layer i, and an extra contribution for the adsorption energy χ_s in the first layer, and is identical to that used by Roe.

The authors showed that the maximization of the partition function leads naturally to the matrix formalism for the treatment of random walk statistics as employed by *DiMarzio and Rubin* (1971), but with weighting factors p_i for *every* layer i. Each segment of a chain of r segments contribute such a factor p_i, also denoted as the *free segment probability*, to the conformation proba-bility. It can be written as the product of three factors. The first factor, $(1-\phi_i)/(1-\phi_*)$, where ϕ_i and ϕ_* are the segment densities in layer i and in bulk, respectively, accounts for the average vacancy expectancy of a site in layer i as compared to the bulk solution. The second factor contains χ and accounts for the difference in the polymer solvent interaction between layer i and the bulk solution. The last factor, $\exp \chi_s$, incorporates the adsorption energy and should thus only be included if i=1. The expression for p_i reads

$$p_i = \left(\frac{1-\phi_i}{1-\phi_*} \right) \exp \left\{ 2\ \chi\ (<\phi_i> - \phi_*) + \delta_{i,1}\ \chi_s \right\} \qquad (2.20)$$

where $<\phi_i>$ is a weighted average of the segment density over the layers i-1, i and i + 1 (according to the coordination around a site in i) and $\delta_{i,1}$ is the Kronecker delta function.

As soon as ϕ_i is known, p_i is also known. The equilibrium values of ϕ_i are found by solving a set of W implicit equations by an iteration procedure based on the matrix formalism. We want to emphasize here that in the Scheutjens-Fleer theory an equilibrium conformation corresponds to a step weighted random walk. Each step is assigned the correct weight according to the mean field concept. The matrix procedure keeps track of all conformations so that it is possible to calculate, in principle, the probability for any specified conformation. Any useful average may thus also be calculated.

2.5 THEORETICAL RESULTS

The qualitative trends predicted by the afore mentioned theories do not differ very much. General features are:
-    there exists a critical, non zero, adsorption energy; no adsorption takes place if the adsorption energy is lower than this critical value.
-    adsorption isotherms for high chain lengths are of the high affinity type.
-    both p and θ increase with increasing adsorption energy.
-    θ increases with chain length, but levels off at high chain length.
-    at given ϕ^* the adsorbance increases with chain length.
-    the solvent effect is pronounced: the adsorbance increases and p decreases with χ.

However, the quantitative details can be rather different. E.g., for the dependency of adsorbance on chain length (at fixed concentration) in theta solvents Hoeve predicts that Γ is approximately proportional to $r^{0,5}$ for long chains.

Silberberg finds that, in such solvents, Γ reaches a limit at very high chain length, whereas Roe predicts rather a levelling off (for Γ_{ex}).
Scheutjens and Fleer calculate that the adsorbance from theta solvents increases nearly proportionally with log r in the range 20 < r < 1000 (because of computing time limitations they could not calculate results for longer chains). All the theories agree that in athermal solvents (χ = 0) the adsorbance tends to a limiting value at high r.

Hoeve assumed an exponential segment density profile whereas Silberberg approximated it by a step function. Both Roe and Scheutjens et al. were able to calculate the profile without any assumption about its general shape. Close to the surface the profiles found from their theories are approximately

exponential and differ only slightly. At larger distances, the theory of Scheutjens and Fleer predicts considerably higher densities than Roe's theory. This is due to the occurrence of long dangling tails which dominate the segment density in the outskirts of the absorbed layer. Only the Scheutjens-Fleer theory avoids approximations which obscure the occurrence of tails.

Although this latter theory requires the use of a large computer for the evaluation of numerical results, it has a number of distinct advantages.

  i)   it is based on a consistent application of the mean field concept, without further approximations

 ii)   it is not restricted to long chains, but applies equally well to oligomers; this applies also to Roe's theory but not to those of Hoeve and Silber-berg.

iii)   detailed information about the conformation of the absorbed chains, in terms of loops, trains and tails, is obtained.

A big problem in the application of a lattice theory to an experimental system is how a polymer segment should be defined. In terms of the lattice model of Roe and Scheutjens et al., it is a volume of polymer equal to the volume of a solvent molecule. If the solvent consists of small molecules, as in the case of water, this means that the number of segments per chain is very high, and then a serious overestimate of the number of possible conformations is to be expected.

Also, the effects of polydispersity of the polymers and irreversibility of the adsorption are not considered in the theory. Nevertheless, in experiments they may be quite important. In order to explore their consequences on the relations between theory and experiment we consider these aspects more closely in the next sections.

2.6   CHAIN VOLUME AND FLEXIBILITY IN LATTICE THEORIES

2.6.1 *Definition of a statistical segment; introduction of the bulkiness parameter.*

If we want to evaluate predictions of a statistical thermodynamic theory, we must be well aware of the differences between the properties of the model and of the real system to be described by the model. In the theory for the adsorption of polymers we are mainly interested in those properties which determine the *free energy of mixing* and those properties which determine the *conformational entropy* of the polymer molecules. Let us consider those properties in some detail.

The entropy of mixing, ΔS_m, of a polymer solution depends, to a first approximation, only on the numbers of polymer molecules n and solvent molecules n^o and on the corresponding volume fractions ϕ and ϕ^o:

$$\Delta S_m/k = n^o \ln \phi^o + n \ln \phi \qquad (2.21)$$

(*Flory*, 1941 and *Huggins*, 1941; 1942). For the magnitude of ΔS_m, the shape or the flexibility of the polymer molecules is irrelevant. We need only know the molecular volume ratio v_2/v_1 and the numbers n and n^o. *Huggins* (1971) showed that (2.21) could be derived for chains of arbitrary flexibility. The flexibility, according to (2.21), does not contribute to ΔS_m: its effect is cancelled by the introduction of a reference state of equally flexible molecules (pure des-oriented polymer). For the energy of mixing, expressed by the interaction parameter χ, a similar reasoning holds. Since this energy of mixing can be written as $n^o \phi \chi$, it also depends solely on n, n^o and v_2/v_1. Thus, the only fundamental property which must be included in the model in order to describe the free energy of mixing accurately is the ratio between the volume of a polymer molecule and a solvent molecule.

The volume of the real chain is $P v_{mon}$, where v_{mon} is the volume of the monomer unit, and P is the degree of polymerization. The volume of the model chain is $r v_{seg}$, where v_{seg} is the volume of a theoretical segment. Since the model chain and the real chain should have equal volumes we have $v_{seg} = P v_{mon}/r$. Dividing by the volume of the solvent molecule, v_1, gives

$$v_{seg} / v_1 \equiv b = \frac{P v_{mon}}{r v_1} \qquad (2.22)$$

The volume ratio b between a theoretical segment and a solvent molecule may be called the bulkiness parameter. Since v_{mon} and v_1 are constants for a given polymer-solvent pair, b depends only on P/r, the number of monomer units per theoretical segment.

Below we discuss three different ways to estimate P/r. The first of these is based on geometrical considerations i.e. on the thickness of the chain or its average cross sectional area. The other two methods are based on the flexibility of the chain. For reasons to be given below we prefer the first way. Hence, the P/r values consistent with the flexibility of the chain will only be used in order to check to what extent the flexibility is accounted for in the model.

The first method is based on the notion that a lattice model such as employed by Roe or by Scheutjens and Fleer is incapable to cope with anisotropic segments. This is a direct consequence of the way in which the chain statistics

are treated. Thus a segment must have equal length, width and height and all three must be equal to the thickness of a monolayer of tightly packed polymer chains, lying flat on the surface. This thickness, d, is immediately related to the adsorbed amount in a monolayer A^{mon}, and can be estimated, e.g., with the help of suitable molecular models. The segment volume is d^3 and we have $b = d^3/v_1$, or, using (2.22):

$$r/P = v_{mon} / d^3 \qquad (2.23)$$

The reason that we prefer to use this equation as our definition of a theoretical segment is that it is so closely related to the very nature of the lattice model.

However, since conformation changes are important in adsorption, we are also interested in those properties which determine the conformational entropy, i.e. in the flexibility. Therefore, the other two methods of assessing b are based on the conformational partion function Ω^C, and on the mean square end-to-end distance $<h_o^2>$, respectively. The conformational entropy is directly given by $k \ln \Omega^C$. The relation between the conformational entropy and $<h_o^2>$ is less direct, since it may depend on the detailed architecture of the chain (*Flory*, 1969), but in cases where a reliable estimate of Ω^C is not available it may serve as a useful alternative. Thus, let us investigate which values of r/P we find if we demand that the model chain and the real chain have either equal Ω^C or equal $<h_o^2>$.

For a model chain of r segments on a lattice with coordination number Z, we have

$$\Omega^C = z^{r-1} \qquad (2.24)$$

if the effects of self-exclusion are ignored. For real chains, we rely upon Flory's treatment of the statistical mechanics of chain molecules (Flory, 1969). This treatment follows the lines of the *rotational isomeric state approximation* in which each bond in the backbone of a polymer chain is assumed to occur in one or another of several discrete rotational states. We do not attempt to describe Flory's approach here, but merely quote the result that for any long, flexible polymer chain the expression for the conformational partition function takes the simple form

$$\Omega^C = z_p^{P} \qquad (2.25)$$

(cf, *Flory*, 1969, p. 71; p. 226). Here z_p is a characteristic constant for a

given polymer. It is possible, at least in principle, to derive Ω^c for a chain of known architecture, but the parameters from which Z_p follows should be checked by relating them to some experimental quantity such as, e.g., the mean square end-to-end distance or the temperature coefficient thereof. Good examples are the calculations of *Abe et al* (1966) for the polymethylene chain, giving $Z_p \simeq$ 1.85. For vinyl chains, we are only aware of the calculations of *Tonelli* (see *Flory*, 1969, p. 236) for polystyrene. Tonelli shows that for predominantly syndiotactic chains a value of $Z_p = 1.62$ leads to reasonable agreement with observed values of $\langle h_o^2 \rangle$.

Comparing (2.24) and (2.25) we find that the requirement Ω^c (real chain) = Ω^c (model chain) is satisfied if $Z^{r-1} \simeq Z^r = Z_p^P$. Hence,

$$P/r = \log Z / \log Z_p \qquad (2.26)$$

The third alternative is to use $\langle h_o^2 \rangle$ as the basis for the definition of a statistical segment. For a model chain in a lattice with coordination number Z, $\langle h_o^2 \rangle$ can be written (*Yamakawa*, 1971) as

$$\langle h_o^2 \rangle = \frac{1 + z^{-1}}{1 - z^{-1}} \, r \, l_1^2 \qquad (2.27)$$

Eq. (2.27) may be expressed in the contour length, $L = r \, l_1$ of the model chain, where l_1 is the length of a step on the lattice. Thus, we find for the model chain of given contour length L that $\langle h_o^2 \rangle$ is inversely proportional to r:

$$\langle h_o^2 \rangle = \frac{1 + z^{-1}}{1 - z^{-1}} \, L^2/r \qquad (2.28)$$

For the real chain we had eq. (2.7): $\langle h_o^2 \rangle = C \, m \, l^2 = 2 \, C \, P \, l^2$, where l is the bond length, and C the characteristic ratio. If we demand that the real chain and the lattice chain have the same end-to-end distance *and* the same contour length, the number of steps of the lattice chain must be:

$$r = \frac{1 + z^{-1}}{1 - z^{-1}} \, \frac{L^2}{2 \, C \, P \, l^2} \qquad (2.29)$$

Since L could be expressed in P through eq. (2.9): $L = 1.64 \, l \, P$ we find by elimination of L

$$P/r = 0.743 \, \frac{1 - z^{-1}}{1 + z^{-1}} \, C \qquad (2.30)$$

Equations (2.26) or (2.30) serve to define a segment on the basis of
flexibility. We can check for a given chain whether the P/r values found from
them are (approximately) the same as that derived from eq. (2.23) on the basis
of chain thickness. If this is the case we may expect that the lattice model
chain consistently accounts for both the chain volume and the conformational
degrees of freedom of the real polymer molecule. If there is a considerable
difference between the P/r estimates from (2.23) and from (2.26) or (2.30),
respectively, the flexibility is only poorly accounted for in the model and
improvement can only be expected if a new theory using different lattice
statistics is developed. In chapter 6 we apply the above equations to assess
the size of a segment of polyvinyl pyrrolidone.

2.6.2 *A modification of the Scheutjens-Fleer theory*.

The above definitions of statistical segments are inconsistent with lattice
theories such as the Scheutjens-Fleer theory, since the partition function
(eq. 2.19) is derived for segments and solvent molecules of equal size ($b = 1$).
Usually, b is larger than 1. However, it is possible to modify the theory by
assuming that each lattice site may be occupied by either one segment or b
solvent molecules. In that case, the n_i^o lattice sites which remain in layer i
after placing the polymer molecules can be filled with b n_i^o indistinguishable
solvent molecules. Straightforward maximization of the modified partition
function by the procedure employed by Scheutjens and Fleer reveals that the
free segment probability p_i (eq. 2.20) must now be replaced by p_i^b, provided
χ_s in (2.20) is replaced by χ_s/b to keep the adsorption energy per segment
constant (see the definition of χ_s in section 2.3). Since in experiments with
polymer solutions, the polymer-solvent interaction parameter χ is usually
defined per solvent molecule the introduction of b has no effect on χ. Hence,
the expression for p_i now reads:

$$p_i = (\frac{1 - \phi_i}{1 - \phi_*}) \exp \{ 2 \chi (<\phi_i> - \phi_*) + \delta_{i,1} \chi_s/b \} \qquad (2.31)$$

The physical meaning of the replacement of p_i by p_i^b is that a segment can
only be placed in layer i if simultaneously b solvent molecules are removed from
this layer. The volume of the solvent molecule enters, through b, as a parameter
into the adsorption theory (cf. eq. 2.22). Therefore, a change in the solvent
volume, at constant segment volume and constant χ (per solvent molecule) and χ_s
(per segment or per unit of surface area), will affect the theoretical results.
In section 2.6.3 we investigate how the theoretical results depend on b.

Differences between various chain types can, in principle, also be studied by varying the bulkiness parameter at constant v_1. However, we then have to choose what chain property we should keep constant: the chain volume, the adsorption energy per unit volume or the adsorption energy per unit of surface area, etc. Each choice forces us to accept some other parameter to depend on b: at constant chain volume b r is constant, thus $r \sim b^{-1}$; at constant adsorption energy per unit volume $r\chi_s/rb$ is constant, so that $\chi_s \sim b$; at constant adsorption energy per surface area $r\chi_s/r$ $b^{2/3}$ is constant, hence $\chi_s \sim b^{2/3}$. Since in all these cases the monolayer capacity A^{mon} becomes also a function of b and since it is unclear to what physical situation each of these choices corresponds we shall not pursue the investigation of such chain type effects.

2.6.3 *Influence of the bulkiness parameter on theoretical results.*

We investigated the consequences of incorporating the bulkiness parameter into the Scheutjens-Fleer theory. We performed calculations for a simple cubic lattice for different values of b, keeping the energy parameters χ_s (per segment) and χ (per solvent molecule) constant. The data presented in this section apply to $\chi_s = 2$ and $\chi = 0.45$, this choice was made in view of the applicability of the results on the adsorption of PVP on silica from water and from dioxane (see chapter 6). The chain length r was varied between 2 and 1000 segments. The volume fraction ϕ^* of the polymer in the solution was always 10^{-4}. All calculations were performed on a DEC-10 computer, using a modification of a programme written in ALGOL by *Scheutjens* (1979).

Adsorbed amount

In fig. 2.2 we give the adsorbed amount Γ as a function of b, for different chain lengths; b is plotted on a logaritmic scale. We see that, for $b \leq 5$, Γ depends almost linearly on $\log b$: for high chain lengths there is a dramatic decrease with increasing b, while for shorter chains the slope of the curve increases gradually from strongly negative to even weakly positive for dimers ($r = 2$). Since the effect of b depends so strongly on the chain length it is useful to investigate how Γ depends on chain length for different values of the bulkiness parameter. Curves for $b = 1$, 2, 5 and 10, respectively, are given in fig. 2.3, where Γ was plotted against $\log r$. At $b = 1$, Γ increases strongly, and almost linearly with $\log r$, at least if $r > 10$. This result is typical for a relatively poor solvent ($\chi = 0.45$) in the original Scheutjens-Fleer theory (for which $b = 1$). For more bulky polymers the dependence of Γ on r becomes much weaker. The curve for $b = 10$ has a slope which is not much different
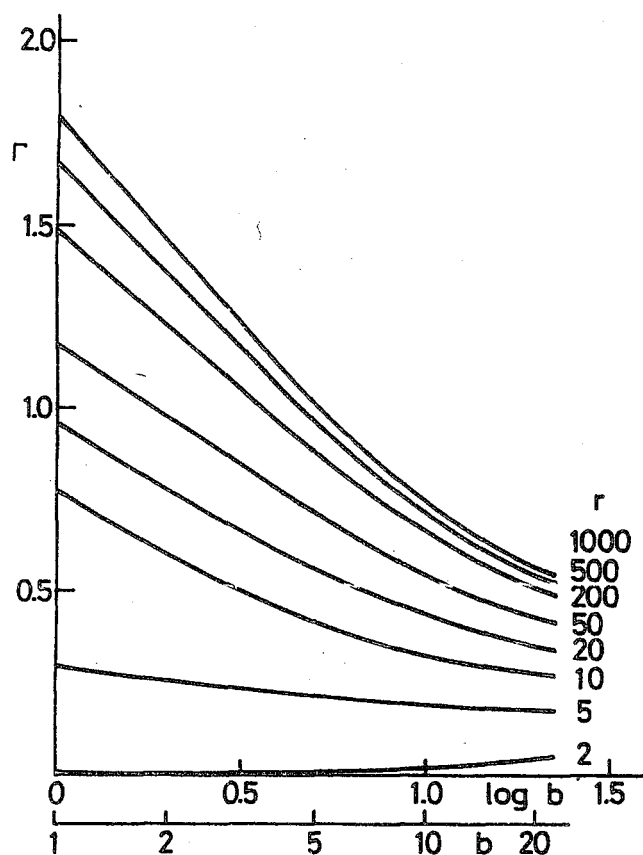
Fig. 2.2. Dependence of adsorbance Γ on bulkiness, for different chain lengths; $\chi_s = 2$, $\chi = 0.45$.
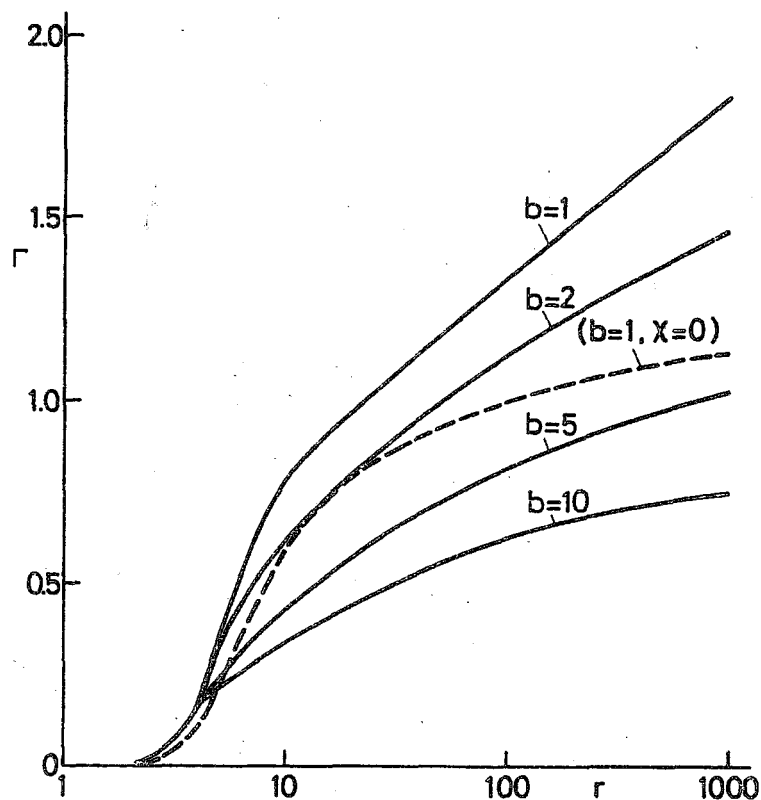
Fig. 2.3. Dependence of adsorbance Γ on chain length r, for a number of values of the bulkiness parameter b. Solid lines refer to a moderately poor solvent ($\chi = 0.45$) and the dashed line is for a good solvent ($\chi = 0$). For all curves, $\chi_s = 2$.

from that for a good solvent ($\chi = 0$) in the original Scheutjens-Fleer theory.
Thus, it looks as if, at high b, the adsorption of long chain molecules occurs
from a thermodynamically good solvent. For very short chains the effect is
reversed: slightly higher adsorbances are found with increasing b.
For the given set of parameters (fig. 2.3) the inversion occurs somewhere
between 2 and 5 segments. At very large r the number of layers of high ϕ_i is
large, so that here the effect of b on Γ is particularly strong.
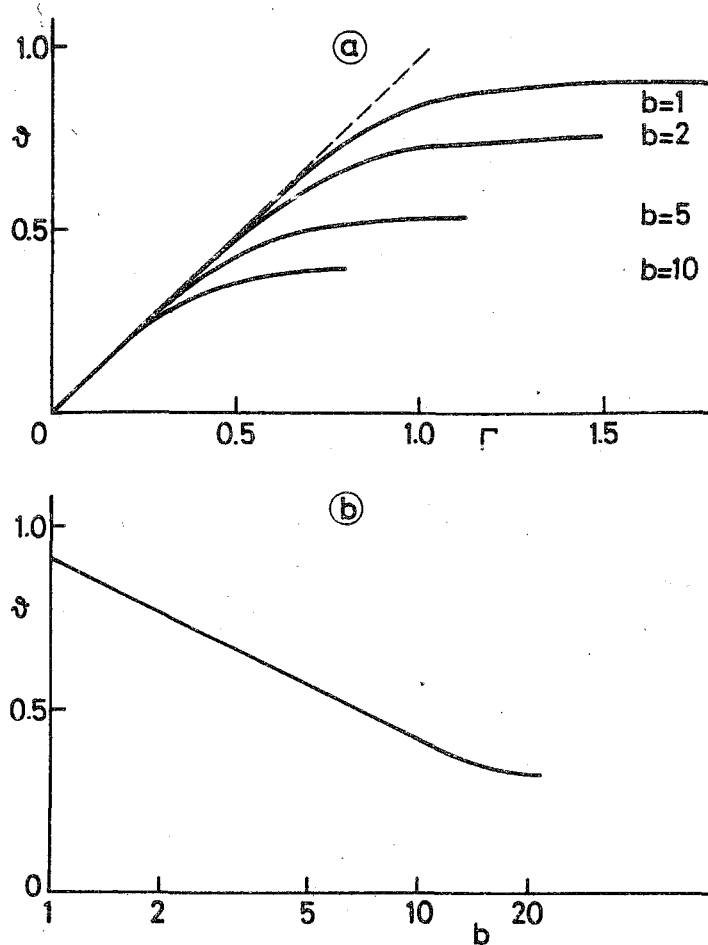
Fig. 2.4 a) Segment density θ in the immediate neighbourhood of the surface, as
a function of adsorbance Γ, for various values of the bulkiness
parameter b.
b) The plateau value of θ as a function of b (logaritmic scale).

Surface occupancy

As could be expected, the surface occupancy θ shows trends as a function
of b similar to those of Γ (see fig. 2.4a). At very low adsorbed amount, all

curves have the same slope (of about 1) but at higher Γ the curves at high b level off to a much lower plateau than those at low b. The plateau level of θ depends again linearly on log b (fig. 2.4b).

Conformation of the adsorbed molecules

The conformation of the adsorbed macromolecules (at given bulk concentration) expressed as the fraction of segments in loops, trains, and tails, respectively, is almost unaffected by the bulkiness of the chain. For instance, the fraction of segments in trains p ('bound fraction') changes by no more than 2 % if b increases from 1 to 10. So the effect of the bulkiness seems to be to merely 'push' macromolecules away from the interface, rather than inducing changes in the conformation of these molecules. Therefore, as the bulkiness increases the adsorbed amount decreases, but the conformation (as judged from the fraction of segments in trains, loops and tails) is essentially unchanged.

2.6.4 Concluding remarks

Since for a given polymer b is inversely proportional to the volume of a solvent molecule v_1, a decrease of v_1 corresponds to an increase of b. Such is the case if we dissolve a given polymer in solvents with different v_1; if all other variables (χ, χ_s, molecular weight) are kept constant, we should find lower adsorbed amounts and also a weaker dependence on M in the solvent with the smaller v_1. Because the water molecule is very small, it may be expected that a polymer molecule in water is very 'bulky'. Hence, we expect that adsorbed amounts of long chain molecules from water are relatively low and depend only weakly on molecular weight. Most organic solvents have molecules about five times as big as the water molecule; our calculations suggest that the corresponding decrease in bulkiness alone causes the adsorbed amounts from these solvents to be much higher and to depend stronger on molecular weight.

We conclude that the scheme outlined in section 2.6.2 enables us to incorporate the volume of a particular chain type into the Scheutjens-Fleer theory. To do this, the free segment probability p_i is brought to the power b, where b is the volume ratio between a segment and a solvent molecule (eq. 2.22); suitable segments were defined in 2.6.1. In this procedure the definition of the adsorption energy parameter χ_s, *per segment* was maintained so that p_i had to be rewritten with χ_s/b instead of χ_s, (eq. 2.31). The scheme cannot consistently cope with stiff chains, since this would involve anisotropic segments, but for flexible chains the flexibility may be reasonably accounted for. In chapter 6 we apply the modified theory to our experimental results.

2.7 POLYDISPERSITY AND REVERSIBILITY

Many authors have discussed the reversibility of the adsorption of flexible polymers. The main argument is that desorption is usually not observed if solvent is used to dilute the system. Other observations, such as adsorption-desorption hysteresis and dependence of adsorption isotherms on the amount of adsorbent are also at variance with theoretical predictions and do indeed suggest irreversible adsorption. Therefore, the application of equilibrium thermodynamics to polymer adsorption is often questioned. Looking for a compromise between the two conflicting views (equilibrium or non-equilibrium) *Lankveld and Lyklema* (1968) assumed that individual segments could adsorb reversibly, establishing a local equilibrium. *Koopal and Lyklema* (1975) found that it was indeed possible to treat the train segments as being in (quasi-) equilibrium with the solution.

However, it is difficult to understand that non-equilibrium persists in a flexible chain which is apparently in local equilibrium with its surroundings. It means that movements of the chain as a whole are effectively prohibited by many entanglements. The explanation forwarded by Lankveld et al. is also unnecessary, since lack of desorption upon dilution is in agreement with theoretical results. The adsorption affinity of long chains is found to be so high, that theoretical equilibrium concentrations may be incredibly low ($\phi_* < 10^{-20}$). Still these results are for adsorbed chains in perfect equilibrium with their surroundings.

Recently, we have shown that many of the experimental observations ascribed to irreversibility can be explained in terms of polydispersity effects (*Cohen Stuart et al.* 1980). It should be born in mind that all theoretical results, (including those mentioned in section 2.5) are valid for monodisperse polymers. In experimental studies, polydisperse samples are often used and the results obtained with such mixtures may differ significantly from those found for pure components. As has been discussed above (see 2.1) in polydisperse polymers preferential adsorption of long molecules over shorter ones occurs. Consequently, experimental data for polydisperse polymers cannot be interpreted in terms of some average molecular weight, but the molecular weight distribution must be taken into account.

The ideas developed by Cohen Stuart et al. are as follows. At low amounts of polymer in the system, the available surface area is large enough to accomodate virtually all the polymer on the surface. In this region the isotherm shows its steep initial rise. As more polymer is added, there is no more unoccupied surface area and competition between the molecules takes place. The preferential adsorption of large molecules causes then a fractionation with the

average molecular weight on the surface shifted to higher values as compared
to that in the solution. This process continues as long as there are larger
molecules in the solution than on the surface.

The isotherm for a simple binary polymer mixture was shown to consist of
three parts: a steep initial rise, a linear part with a slope inversely propor-
tional to the amount of adsorbent (surface area to bulk solution volume ratio)
and a horizontal plateau coinciding with the adsorption plateau of the component
with the highest molecular weight. The results could be generalized for a
polydisperse polymer mixture and an expression was found from which the adsorp-
tion isotherm for such a mixture could be calculated, provided that the molecular
weight distribution function and the dependency of the adsorbed amounts on
molecular weight are known.

Inversely, the molecular weight dependency of the absorbed amount can be
derived from experimental isotherms, if the molecular weight distribution is
given. The procedure developed by Cohen Stuart et al. involves plotting the
adsorbance A as a function of the total amount of polymer in the system *per unit
of surface area*. A tangent drawn to this curve contains all the information
(adsorbance and molecular weight) for a single fraction in the polydisperse
sample.

The displacement process cannot be reversed by diluting the solution with
pure solvent. Since the "isotherm" is not a real one component isotherm, but
reflects the displacement process, it is impossible to "follow the isotherm
back" by dilution alone. Instead the desorption isotherm is a nearly horizontal
"theoretical" line corresponding to the adsorption behaviour of the average
molecular weight that is on the surface.

On the basis of the ideas outlined above we will try to interpret the
experimental data in terms of equilibrium adsorption, taking the polydispersity
of the samples into account.

Chapter 3
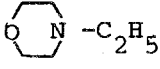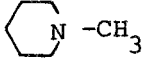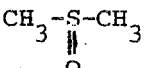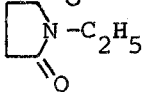
Characterization of Materials

3.1 LOW MOLECULAR WEIGHT SUBSTANCES

The solvents used were water and 1,4 dioxane. The water was distilled once. The dioxane (Baker Analar) was a selected lot containing less than 0.003 % water (w/v) as stated by the manufacturer; it was used without further purification. In order to carefully exclude water, all dioxane solutions were made up in a glove box under P_2O_5-dried air.

Five other chemicals were used in displacement studies (chapter 4). Properties and pretreatment of these chemicals and of dioxane are summarized in table 3.1. This table also contains the abbreviations by which the substances are denoted in the text.

Table 3.1. Properties of low molecular weight chemicals

Name	Abbreviations	Structure	Manufacturer	Mol.weight	Purification:
Pyridine	PYR		Merck (pro analysi)	79.10	—
N-ethylmorpholine	NEM	$-C_2H_5$	Aldrich (analyzed, 99%)	115.18	—
N-methylpyrrolidine	NMP	$-CH_3$	Aldrich (analyzed, 97%)	85.15	distillation
Dimethylsulfoxide	DMSO	CH_3-S-CH_3 ‖ O	Fluka (purum)	78.14	—
N-ethylpyrrolidone	NEP	$-C_2H_5$	Aldrich (analyzed)	113.16	distillation
Dioxane		O O	Baker Analar	88.12	—

3.2 POLYVINYL PYRROLIDONE

The polymer used in this study was commercially produced polyvinyl pyrrolidone (PVP), namely Kollidon from BASF (BRD). Sections 3.3 and 3.4 deal with the solution properties and the molecular weight of the samples used. In this section we review some relevant general properties.

3.2.1 *Preparation and structure*

Polyvinyl pyrrolidone (PVP) is an essentially linear homopolymer prepared by either radical or cationic polymerization of vinyl pyrrolidone. It has the chemical structure:

$$\left[CH_2 - \underset{\underset{\displaystyle N}{|}}{CH} \right]_n \quad \overset{N}{\diagdown} = 0$$
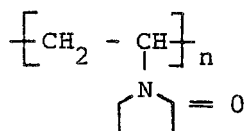
Almost all commercially produced PVP has been prepared in aqueous solution by a radical (redox-) polymerization with hydrogen peroxide together with amines. Average molecular weights ranging from about 10^3 up to 10^6 can be obtained. By virtue of its extremely low toxicity and its complexing properties PVP is applied in many pharmaceutical products. A number of properties of PVP has been summarized by *Herrle* (1965).

In some radical polymerizations branching may occur if chain transfer reactions to the monomer or to an already formed chain have sufficient probability (*Flory*, 1953, p. 257). However, the transfer constant to monomer is as low as $4 \cdot 10^{-4}$ (*Brandrup and Immergut*, 1975). Therefore it is unlikely that any branching occurs if the average degree of polymerization remains below 10^3. Branching at higher chain length would show up as a deviation in the viscosity-molecular weight relationship. In the literature, there is no evidence for such a deviation (*Burchard*, 1967). Hence, we presume that branching in PVP is un-important.

Irregularities in the way monomers are attached to each other (head-to-head instead of head-to-tail) are not very probable because of the strong steric hindrance between the bulky pyrrolidone rings. Like most radical polymers with such bulky side groups, the PVP chain will be predominantly syndiotactic. This view is supported by *Bartels et al.* (1977) who found that PVP forms more stable complexes with syndiotactic polymethacrylic acid (PMAA) than with isotactic PMAA. This can be understood from geometrical considerations, assuming PVP to be syndiotactic.

3.2.2 *Spectroscopic properties*

The UV spectrum of PVP has been studied by *Saidel* (1955) and *Oster* (1952). These authors agree that PVP has its absorption maximum in the far UV region. A single band is found corresponding to the $\pi \rightarrow \pi^*$ excitation of the carbonyl π-electrons (peptide I band). Using a Pye Unicam SP 1800 spectrophotometer we

could record the absorption spectrum of a 5 mg dm^{-3} aqueous PVP solution down to 190 nm (fig. 3.1).
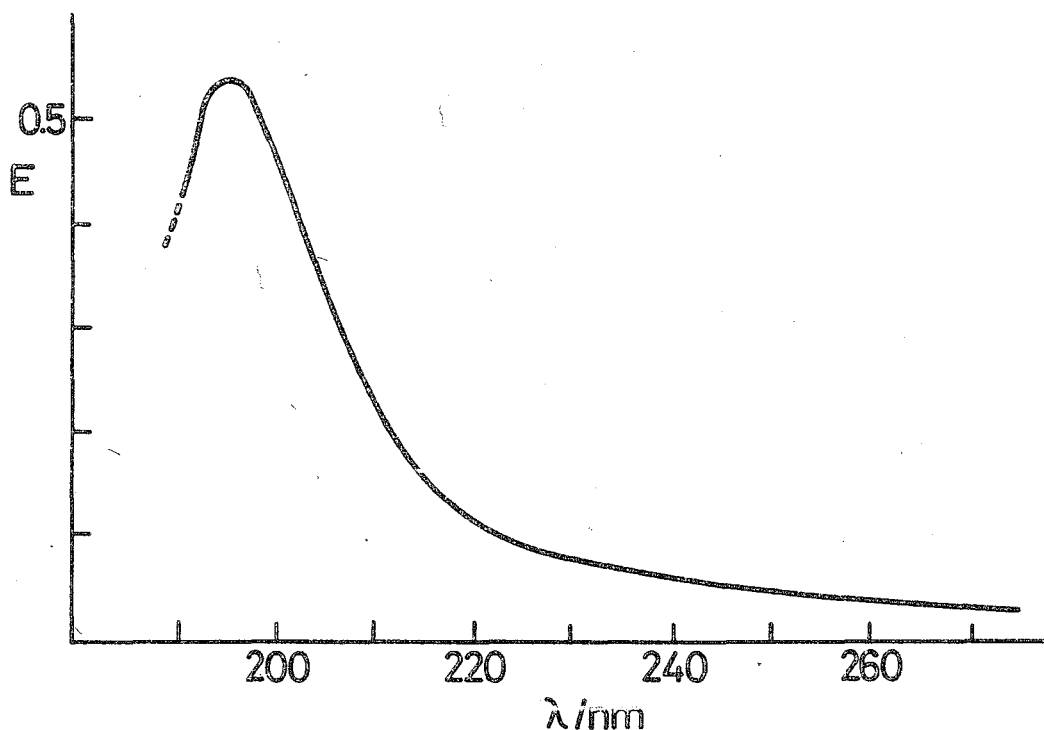
Fig. 3.1. Ultraviolet spectrum of aqueous PVP solution. Pathlength 1.0 cm, concentration 5 mg dm^{-3}.

Clearly, one single absorption band is found, without the fine structure reported by *Oster* (1952). Presumably, this fine structure is an artefact of Oster's measurement caused by stray light or poor matching of the optical paths (e.g. differences between cells). The absorbance per mole of monomer units per dm^3 and per cm pathlength (molar absorptivity) at 196 nm was found to be 5560 dm^3 mol^{-1} cm^{-1}. *Saidel* reports that the UV spectrum of an aqueous PVP solution does not change when the pH is changed from 6.2 to 12.2.

In figure 3.2 we show the infrared spectra of PVP in dioxane and in deuterium oxyde (D$_2$O) in the range of 1400 to 2000 cm^{-1}. Both were recorded on a Hitachi EPI - G3 double beam spectrophotometer against pure solvent using cells with CaF$_2$ windows and adjustable pathlengths. A prominent feature is the strong absorption between 1640 and 1700 cm^{-1} due to the carbonyl group in the pyrrolidone ring. In dioxane we find this band at 1690 cm^{-1} whereas in D$_2$O the peak is situated at 1645 cm^{-1}. The reason for this difference is that in D$_2$O
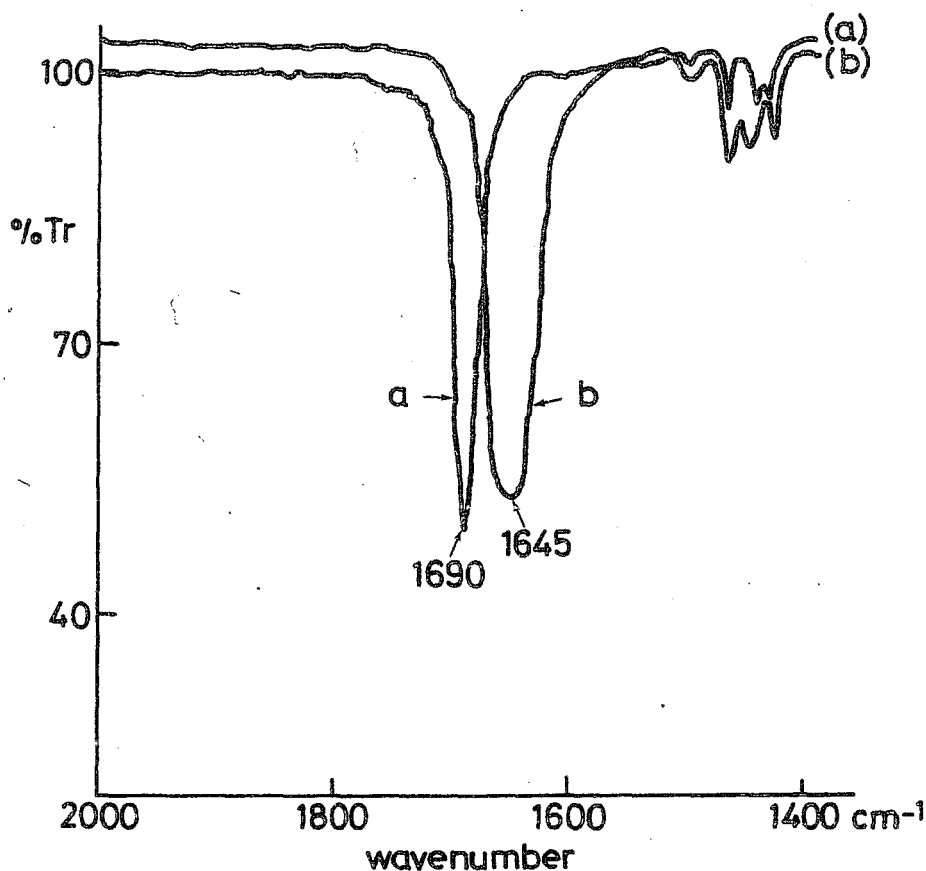
Fig. 3.2. Infrared spectra of PVP in the region 2000 cm^{-1} to 1400 cm^{-1}:
(a) in dioxane, (b) in D_2O. Concentration: 1 g dm^{-3}; pathlength 0.4 mm.

the carbonyl C = O bond is weakened due to hydrogen bonding between the carbonyl group and the deuterons of the solvent.

3.2.3 *Solubility and possibly ionic character*

Stable solutions up to high concentrations of PVP are easily formed in water as well as in many organic media such as alkohols, amines, acids, chloroform, amides and toluene. Traces of water may sometimes have a dramatic effect on the solutions in organic solvents, either stabilizing or destabilizing them. Destabilization by water is found in toluene (*Herrle*, 1965) dioxane and tetrahydrofurane (*Burchard*, 1967), whereas we found that a trace of water seems to be necessary for dissolution in chloroform.

It is known that the carbonyl group of the pyrrolidone ring is capable to bind protons strongly. Thus, hydrogen bonds are formed with many proton-donating

substances. Sometimes very stable complexes are formed, especially with polyacids such as PMAA (*Ohno et al.*, 1978). On the other hand, in aqueous solution strong complexes, with more hydrophobic compounds such as dyes or iodine are also formed. There is evidence that the bound molecules find themselves in hydrophobic apolar surroundings (*Takagishi et al.*, 1977). These observations suggests that the PVP chain has both hydrophilic and hydrophobic parts. In mixed solvents, there is a preference for the solvation with proton donating substances (*Chaufer et al.*, 1975).

Proton binding is not so strong, that PVP in aqueous solution acquires a charge. Electrophoretic measurements by *Sullivan et al.* (1952) demonstrated that PVP at pH 7 is uncharged. Only at extreme pH values (1; 13) the molecule carries some (positive or negative) charge. We conclude that between pH 4 and 10 charge effects on the adsorption from aqueous solution are of minor importance.

3.3 SOLUTION PROPERTIES OF PVP

As has been pointed out in section 2.1, the solvent quality plays an important role in the adsorption of polymers. The interaction between the polymer and the solvent is quantitatively expressed by means of the well-known Flory Huggins parameter χ, which was theoretically defined in section 2.3. Through simple thermodynamic relations, χ may be expressed in a number of measurable solution properties. In this section we review some of the expressions needed to derive χ from experimental data. We want to obtain values of χ for PVP in aqueous and dioxane solution, respectively, and we shall discuss the meaning of these values in the context of adsorption.

3.3.1 *Expressions to evaluate χ from experimental data*

In section 2.6 we mentioned already that for a polymer solution the excess free energy of mixing (with respect to the reference state of pure components) ΔG_m, can be quite generally shown to contain an important configurational entropy term, ΔS_m:

$$- \Delta S_m/k = n^o \ln \phi^o + n \ln \phi \qquad (2.21)$$

where, as before, n^o and n are the numbers of molecules of solvent and polymer, respectively, and ϕ^o and ϕ are the corresponding volume fractions.

Due to the interaction with the solvent ΔG_m may contain a number of other contributions, which we shall denote as the *residual* excess free energy of mixing, ΔG_m^R (*Orwoll*, 1977):

$$\Delta G_m^R = \Delta G_m + T \Delta S_m \tag{3.1}$$

Flory (1941) proposed a simple expression for ΔG_m^R on the basis of a quasi-crystalline solution model in which polymer segments and solvent molecules have equal size:

$$\Delta G_m^R / kT = n^o \phi \chi \tag{3.2}$$

According to this, χ has the meaning of a free energy, expressed in units kT. Inserting (3.2) and (2.21) into (3.1) and differentiating with respect to n^o we obtain

$$\chi \phi^2 = (\mu_1 - \mu_1^o)/RT - \ln(1-\phi) - (1 - \bar{v}_1^o/\bar{v}) \phi \tag{3.3}$$

where $\bar{v}^o$ and $\bar{v}$ are the molar volumes of solvent and polymer, respectively, and $\mu_1 - \mu_1^o$ is the excess chemical potential of the solvent with respect to the reference state. As the excess chemical potential is, in principle, measurable, equation (3.3) serves as a suitable experimental definition of χ.

Vapour pressure

The vapour pressure, over a polymer solution is determined by the (excess) chemical potential of the solvent according to (3.3). If the solvent vapour behaves as an ideal gas, we may express the chemical potential in the activity ratio P_s/P_o of the solvent vapour:

$$\mu_1 - \mu_1^o = RT \ln P_s/P_o \tag{3.4}$$

where P_s and P_o are the vapour pressures of the solution and the pure solvent, respectively, both at the same temperature T_o. Also, P_s may be expressed as the vapour pressure over pure solvent at a lower temperature T. If the temperature-pressure relationship for the solvent is known, P_s/P_o can be determined from temperature measurements. Since, at low ϕ_2, P_s/P_o must be close to unity, all terms in 3.3 become vanishingly small and χ cannot be determined with sufficient accuracy. Therefore, in practice vapour pressure measurements can only be used for concentrated solutions ($\phi > 0.05$).

Light scattering and osmotic pressure

Expansion of the logarithmic term in (3.3) and neglecting the molar volume ratio $\bar{v}^{o}/\bar{v}$ led *Flory* (1953) to the conclusion that the second virial coefficient of osmotic pressure, B_2, is related to χ:

$$B_2 = V_2^{\,2} \, (1/2 - \chi) \, / \, \bar{v}^{o} \tag{3.5}$$

Here, V_2 is the specific volume of the polymer in the solution. B_2 may be obtained both from light scattering experiments and from direct osmometry. Newer theories, discussed by *Yamakawa* (1971, p. 149), write B_2 as:

$$B_2 = V_2^{\,2} \, (1/2 - \chi) \, f \, \{M, \, (1/2 - \chi)\} \, / \, \bar{v}^{o} \tag{3.6}$$

where $f \, \{ M, \, (1/2 - \chi) \}$ is a slightly decreasing function of M and $(1/2 - \chi)$. At low M and small $(1/2 - \chi)$, f becomes equal to 1. From theoretical considerations (*Kurata et al.* 1958, *Zimm et al.*, 1953) it is concluded that a plot of B_2 against $\sqrt{M}$, extrapolated to zero molecular weight, leads to a correct χ value. Equation (3.6) was developed for dilute solutions and its validity is therefore limited. For high molecular weights, ϕ should not exceed 0.01.

Viscometry

Just as the *interaction* between two polymer coils (intermolecular interaction) can be described in terms of the interaction of segments in these coils (i.e. in terms of χ), the *size* of a given coil is determined by the interaction between parts of the *same* chain (intramolecular interaction); it is thus again a function of χ. Of course the coil size depends also on the length of the chain. Many theories have been proposed for the relationship between the intrinsic viscosity $[\eta]$, M and χ. The reader is referred to *Yamakawa* (1971) for a comprehensive review. Here we merely note that the results of these theories can all be expressed in two fundamental parameters, namely the molecular weight M, and the so-called excluded volume parameter Z. Therefore the general scheme is often denoted as the two-parameter theory.

Under conditions where random flight statistics are applicable (theta conditions), the mean square end-to-end distance $\langle h_o^{\,2} \rangle$, given by (2.7) can be written:

$$\langle h_o^{\,2} \rangle = 2 \, C \, l^2 \, M/M_o \tag{3.7}$$

where we used $m = 2 M/M_o$; M_o is the molecular weight of the monomer unit. Since C, 1 and M_o are all constants, $<h_o^2>/M$ is again a characteristic constant for a given polymer. It can be shown that $<h_o^2>$ is proportional to the mean square radius of gyration under theta conditions, $<s_o^2>$

$$<h_o^2> = 6 <s_o^2> \qquad (3.8)$$

Both $<h_o^2>$ and $<s_o^2>$ are measures for the radius of the unperturbed coil. Kirkwood and Riseman (1948) showed that the intrinsic viscosity in the theta solvent, $[\eta]_\theta$, is proportional to the *coil volume per segment*:

$$[\eta]_\theta = \Phi_o \frac{<h_o^2>^{3/2}}{M} = K_o M^{1/2} \qquad (3.9)$$

where Φ_o is a viscosity constant, and K_o is defined by

$$K_o = \Phi_o \frac{<h_o^2>^{3/2}}{M} \qquad (3.10)$$

Strictly, Φ_o, and thus K_o, are only constant if the draining behaviour of the coil is constant. For non-free draining coils, Φ_o has been calculated as 2.87×10^{23} mol^{-1}. Experimentally, a well-established value is between 2.5 and 2.6×10^{23} mol^{-1} (*Yamakawa*, 1971, section 3.9).

If the polymer coil is in a better solvent, the effects of self-exclusion cause the chain to expand (cf. section 2.3). The departure from random flight, or *unperturbed* dimensions is given by an expansion factor, e.g.

$$<h^2> = \alpha_h^2 <h_o^2> \qquad (3.11a)$$

$$<s^2> = \alpha_s^2 <s_o^2> \qquad (3.11b)$$

Here, $<h^2>$ and $<s^2>$ are the mean square end-to-end distance and radius of gyration, respectively, and α_h and α_s are the corresponding expansion coefficients. In a similar way, the expansion of the hydrodynamically effective coil radius can be described by means of an expansion factor α_η. The intrinsic viscosity $[\eta]$, being proportional to the hydrodynamic volume of the coil, see (3.9), should thus expand as:

$$[\eta] = \alpha_\eta^3 [\eta]_\theta \qquad (3.12)$$

The two parameter theory expresses all these expansion coefficients as a function of the *excluded volume parameter* z, a dimensionless quantity defined by:

$$z = \frac{4}{3^{3/2}} \; C_M \; (1/2 - \chi) \; M^{1/2} \tag{3.13}$$

where C_M is a constant:

$$C_M = 0.857 \; \frac{v_2^2}{\bar{v}^o \; N_{av}} \; \left[\frac{<h_o^2>}{M} \right]^{-3/2} \tag{3.14}$$

(*Yamakawa*, 1971, p. 157 and 71, resp.); N_{av} is Avogadro's number. As can be seen, z contains both the polymer-solvent interaction (through χ) and M. For a theta solvent, $\chi = 0.5$ and $z = 0$.

Flory's original approach did not differentiate between α_h, α_s, and α_η. The well-known Flory equation reads for all three expansion coefficients, denoted as α:

$$\alpha^5 - \alpha^3 = 2 \; C_M \; (1/2 - \chi) \; M^{1/2} = \frac{3^{3/2}}{2} \; z \tag{3.15}$$

The Flory-Fox-Schaefgen (FFS) equation (*Flory* and *Fox*, 1951) is obtained from (3.9), together with (3.10), (3.12) and (3.15):

$$[\eta]^{2/3} / M^{1/3} = K_o^{2/3} + 2 \; C_M \; (1/2 - \chi) \; K_o^{5/3} \; M / [\eta] \tag{3.16}$$

Kurata (1958) and *Yamakawa* (1958) were the first to emphasize the differences between α_η and other expansion coefficients. The expansion coefficients can be written as a power series in z. For α_h and α_s they find

$$\alpha_h^2 = 1 + 1.333 \; z - 2.075 \; z^2 + \ldots \tag{3.17}$$

$$\alpha_s^2 = 1 + 1.276 \; z - 2.082 \; z^2 + \ldots \tag{3.18}$$

The hydrodynamic expansion coefficient is expressed in the following series:

$$\alpha_\eta^3 = 1 + 1.55 \; z - \tag{3.19}$$

(*Yamakawa*, 1971, p. 301).

Burchard (1961), and later Stockmayer and Fixman (1963) realized that
eq. (3.19) provided a basis for an expression for $[\eta]$. Combining (3.19) with
(3.9) and (3.12), this Stockmayer-Fixman (SF) equation is found to be:

$$[\eta] = K_o M^{1/2} \{ 1 + 1.55 K_o z / M^{1/2} \} \qquad (3.20)$$

According to this equation, a plot of $[\eta]/M^{1/2}$ against $M^{-1/2}$ should give a
straight line from the slope of which χ can be evaluated with the help of (3.13).
In the neighborhood of the theta temperature (small z) the series of (3.19)
converges to $\alpha_s^{2.43}$. In a discussion of experimental results, Yamakawa (1971,
p. 384) shows that at small z, α_η^3 is found to be smaller than $\alpha_s^{2.43}$. Therefore,
the coefficient of z in (3.19) should also be smaller than 1.55. A best fit of
the experimental results is obtained with

$$\alpha_\eta^3 = 1 + 1.05 z \qquad (3.21)$$

for values of $\alpha_\eta^3 < 1.6$ which implies a power law

$$\alpha_\eta^3 = \alpha_s^{1.65} \qquad (3.22)$$

The numerical constant in (3.20) is thus also somewhat uncertain, and this affects
the reliability of the χ-value derived from the slope of the SF plot.

3.3.2 PVP in aqueous solutions

Aqueous PVP solutions have been extensively investigated. Therefore we derive
χ-values entirely from data in the literature. Molyneux (1975) collected a large
number of data about aqueous solutions of synthetic polymers, including PVP.
He calculated χ from vapour pressure measurements by Dole and Faller (1950).
However, at lower water content these data, with eq. 3.3, would lead to strongly
negative χ-values. Molyneux assumed that this was due to the presence of strongly
hydrophylic impurities in the polymer sample. He estimated the amount of water
bound by these impurities and subtracted it from the total amount of water taken
up by the polymer. From the thus corrected data he calculated new χ-values
according to eq. (3.3) over the concentration range $0.5 < \phi < 1$. From the re-
sults, it seems that in the region $\phi = 0.6 - 0.9$, χ is slightly higher, than
0.5, and rises with decreasing water content. At polymer weight fractions higher
than 0.9 the results become less reliable due to uncertainties in the applied
correction. Measurements by Mc Kenzie et al. (1971) at 22° C and of Tadokoro
et al. (1965) agree rather well with those of Dole and Faller, provided that

the same correction is applied. *Tadokoro et al.* report that the solvent uptake at low, fixed vapour pressure increases with temperature within the range + 30°C to + 50°C. This is indicative of endothermic mixing. *Mc Kenzie et al.* found increasing sorption with decreasing temperature in the temperature range - 40°C to + 22°C, indicating that the mixing is exothermic at low temperatures. *Breitenbach et al.* (1954) studied swelling equilibria at polymer volume fractions of about 0.06. In the temperature range of 20°C to 70°C, the mixing was found to be exothermic, in contrast to the results of Tadokoro. This finding is confirmed by osmotic measurements by *Vink* (1971). The transition from endothermic to exothermic mixing seems to occur at a water activity ratio P_s/P_o of 0.5, corresponding roughly to a 1 : 1 (water: monomer unit) ratio. To explain this, Molyneux suggests that bridging of water molecules between neighbouring carbonyl groups occurs at the lower activities.

Vink (1971) measured osmotic pressures of aqueous PVP solutions in the concentration range $0.03 < \phi < 0.3$. From his data χ values can be derived increasing from 0.480 at low ϕ, to about 0.54 at the highest concentration.

Burchard (1967) derived second virial coefficients from light scattering data obtained with dilute solutions. He plotted B_2 as a function of $M^{1/2}$. In contrast to what is to be expected from eq. (3.6) this plot deviates strongly from a straight line. At low M, an upward bend is found which makes extrapolation to M = O somewhat unreliable. Nevertheless, χ was estimated from B_2 to be equal to 0.465 ± 0.003, which is considerably lower than Vink's value of 0.480. The light scattering data also show that PVP in aqueous solution tends to form associates, especially at the higher molecular weights. Burchard concludes that dilute PVP solutions in water are anomalous to some extent and cannot completely be described by the two parameter theory.

Burchard presents also a SF plot of viscometric results. The intercept of such a plot is equal to K_o, and the slope should according to (3.20) be equal to $1.55\ K_o\ z/M^{1/2}$. As has been discussed above, the coefficients of z in (3.20) should probably be lower than 1.55. This is consistent with Burchard's results for PVP in a number of different theta solvents. Comparing expansion factors α_s determined by light scattering for the radii of gyration with viscometric expansion factors, he finds:

$$\alpha_\eta^3 = \alpha_s^{1.90 \pm 0.15} \qquad\qquad (3.23)$$

which implies, for low z, a coefficient of 1.21 ± 0.10 in (3.19) and (3.20). Furthermore it was found by Burchard that unperturbed dimensions as determined

from light scattering agreed reasonably well with those from viscometry.
Therefore we assume that the constant Φ_o, reflecting the draining behaviour of
PVP in water, is not much different from the often found value of 2.5×10^{23}
mol^{-1}. Using these results, together with the following values: $V_2 = 0.785$
$cm^3 \ g^{-1}$ (*Brandrup* and *Immergut*, 1975), $\bar{v}^o = 18 \ cm^3 \ mol^{-1}$ and $N_{av} = 6.02 \times 10^{23}$
mol^{-1} we find from the SF plot $\chi = 0.489$ (Burchard did not calculate χ-values).

We also plotted Burchard's result according to the FFS equation (3.16),
see fig. 3.3. From this plot we find, with the same values of the parameters,
$\chi = 0.488$.
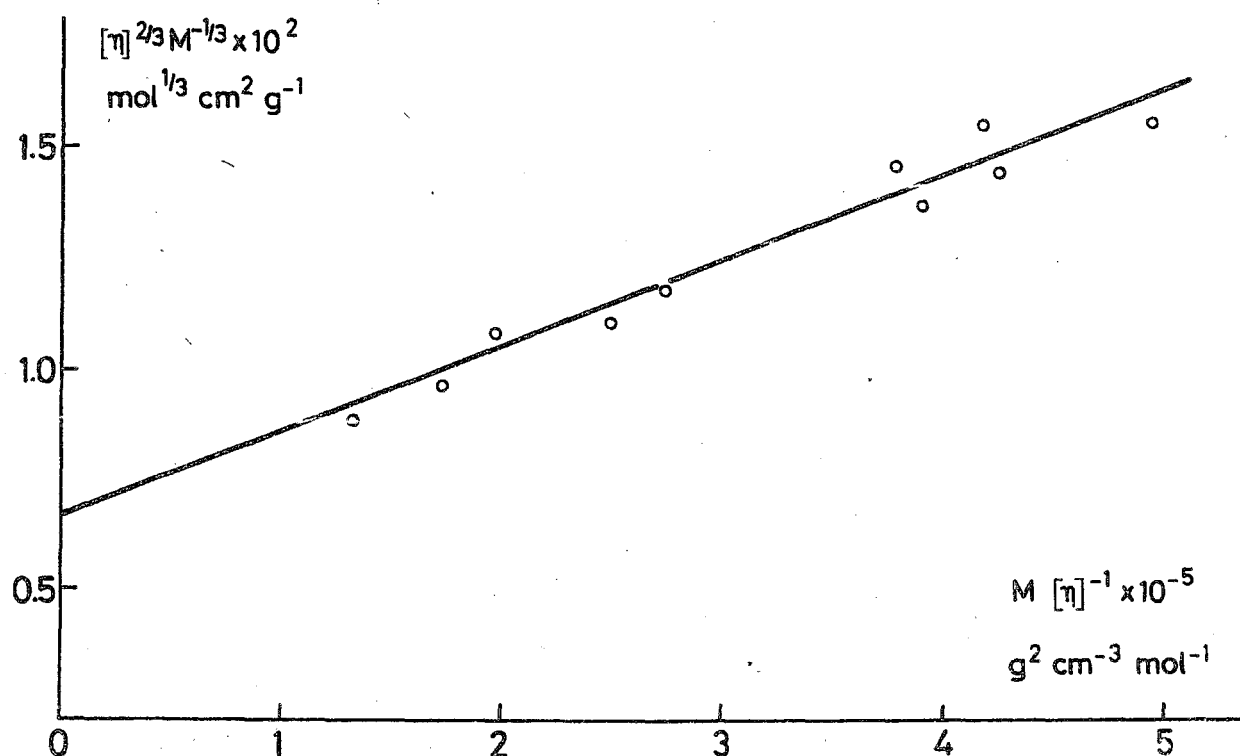
Fig. 3.3. Flory-Fox-Schaefgen plot of viscometric data from *Burchard* (1967)
for PVP in aqueous solution.

The results of *Dole* and *Faller*, *Mc Kenzie et al.* and *Vink* for the concen-
trated and semi dilute solution and those of Burchard for the dilute solution
are summarized in fig. 3.4.
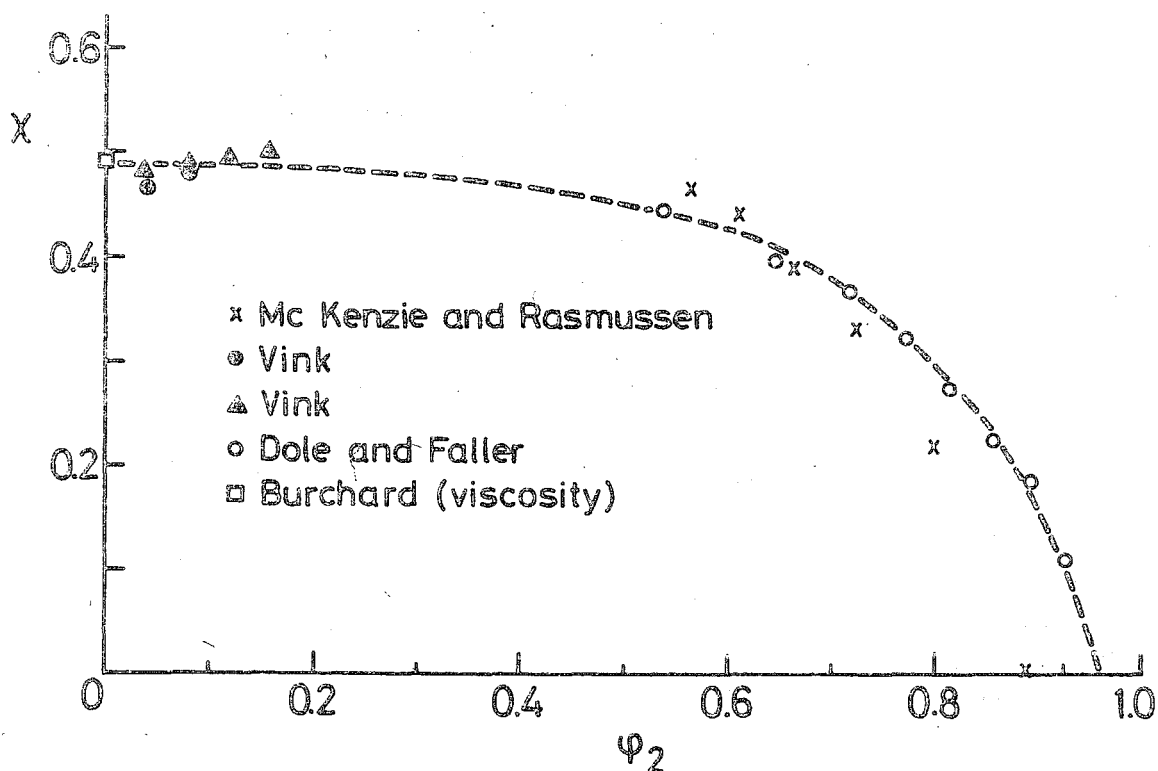
Fig. 3.4. Values of the interaction parameter (χ) as a function of PVP concentration, in aqueous solution. Data were obtained from *Mc Kenzie* and *Rasmussen* (1971), *Vink* (1971), *Dole* and *Faller* (1950) and *Burchard* (1967).

The correction applied by Molyneux was omitted because its justification is open to doubt. As can be seen, χ is slightly below 0.5 in the dilute solution and increases slightly with ϕ. Between $\phi = 0.15$ and $\phi = 0.5$ we have no results but at $\phi = 0.5$ χ is about 0.45. By interpolation one might expect χ to be around 0.5 in the range $\phi = 0.15$ to 0.5. At higher ϕ, χ decreases and eventually becomes negative. Rather than ascribing this behaviour to hydrophilic impurities we believe that PVP itself, at these high volume fractions, binds water strongly. The description of the 'solution' in this region by ordinary Flory-Huggins theory is probably not accurate enough.

3.3.3 PVP in dioxane solution

For PVP in dioxane, the only available data were reported by *Burchard* (1967), for the dilute solution. This author employed both light scattering and viscometry and concluded that the behaviour of PVP in dioxane can be readily described by the two-parameter theory. A theta temperature of $-10^{\circ}C$ is found, and at $20^{\circ}C$ the expansion of the molecule can be described by a value of $z/M^{1/2}$ of about 6.5×10^{-4}. The temperature dependence of z, and thus of $(1/2 - \chi)$,

satifies the relation $z = z_o (1 - \frac{\Theta}{T})$, where z_o is the volume of z at infinitely high temperature, and Θ is the theta temperature. From Burchard's results, $z_o/M^{1/2} = 6.42 \cdot 10^{-3}$ is obtained.

The Flory-Huggins expression (3.5) for the second virial coefficient leads to $\chi = 0.481 \pm 0.001$. Burchard gave also a SF plot. Using $V_2 = 0.78 \ cm^3 \ g^{-1}$, $\overline{v}^o = 85.24 \ cm^3 \ mol^{-1}$, $\Phi_o = 2.5 \ x \ 10^{23} \ mol^{-1}$ and a coefficient of 1.2 instead of 1.55 in eq. (3.22) we derived $\chi = 0.491$ from the slope and intercept of this plot. We made a FFS plot from the same data and found, with the same parameters, $\chi = 0.494$ (fig. 3.5).
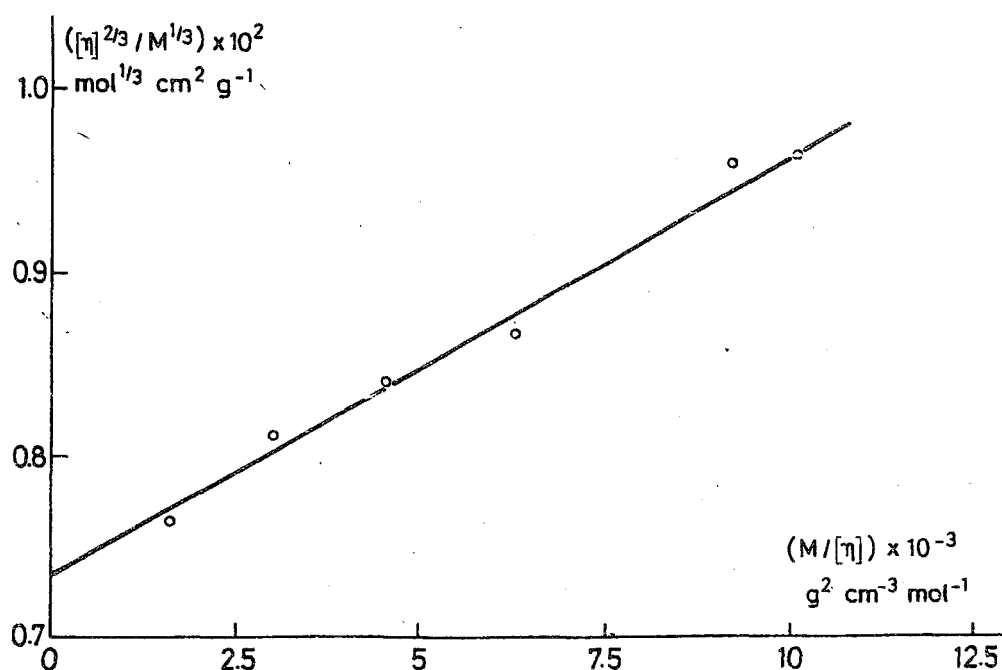
Fig. 3.5. Flory-Fox-Schaefgen plot of viscometric data from *Burchard* (1967) for PVP in dioxane solution.

Sometimes, χ is split up into a temperature dependent χ_H and a part χ_S, independent of T:

$$\chi = \chi_S + \chi_H \qquad (3.24)$$

It can be calculated from the temperature dependence of χ, that at $20^o C$ χ_S is 0.441 and χ_H is only 0.053. Thus χ is mainly entropic at this temperature. *Burchard* found also, that by adding small amounts of water the solvent becomes

poorer, as if the effective χ increases. At 20°C, a mixture of 95% dioxane and 5% water behaves as a theta-solvent. Addition of more water causes phase separation. In order to maintain a constant solvent quality it is thus important to rigoroulsy avoid contamination of the solutions with water.

In the semi-dilute and concentrated regime, data for χ are not available. We carried out vapour pressure measurements using an apparatus designed and tested by *Weldring et al.* (1975). It consists of a double-walled vertically mounted glass cylinder, about 90 cm high and with 6 cm inner diameter. Between the inner and outer wall, water of constant temperature is circulated. The cylinder can be evacuated to very low pressure. Vapour of a known activity may be introduced by connecting the column to a vessel containing a suitable solution of pure solvent kept at a suitable temperature. The temperature of this vessel can be regulated between -5°C and $+30^{\circ}$C. Dioxane vapour activity was controlled by means of temperature regulation. The activity ratio P_1/P_2 between the vapour pressure over pure dioxane at temperature T_1 and at T_2, respectively, can be calculated from the empirical expression (*Gallaugher* and *Hilbert*, 1937).

$$\log P_1/P_2 = -1866.7 \ (1/T_1 - 1/T_2) \tag{3.25}$$

The uptake of solvent by the polymer is measured gravimetrically. The polymer sample is placed on a small pan, suspended on a quartz spring with known force-elongation characteristics. The position of the pan, which is a function of its weight, is measured with a kathetometer. In fig. 3.6 the solvent uptake at 20°C is plotted as a function of the activity ratio P_s/P_o for two samples, Kollidon 25 and Kollidon 90. The theoretical curve, corresponding to $\chi = 1/2$ is drawn in the same figure. The lines indicated 1 correspond to the first dissolution curve, starting from dry PVP. Curves 2 are obtained on lowering the activity of dioxane and curves 3 were found upon increasing the activities again.

It is seen that dry PVP does not take up appreciable amounts of dioxane until P_s/P_o is higher than 0.9. At this point the solvent becomes able to break the strong polar bonds that hold the segments together, and the uptake of solvent increases steeply. A very viscous solution is formed. Clearly, lines 1 do not represent equilibrium states, for the lines 2, obtained upon decreasing the vapour pressure show much higher solvent contents in the polymer. If P_s/P_o is again increased, line 3 is found, which is only slightly lower than the desorption line 2.

Since the points obtained upon lowering and upon raising P_s/P_o do not constitute a single curve, we cannot conclude that they correspond to equilibrium
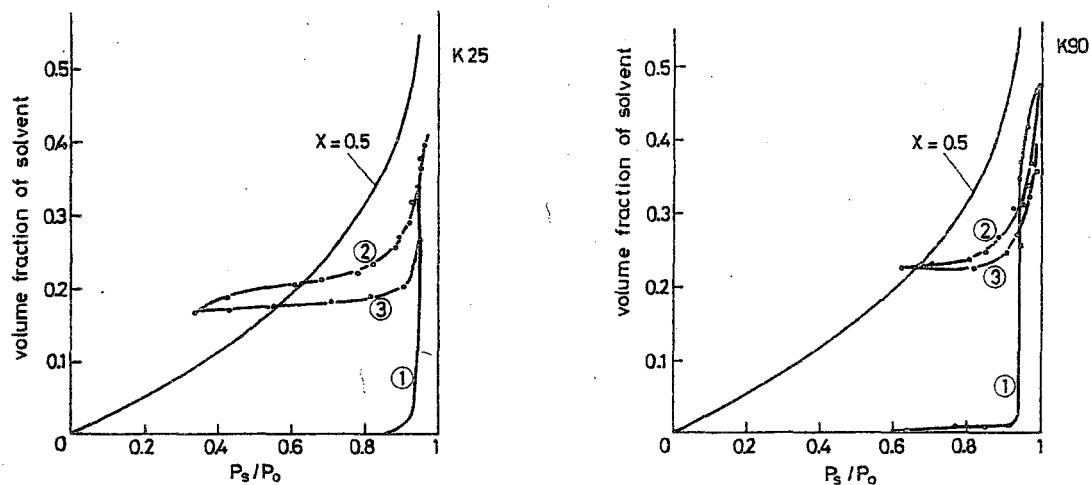
Fig. 3.6. Composition of polymer solution as a function of solvent vapour pressure, for PVP in dioxane at 20°C, left: K_{25}, right: K_{90}

situations. Also, long times of about one week or more were required to reach a steady value for the solvent uptake. Probably, diffusion in the highly viscous, concentrated solution is too slow. The results with Kollidon 25 are less reliable because the vacuum could not be properly maintained during the complete experiment. Therefore we believe fig. 3.6 b to represent the best result. Here, curves 2 and 3 do not differ too much, and it seems possible that in going from curve 2 to curve 3, somewhere an equilibrium line is crossed. We tentatively assume that the equilibrium curve lies between curve 2 and 3 in fig. 3.6 b. Unfortunately, it was not possible to reduce the dioxane vapour pressure sufficiently to return to the dry solid PVP. However, both figures 3.6 show the surprising fact that the sorption curves 2 and 3 cross the theoretical line for $\chi = 1/2$ at an activity ratio of about 0.6. This would mean that at low activities, χ becomes low, may be even negative. A correction, as applied by Molyneux to data for the aqueous PVP solution (Molyneux, 1975, chapter 7) could possibly modify the data, such that χ becomes a monotonously increasing function of concentration. However, as stated before, such a correction is somewhat doubtful as long as the causes for an unexpected solvent uptake curve are insufficiently studied. Therefore we omitted such a correction and calculated χ-values from the vapour pressure results by means of eq. (3.3).

In fig. 3.7 we have summarized the obtained χ-values together with the results of Burchard for the dilute solution. In the range between the very dilute solution $\phi \simeq 0$ and $\phi = 0.5$ we have estimated χ-values by means of

interpolation (broken line). Probably, χ increases monotonously with ϕ from about 0.49 at $\phi=0$ to a maximum of 0.9 at $\phi \simeq 0.7$. At higher ϕ, χ decreases steeply. Whether this decrease must be ascribed to poor equilibration during the measurements or to the presence of impurities in the PVP samples cannot be concluded from the present results.

Fig. 3.7. χ-values for PVP in dioxane from vapour pressure measurements and from viscometry, as a function of concentration. Viscometric data were taken from *Burchard* (1967).

3.3.4 *The meaning of experimentally determined χ-values in adsorption theory*
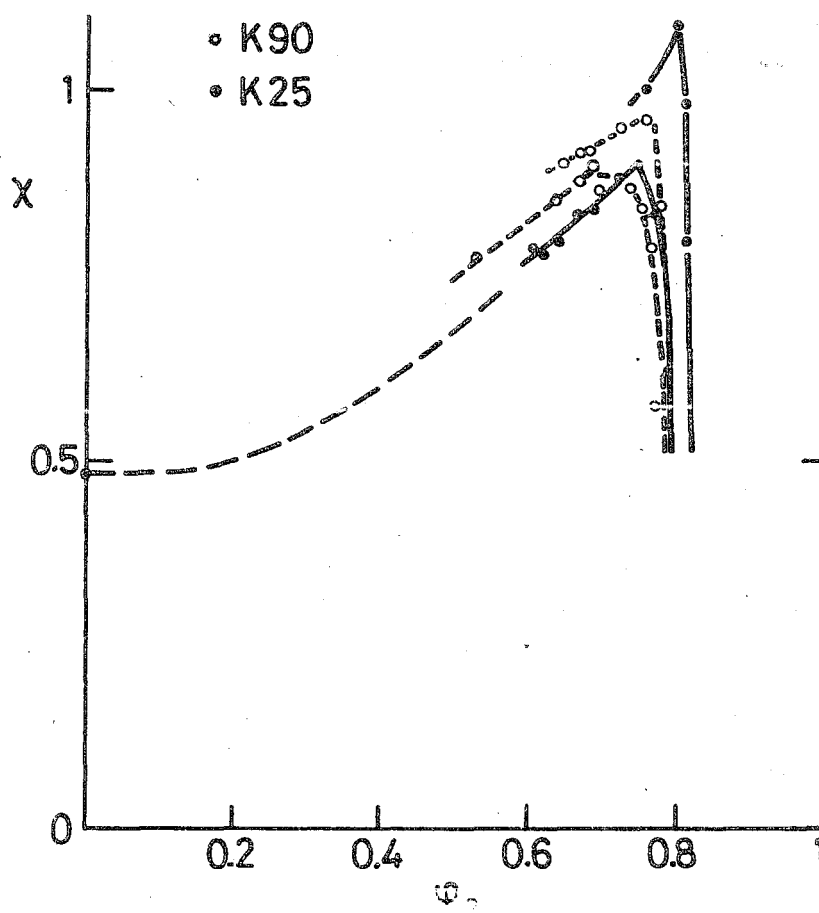
In the treatment outlined in 3.3.1 the χ parameter was regarded as a constant for a given polymer-solvent pair. It should be independent of the polymer concentration. But from the results discussed in 3.3.2 and 3.3.3 (fig. 3.4 and 3.7, respectively) it is obvious that the experimentally determined value of χ varies considerably with concentration.

This means that a detailed description of the solution is more complicated than eq. (3.2) suggests. A more sophisticated description should include, e.g., differences in size between segments and solvent molecules, effects of non-random mixing and changes in orientational freedom of segments and solvent molecules with concentration. Detailed theories incorporating these effects have been formulated by *Flory* (1964, 1965, 1970), *Huggins* (1971) and *Maron* (1959). Such corrections lead possibly to satisfying results for a number of polymer-solvent pairs, but the treatment of aqueous solutions, where strong solvation and hydrophobic effects may occur within the same molecule seems to be even more complicated.

A second unexplained fact is that in dilute solutions almost all χ-values are found in a narrow range ($0.4 < \chi < 0.5$), although from a theoretical point of view one would expect that for a wide range of different polymers χ may assume all kinds of values between, e.g., $- 0.5$ and $+ 0.5$. Parallel to this is the finding that the two parameter theory for dilute solutions, in spite of considerable successes is unable to explain why z-values derived from reasonable estimates of the dimensions of polymer segments are always much larger than those experimentally found. *Yamakawa*, in his book, prefers to adopt z as a basic parameter formally representing the interactions between segments. He does not attempt to relate it to molecular parameters (chapter III, section 17). Following this, we prefer to regard χ as the residual excess free energy of mixing per solvent molecule (eq. 3.3). Then it can be defined unambiguously in terms of experimental data, and it accounts for all free energy contributions which are not included in eq. (2.20). (*Orwoll*, 1977).

We may ask what the meaning is of the χ parameter defined in this way, in the context of adsorption theory. From the theoretical treatments presented in chapter 2, it is clear that in the case of adsorption *changes in conformation* make an important contribution to the change in free energy. In addition to these contributions, we have the free energy of mixing. For the calculation of this mixing contribution (which is entirely based on χ) we imagine the adsorbed layer - with its density gradient perpendicular to the surface - as being built up from thin layers of constant segment density parallel to the wall. For each of these layers the mixing term is calculated from the number of

polymer-solvent contacts.

In order to incorporate the experimental concentration dependent value of χ in this model it is thus necessary to assume that the mixing properties in a density gradient consisting of a number of such layers can be described by an equal number of χ parameters, each of which is measured in a macroscopic, isotropic solution of the same segment density as that in the corresponding thin layer. This implies that χ should be independent of the dimensions of the region to which it is applied. It can only be safely used if it is uniquely related to local segment-solvent interactions with a range comparable to the thickness of an elementary model layer.

We conclude that the use of experimental χ-values is not justified if χ contains contributions due to, e.g., conformation changes, involving the polymer molecule as a whole. Therefore replacement of the theoretical χ by the experimental function $\chi(\phi)$ requires that we assume that such contributions are negligible.

3.3.5 *The characteristic ratio for the end-to-end distance*

Flory (1969) defined the characteristic ratio C for the end-to-end distance, eq. (2.7) as:

$$C = \frac{\langle h_o^2 \rangle}{m\, l^2}$$

For PVP, this value can be deduced from the data of *Burchard* (1967). In three different theta solvents, namely H_2O/acetone (28:72), EtOH/hexane (25:75) and Methylglycol - dibutylether (49:51) and at $20^{\circ}C$ the mean square radius of gyration was measured as $(9.7 \pm 0.4)\,10^2$ nm^2. With $l = 0.154$ nm for the carbon-carbon covalent band, this leads to $C = 10.3 \pm 0.1$. This is a value comparable to that of other atactic vinyl chains, such as 10.0 for polystyrene (*Flory*, 1969).

In a number of other theta solvents, namely dioxane ($- 10^{\circ}C$), H_2O/dioxane (26:74), H_2O/tetrahydrofuran (45:55) and tetrahydrofurane ($- 10^{\circ}C$) it was found that $\langle s_o^2 \rangle = 6.7\,10^2$ nm^2. Consequently, $C = 7.1$ in these solvents. The difference of about 30% between both groups of solvents is not easily explained; it seems to indicate that the PVP molecules are more flexible in the latter four solvents.

3.4 MOLECULAR WEIGHT AND MOLECULAR WEIGHT DISTRIBUTION

Many experimental and theoretical studies have revealed the importance of the chain length on the adsorption behaviour of polymers. Therefore a thorough study requires the use of well defined samples with a narrow molecular weight distribution. However, the direct synthesis of such PVP samples has not been described and seems beyond the present possibilities so that a fractionation technique must be invoked.

Also, it may be interesting to study the effect of the molecular weight distribution on the adsorption. Since we did both kinds of experiments (chapter 4) we describe here the characterization of commercial samples with a wide molecular weight distribution, and of the fractions obtained from them.

3.4.1 *Samples with broad molecular weight distributions*

Five commercial PVP-samples, manufactured by BASF (BRD) were used in this study. We measured their molecular weights by viscometry in aqueous solutions. A Fica Viscomatic automatic viscometer was used to determine flow times at six different concentrations. The temperature was $20^{\circ} \pm 0.005 \,^{\circ}C$. Between different polymer samples the temperature variation was less than $0.01 \,^{\circ}C$. Intrinsic viscosities $[\eta]$, were calculated according to *Huggins* equation:

$$\eta_{sp}/c = [\eta] + [\eta]^2 k_H c \qquad (3.26)$$

The relation between M and $[\eta]$ is given by the well known *Mark-Houwink-Sakurada* (MHS) equation:

$$[\eta] = K M^a \qquad (3.27)$$

where, for polydisperse samples, M must be replaced by the viscosity averaged molecular weight M_v. The constants K and a have to be determined empirically with the help of a suitable calibration technique. A number of values has been determined by various authors; those given by *Frank* and *Levy* (1955) are the most widely used. However we prefer to adopt K and a values given by *Burchard* (1967) for mainly two reasons.

First, *Frank* and *Levy* used light scattering for the calibration. As has been convincingly shown by Burchard, PVP molecules in aqueous solution associate to some extent, leading to curved Zimm-plots. If this is not recognized, evaluation of the data leads to an overestimate of the molecular mass, especially at high M. Burchard avoided this complication by recalibrating his samples in

ethanol, where association phenomena are absent. He showed also that by a suitable correction the light scattering results in water can be brought into perfect agreement with those in ethanol.

Second, Frank and Levy were mislead by the reasonable agreement between their calibration results in water and in chloroform. In chloroform, which is rarely completely free of water, strong preferential solvation by water may occur, leading to higher apparent molecular weights. Such preferential solvation has been studied in the binary solvent cloroform/ethanol (*Chaufer et al.*, 1975) and may be even more pronounced in the case of chloroform/water. Frank and Levy also published MHS constants for PVP in methanol. Because in methanol, as in ethanol, neither preferential solvation nor association phenomena may be expected to play a role, agreement with Burchard's results for this solvent may be expected and is indeed found.

Burchard's MHS relation for PVP in water is:

$$[\eta] = 1.26 \ 10^{-5} \ M_V^{0.7} \tag{3.28a}$$

The MHS equation (3.27) implies a linear relationship between log $[\eta]$ and log M with a single slope a. However, experimentally one finds that in good solvents a deviation from the linear relation log $[\eta]$ = a log M occurs at low M. Another linear relationship is then found, which a slope which is always nearly equal to 0.5, irrespective of the slope in the range of high M (*Bianchi* and *Peterlin*, 1968). This is obviously due to the fact that the dimensions of small coils are hardly affected by the nature of the solvent. Bianchi and Peterlin investigated some 10 low molecular weight polymers and concluded that $[\eta]$ in good solvents must gradually approach $[\eta]_\theta$ in the limit of small M. The remaining question is at what molecular weight the transition from one power law to the other occurs. This is determined by the fact that the first linear part of the log $[\eta]$/log M curve should have the intercept K_o (see fig. 3.8). Values for K_o in various theta solvents have been reported in the literature. *Burchard* (1967) gives a value of 8.27 10^{-5} dm^3 g$^{-3/2}$ mol$^{1/2}$ at 20°C in H$_2$O/acetone (28:72) whereas *Elias* (1961) finds 7.5 x 10^{-5} dm^3 g$^{-3/2}$ mol$^{1/2}$ at 25 in H$_2$O/acetone (33.2:66.8). In water, a K_o value of 8,2 x 10^{-5} (same units) is found from Burchard's SF plot. We shall therefore use Burchard's value 8.27 x 10^{-5} also in pure water (20°C).

From the intercepts and slopes of the two linear parts of the log $[\eta]$/log M curve the point of intersection is easily found. The result is M = 12180. Therefore we choose for the MHS equations in water at 20°C

$$M \geq 12000 \quad [\eta] = 1.26 \ 10^{-5} \ M_V^{0.7} \tag{3.28a}$$

$$M \leq 12000 \quad [\eta] = 8.27 \ 10^{-5} \ M_V^{0.5} \tag{3.28b}$$

log[η]

slope 0.5

K_o

K

0

log M
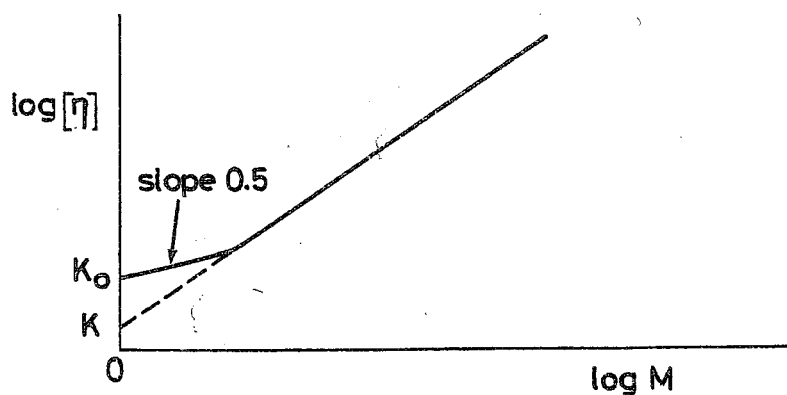
Fig. 3.8. Schematic representation of log [η]/log M plot, showing K_o and K.

Viscosity averaged molecular weights for each of the samples K_{12}, K_{17}, K_{25}, K_{30} and K_{90} were calculated according to (3.28) and the results are summarized in table 3.2.

Table 3.2. Intrinsic viscosities and average molecular weight of commercial PVP samples

SAMPLE CODE	[η] x 10^-3 dm^3 g^{-1}	M_v a) g mol^{-1}	M_n b) g mol^{-1}	M_w b) g mol^{-1}	M_v c) g mol^{-1}	M_v/M_n
K_{12}	4.957	3590	1700	3200	2850	2
K_{17}	7.791	8875				
K_{25}	16.40	28100	9400	17400	16000	3
K_{30}	22.15	43200				
K_{90}	160.4	731000	178000	933000	670000	4,5

a) Viscosity averaged molecular weight calculated from the intrinsic vicsocity according to eqn. (3.28).

b) Average molecular weight calculated from the GPC results.

c) Viscosity averaged molecular weight calculated from the GPC results, assuming for the GPC solvent Mark Houwink exponents of 0.61 for M > 12000 and 0.5 for M < 12000 (eq. 3.32a and 3.32b, respectively).

Gel permeation chromatography (GPC) is at present the best technique for studying the molecular weight distribution. Distribution curves, obtained by GPC were provided by the manufacturer. Unfortunately, these distributions did not agree with the viscosity averaged molecular weights, probably because they belonged to polymer samples different from those employed in the present study. Therefore the samples K_{12}, K_{25} and K_{90} were analyzed by GPC at AKZO Research Laboratories[*]. The instrument used was a Waters Associate Gel Permeation Chromatograph, operated with a chloroform/ethanol (98:2) mixture at 25°C as the solvent, and Staragel (Waters Associate) as the stationary phase. For the calibration, a relation between the molecular weight and the elution volume must be known, which can be done using well-defined narrow PVP fractions. However, such fractions were not available and therefore polystyrene (PS) calibration standards were used. In this case an extra relation between the molecular weights of PVP and PS at the same elution volume has to be found. A commonly used procedure (*Coll* and *Gildings*, 1970; *Doi*, 1975; *Dawkins*, 1972) to find such a relation is the following.

It is assumed that polymer molecules with equal hydrodynamic volumes are eluted at the same elution volume, irrespective of their chemical nature. These hydrodynamic volumes V_H are found from Einstein's law:

$$V_H / K_H = [\eta]_{cal} M_{cal} = [\eta]_x M_x \qquad (3.29)$$

where K_H is a hydrodynamic constant, $[\eta]$ the intrinsic viscosity and M the molecular weight. Indices cal and x refer to the calibration standard (PS) and the unknown sample (PVP), respectively. The intrinsic viscosity is related to M through the MHS equation (3.27). Inserting this equation into (3.29) with K_{cal} and a_{cal} as the MHS constants for the calibration standard and K_x and a_x for the unknown we obtain:

$$\log M_x = \frac{a_{cal} + 1}{a_x + 1} \log M_{cal} + \frac{\log K_{cal}/K_x}{a_x + 1} \qquad (3.30)$$

For the polystyrene standards in chloroform/ethanol (98:2) the following MHS constants were used ($[\eta]$ in $dm^3 g^{-1}$) (*Goedhart*, 1978):

$$M \geq 15,000 \quad [\eta] = 1.536 \times 10^{-5} M^{0.7075} \qquad (3.31a)$$

$$M \leq 15,000 \quad [\eta] = 11.08 \times 10^{-5} M^{0.502} \qquad (3.31b)$$

[*] We gratefully acknowledge the cooperation of Dr. D.J. Goedhart who performed the GPC analysis and calibrated the results.

As has been pointed out above, two pairs of MHS constants are needed to describe the intrinsic viscosity in good solvents down to low molecular weights. For PVP in the chloroform/ethanol (98:2) mixture the constants of the MHS equation have not been measured. However, both *Burchard* and *Frank* and *Levy* find that chloroform is a moderately good solvent for PVP. Addition of a little ethanol to the solvent leads probably to some preferential solvation (*Chaufer et al.*, 1975) and perhaps to some expansion of the coil. Assuming this expansion to be negligible we use results for PVP in chloroform. For reasons discussed above, we regard Burchard's results as the most reliable ($[\eta]$ in $dm^3\ g^{-1}$):

$$[\eta] = 4.2 \quad 10^{-5} \quad M^{0.61} \tag{3.32a}$$

This equation applies only for high molecular weights. As shown above we can include the low molecular weight range by setting the MHS exponent equal to 0.5. In order to calculate the complete MHS equation for low molecular weight PVP in chloroform, we arbitrarily put the validity limit at M = 15.000. The resulting equation reads:

$$M \leq 15,000 \quad [\eta] \quad = \quad 12.10 \times 10^{-5}\ M^{0.5} \tag{3.32b}$$

From eq. 3.31 and 3.32 we see that for $M \geq 15,000$

$$a_{cal} = 0.7075 \qquad K_{cal} = 1.536 \quad 10^{-5}$$
$$a_x \quad = 0.61 \qquad K_x \quad = 4.2 \quad 10^{-5}.$$

whereas for $M \leq 15,000$

$$a_{cal} = 0.502 \qquad K_{cal} = 11.08 \quad 10^{-5}$$
$$a_x \quad = 0.5 \qquad K_x \quad = 12.10 \quad 10^{-5}$$

With these constants, the molecular weight distribution curves were calculated. The curves are drawn in fig. 3.9. From the curves, number averaged, weight averaged and viscosity averaged molecular weights can be calculated through well known equations. These values are tabulated in table 3.2.
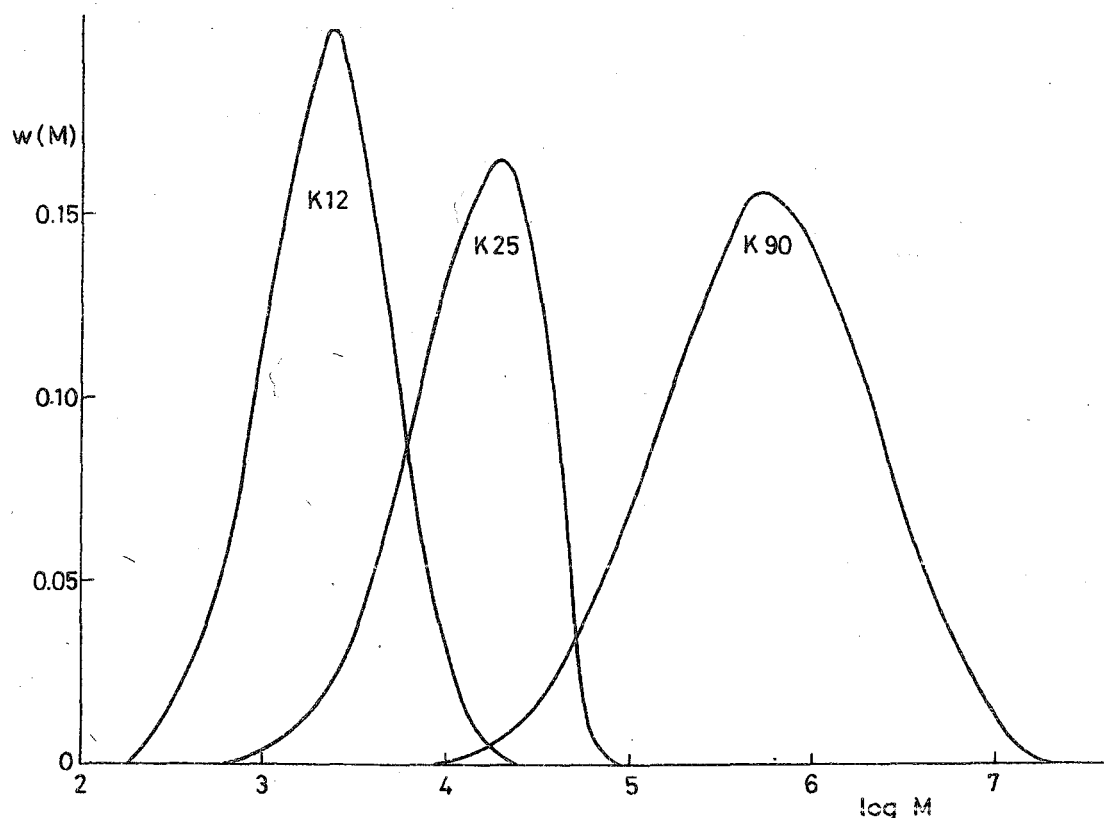
Fig. 3.9. Weight distribution curves for commercial PVP samples (K_{12}, K_{25} and K_{90}, BASF, BRD) as determined by Gel Permeation Chromatography (D.J. Goedhart, AKZO Research Laboratories, Arnhem, The Netherlands).

3.4.2 *Fractionated samples*

Narrow fractions were prepared from the samples described in the previous section by fractional precipitation. For K_{17}, K_{25}, K_{30} and K_{90} we adopted the method of *Scholtan* (1957). A solution of 10 g of the polymer in 1.5 to 2 l water was placed in a large separation funnel and acetone was added under stirring. The temperature was kept constant at 21,5 °C. When the solution became turbid, some more acetone was added (50 - 300 ml) in order to produce a sufficient amount of gelphase. The solution was stirred for one more hour and left to sediment for about 3 days. The viscous gelphase was drained and more acetone was added to the solution to precipitate the next fraction. Each polymer sample was separated into about ten fractions, which were then rinsed with fresh acetone, dissolved into an excess amount of water and freezedried.

Fractions of K_{12} were prepared in the following way. 51 gr of the polymer was dried by evacuating overnight at 70°C. Then the polymer was dissolved in 200 ml hot toluene (90°C) in a stirred 500 ml reaction flask, equipped with a

reflux condensor. A clear, viscous solution was obtained. By stepwise lowering the temperature of this solution, at every step separating the clear supernatant from the sedimented gelphase by careful decantation, we obtained 9 fractions. Each fraction was diluted with ethanol and the solvent mixture was removed in a rotating evaporator. After subsequent vacuum drying at $70^{O}C$ they were dissolved in water and freezedried.

All fractions used in adsorption studies were characterized by viscometry in aqueous solution by the same viscometric measurements as described for the original samples (section 3.4.1) and using again eqns. (3.26) and (3.28). We attempted to characterize the fractions obtained from K_{12} also by osmometry, using a Knauer VapourPressure Osmometer. However, unexpectedly low molecular weights were found, probably because low molecular weight impurities entered the solutions.

From table 3.3 it can be seen that the fractionation method easily leads to samples of widely different M_v. That the molecular weight distribution is considerably narrowed is suggested by fig. 3.10, where GPC curves for fraction $K_{25/4}$ and for the unfractionated sample K_{25} are shown. Since the curves of fig. 3.10 were measured in a different column than the one mentioned in section 3.4.1, the results could not be calibrated and we cannot estimate Mw/Mn.
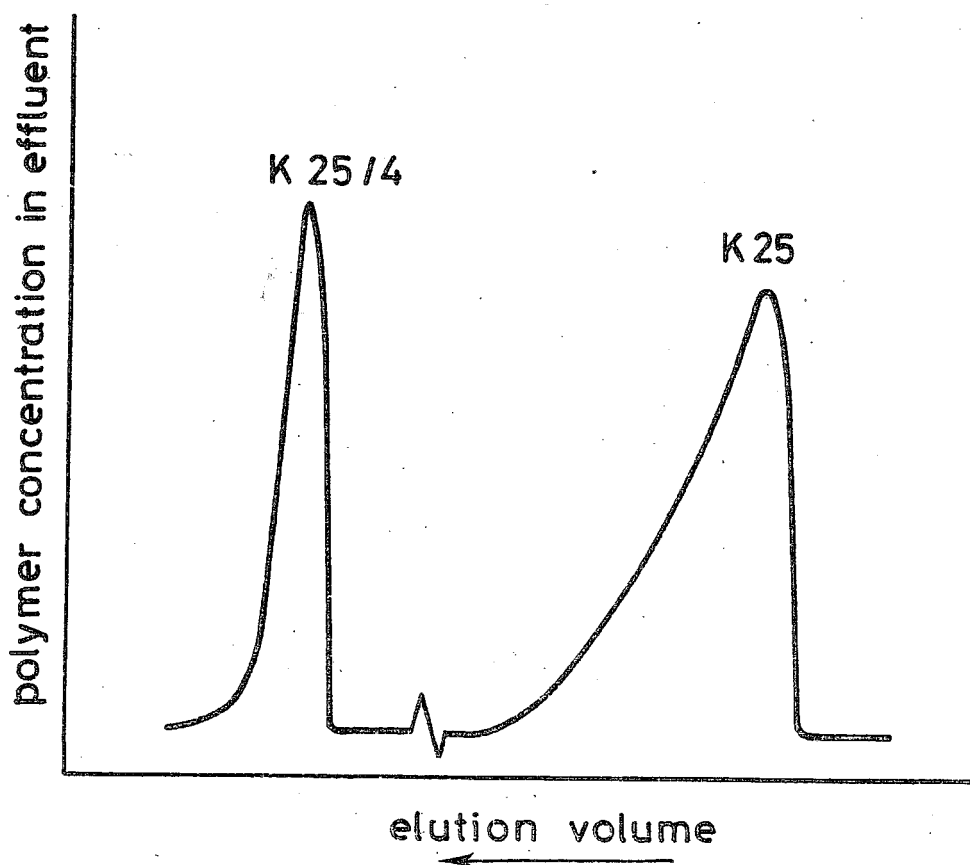
Fig. 3.10. Gel Permeation Chromatogram of fractionated PVP sample $(K_{25/4})$ and unfractionated sample (K_{25}).

Table 3.3. Viscometric characterization of PVP fractions

		VISCOMETRY		FRACTIONATION	
		$[\eta] \times 10^3 \ dm^3 g^{-1}$	$Mv \ g \ mol^{-1}$	temp. $^{\circ}C$	% acetone
K_{12}	$K_{12/1}$	4.35	2 770	- 16	-
	$K_{12/3}$	4.60	3 090	+ 16	-
	$K_{12/4}$	4.80	3 370	+ 25	-
	$K_{12/6}$	5.15	3 880	+ 52	-
K_{17}	$K_{17/2}$	14.53	23 700	-	78.64
	$K_{17/3}$	9.70	13 300	-	79.82
	$K_{17/4}$	12.2	18 400	-	80.87
	$K_{17/6}$	9.65	13 200	-	82.68
	$K_{17/7}$	7.88	9 080	-	83.46
	$K_{17/8}$	6.20	5 620	-	84.42
K_{25}	$K_{25/2}$	3.94	98 400	-	75.18
	$K_{25/3}$	3.104	70 000	-	76.16
	$K_{25/6}$	1.785	34.800	-	80.20
K_{30}	$K_{30/4}$	3.175	72 300	-	75.41
K_{90}	$K_{90/2}$	27.50	1 580 000	-	69.99
	$K_{90/3}$	12.68	523 000	-	70.21
	$K_{90/8}$	4.14	105 000	-	71.79
	$K_{90 \ VI}$	11.15	435 000	-	-
	$K_{90 \ VII}$	7.74	258 000	-	-
	$K_{90 \ V}$	12.74	525 000	-	-

3.5 SURFACE ACTIVITY OF PVP

It has been noted in the literature that PVP does not posess appreciable surface activity (*Schwartz et al.*, 1960), but from at least two other studies it is concluded that PVP adsorbs readily at the aqueous-air interface.

Glass (1968) conducted surface tension measurements at three temperatures using the drop weight method. Surface pressures of the order of 5 mN m^{-1} were found at the higher concentrations (0.01 %). However, the droplet lifetimes were short (10, 30 and 60 sec) as compared to normal equilibration times for polymer adsorption. It is thus possible that larger surface pressures develop

in the course of time. The short droplet lifetimes in these measurements did not allow to conclude a time dependence.

In contrast, *Kul'man* (1970), employing the 'embedded bubble method', (see *Adamson*, 1967, p. 28), measured the surface pressure over longer times. In these measurements, the surface pressure developed very slowly. At 25°C it took more than 20 hours for a 1% solution to reach a constant surface pressure of about 17 dyne cm^{-1}; at 50°C the changes were faster but the final surface pressure was almost the same (16.5 dyne cm^{-1}). From these studies, it appears that PVP displays at least some, although low, surface activity. This may be related to the hydrophobic nature of the backbone chain. The time effects are of the same order of magnitude as those found by *Lankveld* and *Lyklema* (1968) for the interface between paraffine and an aqueous polyvinyl alcohol solution. Both reconformation and displacement of small molecules by larger ones may be rate determining processes, but since we do not know if the same time effects are also found with monodisperse samples, it is impossible to distinguish between the two.

3.6 SILICA

Throughout this study, Cab-O-Sil M_5, manufactured under license by G.L. Cabot Inc., and virtually identical to Aerosil 200 (Degussa), was used as the adsorbent. The surface of this pyrogenic silica has been the subject of numerous studies. Below we give a few of the most important results.

3.6.1 *Preparation and specific surface area*

Pyrogenic (fumed) silicas are prepared from $Si Cl_4$ by oxidation in a hydrogen/air mixture at high temperatures (1000 °C). Amorphous SiO_2 particles are obtained on the surface of which ≡ Si-O-Si ≡ (siloxane-) bonds predominate. A few ≡ SiOH (silanol) surface groups are also formed. As the siloxane bond apparently does not bind water, it is assumed to be hydrophobic (*Young*, 1958) and the hydrophylic properties of silica surfaces must be exclusively ascribed to these few silanol groups.

The determination of the specific surface area by means of BET gas adsorption has been investigated by *Koberstein* and *Voll* (1970). Their results indicate that fumed silicas are essentially nonporous. Both argon and nitrogen can be used for the determination of the specific surface area, but for accurate measurements argon is to be preferred because it does not interact specifically with the surface silanol groups. The specific surface area determined by means of electron microscopy is in good agreement with the gas adsorption results.

Cab-O-Sil M_5 has a specific surface area of $200 \pm 20 \text{ m}^2 \text{ g}^{-1}$ as stated by the manufacturer. This value agrees rather well with results obtained by *Rubio* and *Kitchener* (1976) and by *Morrissey et al.* (1974). The primary particles have a diameter of about 10 nm (*Koberstein et al.*, 1970). It is generally agreed that heating at temperatures beyond 600°C causes a reduction in specific surface area due to a sintering process (*Rubio et al.*, 1976).

3.6.2 *The nature of the silica surface*

The surface of fumed silica carries a number of silanol groups. These are mainly of two kinds: 'free' silanols which do not interact with other OH groups and 'perturbed' or 'bound' silanols which are close enough to other OH groups to form a hydrogen bond. In the infrared spectrum, these two kinds appear as quite different species, characterized by a narrow absorption band at 1736 cm^{-1} and a very broad band, centered around 3650 cm^{-1}, respectively (*Kiselev*, 1975). The concentration of surface silanol groups can be measured by means of a variety of chemical methods (*Wartmann*, 1958; *Hertl* and *Hair*, 1968) or by means of adsorption from solution (*Bijsterbosch*, 1974).

At high temperatures, 2 silanol groups which are close enough together undergo a reversible condensation reaction to form a siloxane bond under evolution of water

$$2 \quad \equiv \text{SiOH} \quad \underset{\leftarrow}{\rightarrow} \quad \equiv \text{Si-O-Si} \equiv \quad + \text{ H}_2\text{O}$$
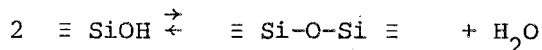
Hence, a heat treatment reduces the number of surface hydroxyl groups and makes the silica surface more hydrophobic.

At very high temperatures ($1100 \, ^{\circ}$C) only isolated hydroxyls which cannot react in this way remain (*Curthoys et al.*, 1974). The concentration of the hydroxyl groups on the surface as a function of temperature has been studied by many authors with chemical, isotope-exchange, and spectral methods. *Young* (1958) compiled a number of results indicating that the hydroxyl group density decreases from about 4.6 nm^{-2} at 180°C to values as low as 0.5 nm^{-2} at 1000°C. Fig. 3.11 shows also a compilation of results by *Kiselev* (1975, p. 80) and *Bode et al.*, (1967). Various models have been proposed to describe the arrangement of silanol groups on the silica surface (*Peri* and *Henseley*, 1968; *Armistead*, 1969). but as yet no general agreement exists.
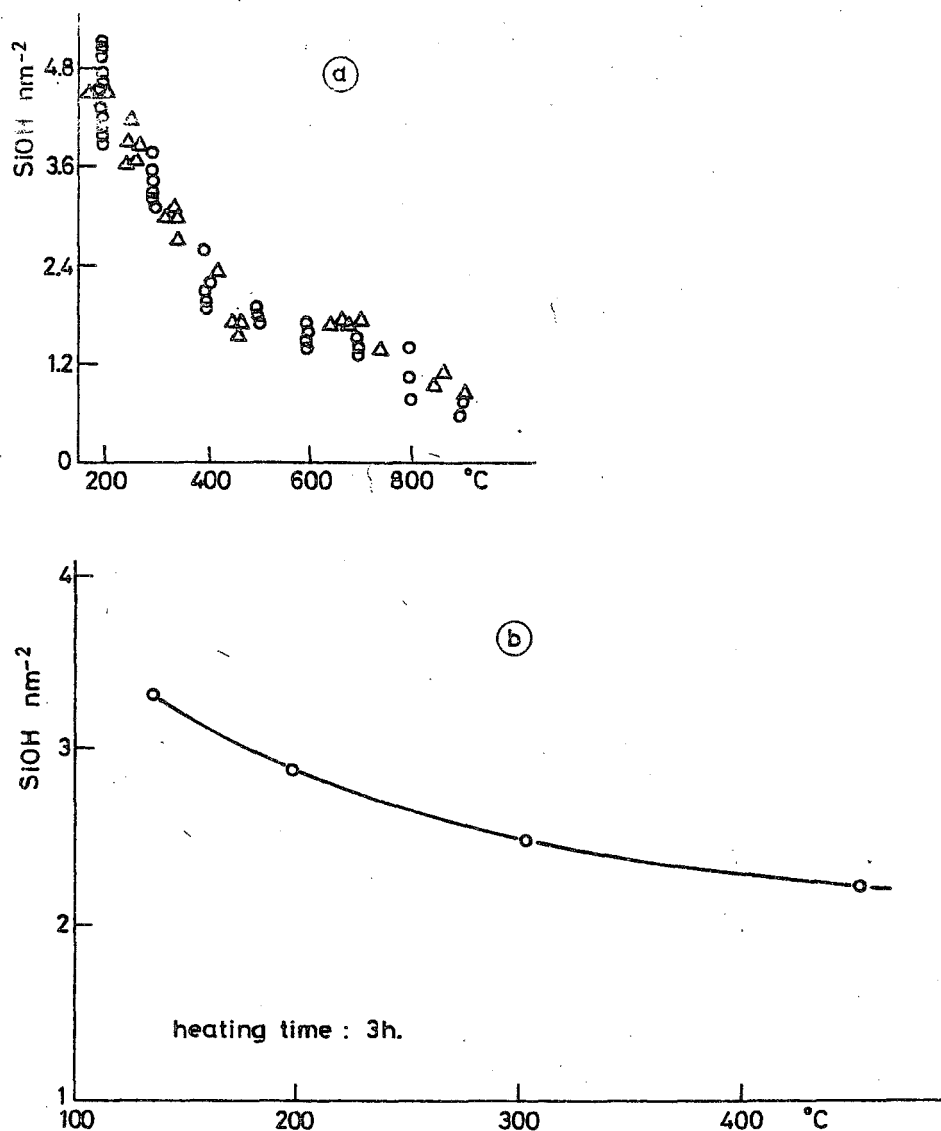
Fig. 3.11. Concentration of surface silanol groups as a function of the
temperature of heat treatment (under vacuum). Data from (a) *Kiselev*
(1975, p. 80) and *Bode et al.* (1967, p. 578).

However, it is clear that the silica surface is heterogeneous with respect
to adsorption and that the degree of heterogeneity depends on pretreatment
conditions. On a fully hydroxylated and largely hydrophilic surface hydrogen
bonding will be an important adsorption mechanism. The surface of silica heated
at $1000^{\circ}C$ will be largely hydrophobic so that adsorption by means of
hydrophobic bonding or Van der Waals forces is more likely to occur. If a
substance is only capable to adsorb through the latter mechanism, we may expect
a strong dependency of the adsorbance on the preheating temperature. Such a
dependency has been found in the case of the adsorption of partially (2%)
esterified polyvinyl alcohol. The adsorbance of this substance increases from
essentially zero on a fully hydroxylated silica to about 0.75 mg m^{-2} on silica
preheated at $800^{\circ}C$ (*Tadros*, 1978; *Trienekens*, 1976).

From the survey of the properties of PVP in the preceding sections (3.2.3) we know that PVP is capable of forming strong hydrogen bonds. Therefore it can be expected to adsorb from non aqueous solution onto silica through hydrogen bonding. However, parts of the chain are hydrophobic, which gives rise to a weak surface activity in aqueous solution. Therefore it is possible that hydrophobic bonding also plays a role in the adsorption at the silica/water interface.

3.6.3 *Dispersions of silica in water and in dioxane*

The point of zero charge of fumed silica in water was found to be between pH 2 and 4 (*Abendroth*, 1970). Therefore in the salt-free aqueous medium at neutral pH ($\simeq$ 7) a silica dispersion is stabilized by some negative charge (*Abendroth,* 1972). From photoncorrelation spectroscopy it is known that in dispersions the primary silica particles are present in the form of aggregates, probably branched chains. (*Winter*, 1973; *Bode et al.*, 1967). These aggregates can be degraded to some extent by strong shearing forces (ultrasonication), but do not disappear, even on prolonged treatment. Nevertheless, sedimentation of the stable aqueous dispersion on standing, even after months, is hardly observed.

Surprisingly, silica forms also a completely stable sol in dioxane, in spite of the low dielectric constant of this solvent (2.2 at 25°C). Perhaps dioxane, as a strong proton acceptor, is able to take up a few protons from the silica giving the surface a few negative charges. The resulting electrostatic repulsion is apparently just strong enough to prevent aggregation by the Van der Waals forces in this solvent. These forces are probably weak since the refractive indices of silica and dioxane are very similar (1.452 and 1.4224, respectively). However, we have no evidence for the existence of surface charge on silica in dioxane. On the surface of crystalline silica (quartz) the electrokinetic potential was found to be zero in dioxane containing small amounts of water (up to 0.5%) (*Shukov et al.*, 1970).

Chapter 4

Experiments on the adsorption and desorption of PVP

4.1 ADSORPTION EXPERIMENTS

We investigated the adsorption of PVP from aqueous and from dioxane solutions. Properties of PVP and dioxane have been discussed in chapter 3. In this section we describe the experimental methods. Results are given and discussed in section 4.2. For most experiments, the silica was treated at $140^{\circ}C$ for 16 hours under atmospheric conditions, and subsequently cooled in a desiccator with $CaCl_2$ as the drying agent. This treatment removes adsorbed water, but does not affect the number of silanol groups on the surface (see 4.2.4). Silica dispersions (sols) were prepared by placing a known weight of silica in a volumetric flask, after which part of the solvent was added. Ultrasonication at 25 kHz (Branson PP 300) was then applied for 15 minutes, and further solvent was added up to the mark. In all cases this procedure resulted in dispersions of sufficient stability in both water and dioxane; no sedimentation could be observed over a period of several weeks.

Adsorption experiments were carried out by bringing together known volumes of sol and polymer solutions in small vessels, which could be firmly closed by suitable caps. Thorough mixing was accomplished by slow end-over-end rotation for 16 hours. The adsorbed amount of polymer was determined by the depletion method. To this end, the samples were centrifuged for 20 minutes at 15,000 g and the polymer concentration in the supernatant was measured.

The concentration of PVP in aqueous solutions is readily determined employing the intense UV absorption of the polymer at 196 nm (see 3.2.2). The absorbance measured is directly proportional to the concentration of monomer units, and thus to the weight concentration of PVP in the solution; it does not depend on the average molecular weight of the sample. In this respect it is more reliable than a colour reaction (e.g. the formation of a reddish-brown complex with KI/I_2). However, the measurement of this far UV absorbance is only possible in aqueous solutions. Also, many compounds including simple salts and trace impurities may interfere. Therefore the samples must be prepared with great care. Absorbance measurements were made in 10 mm quartz cells with a Pye Unicam SP 1800 double beam spectrophotometer at a slit width of 0.63 mm. A good straight calibration line was obtained up to 10 mg dm^{-3} (see fig. 4.1). At higher concentrations deviations from the straight line occur, due to stray light reaching the detector. Samples with higher concentrations than 10 mg dm^{-3} were therefore diluted.
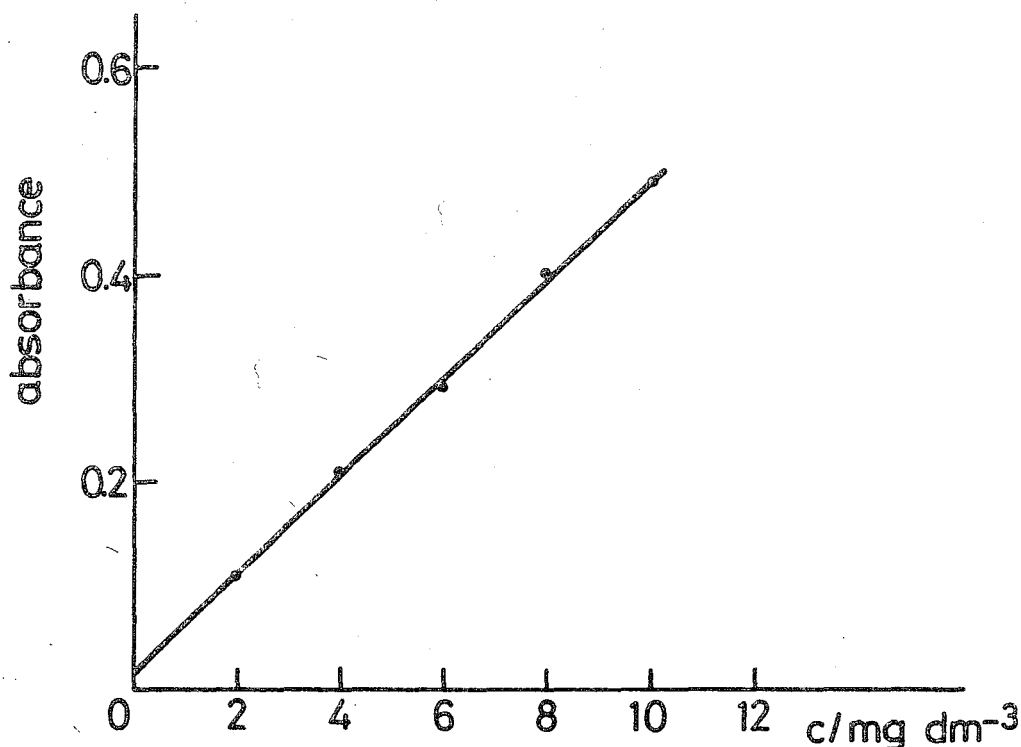
Fig. 4.1. Ultraviolet absorbance of aqueous PVP solutions as a function of
concentration c. Pathlength: 10 mm; wavelength: 196 nm.

The concentration of PVP in dioxane could be determined by evaporating the
solvent from a 1.0 or 0.5 ml aliquot at $80^{\circ}C$ in an evacuated stove. The dry
polymer was redissolved in water and the concentration was determined spectro-
photometrically as described above. The procedure was tested starting from
PVP solutions of known concentration in dioxane, and found to be satisfactory.
For accurate measurements we prepared a blank by mixing pure dioxane with silica
and treating the supernatant as described above.
Adsorbed amounts were always expressed in mg m^{-2}, adopting a specific surface
area of 200 m^2 g^{-1} for the adsorbent (see chapter 3).

4.2 RESULTS AND DISCUSSION

4.2.1 *Adsorption time*

The amount of K_{90} adsorbed from water was measured after 1, 3, 6, 24 and
96 hours of mixing. The silica concentration was 1.47 g dm^{-3} and the starting
concentration of the polymer 780 mg dm^{-3}. The results are plotted in fig. 4.2.
It can be seen that the adsorbed amount A increases during the first 10 hours,

after which a virtually constant value is reached. A similar result was obtained
for the adsorption from dioxane. Maxima, such as those reported by *Gargallo*
(1977) could not be detected.
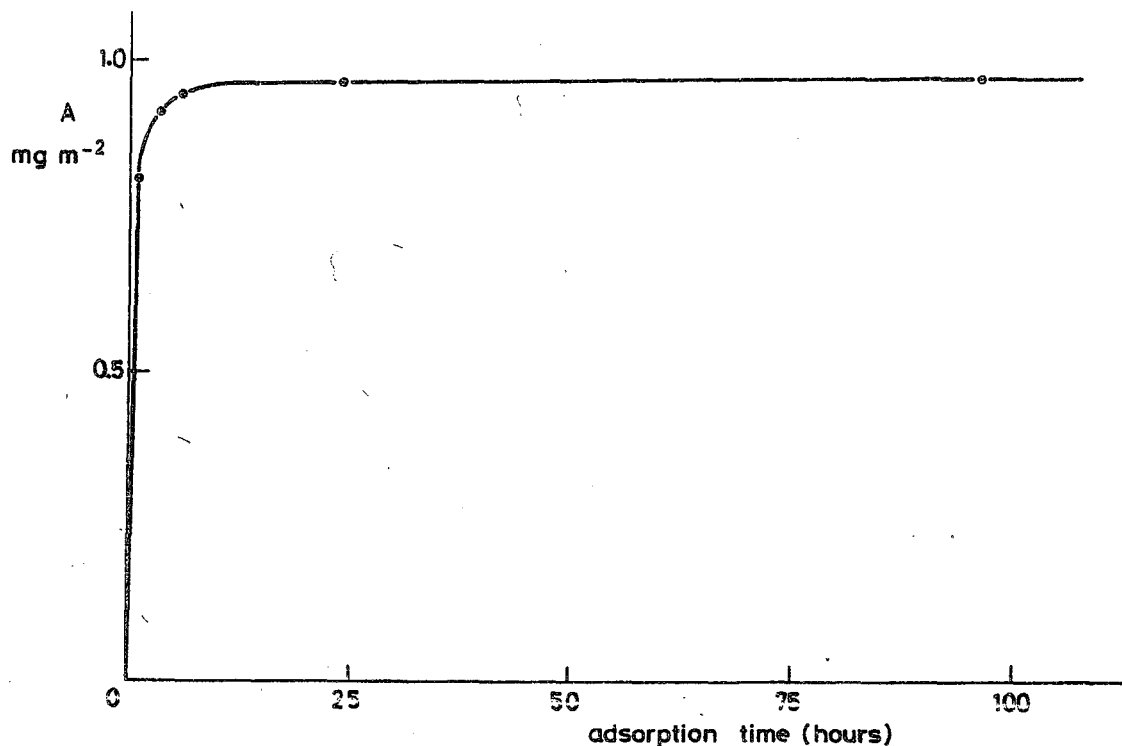
Fig. 4.2. Adsorbed weight of PVP K_{90} as a function of time. Solvent: water.

In one experiment the weight adsorbed from dioxane continued to increase over
a period as long as 600 hours. It could be demonstrated though, that this was
due to the penetration of atmospheric moisture into the sample bottle. With
increasing water content, the solvent becomes poorer and PVP tends to adsorb
in larger amounts. This unusually strong time dependence is not present if
completely air-tight bottles are used, and if the solutions are handled in
a moisture-free atmosphere. For this reason we carried out all adsorption
experiments in dioxane in a glove-box filled with P_2O_5-dried air.

Time dependencies of the type represented in fig. 4.2 are frequently
observed in polymer adsorption (*Koopal*, 1978, p. 67; *Vander Linden*, 1976,
p. IV 8). It is sometimes assumed that reconformation processes play an impor-
tant role in determining the rate of adsorption. However, for polydisperse
polymers, this is not the only possibility since small chains on the surface
may be replaced by bigger ones, leading to a slow increase in the adsorbed
amount. The time scale of such processes is not known, but it is to be expected
that they contribute significantly to the overall time dependence. On the basis

of the observations mentioned above, and for practical reasons, we chose 16 hours as the adsorption time in all experiments.

4.2.2 *Effect of molecular weight*

In the previous chapter (3.4.2) we described the properties of narrow molecular weight fractions of PVP. A number of these were used to determine the dependence of the adsorbed amount on molecular weight both from water and from dioxane. Isotherms were measured over the concentration range from zero to 1000 mg dm^{-3}. A few representative examples for dioxane are given in fig. 4.3. The silica concentration was kept constant at 3.25 g dm^{-3} for the experiments in dioxane and at 3.41 g dm^{-3} for the experiments in water.

The adsorbed weights for all fractions at an equilibrium PVP concentration of 800 mg dm^{-3} were taken from these isotherms and plotted against log M_v, where M_v is the molecular weight of the fraction calculated from its intrinsic viscosity (see table 3.3). Fig. 4.4 summarizes the results for both solvents.
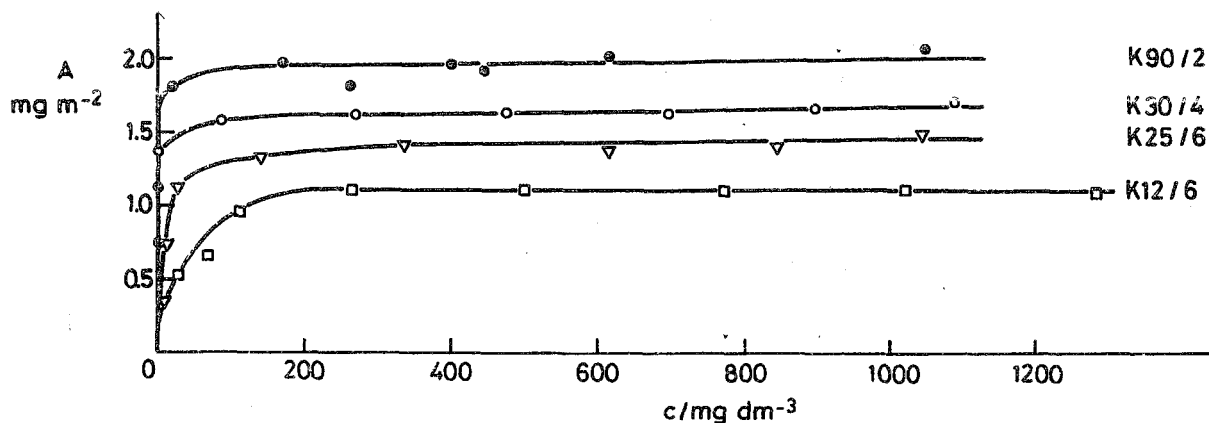
Fig. 4.3. Adsorption isotherms of PVP from dioxane, for 4 different fractions:

$K_{12/6}$ (M_v = 3880)

$K_{25/6}$ (M_v = 31,800)

$K_{30/4}$ (M_v = 72,300)

$K_{90/2}$ (M_v = 1,580,000)

The amounts adsorbed from water range from 0.2 to 1.0 mg m^{-2}. Below $M_v = 10^4$ the adsorbed amount increases strongly with increasing log M_v but for $M_v > 10^6$ A seems to attain a limiting value which is slightly higher than 1 mg m^{-2}. In dioxane the adsorbed amount rises also with increasing M_v but much higher adsorbances are reached than in the case of water. Again, the dependence of A en M_v becomes weaker for higher M but a plateau is not yet reached for M_v < 1.6 x 10^6.
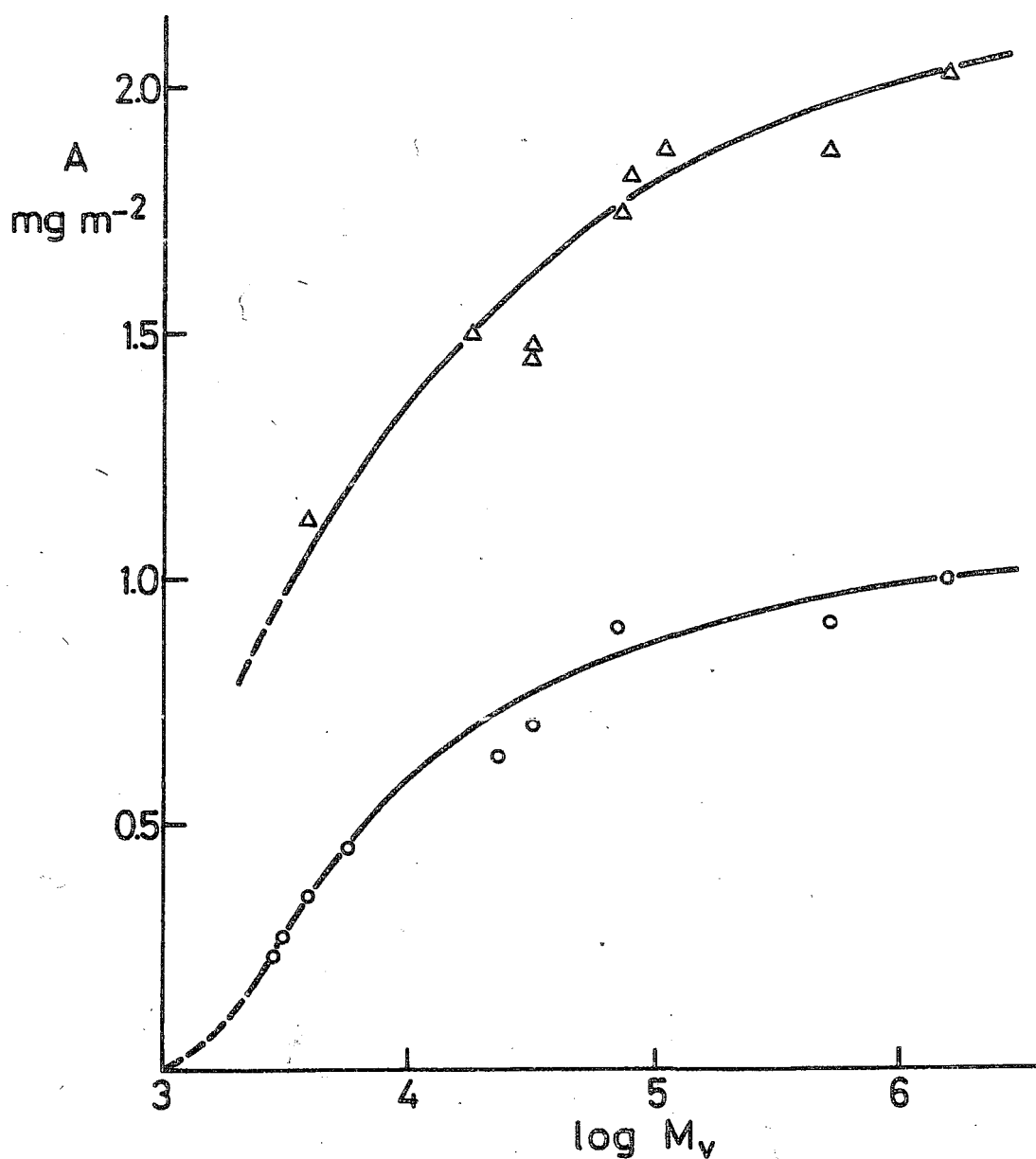
Fig. 4.4. Adsorbed amount of PVP at c = 800 mg dm^{-3}, as a function of molecular weight.

△ from dioxane

○ from water

At very low M_v both curves tend to very low adsorbed amounts. This means that short chains (oligomers) adsorb only weakly from these solvents. This agrees with the observation that the adsorbed weight of the monomeric analogue N-ethyl-pyrrolidone, at the same concentration of 800 mg dm^{-3}, is undetectably small.

The results presented in fig. 4.4 show that the adsorption depends strongly on the solvent used. Generally, this may be caused by two factors, namely the polymer-solvent interaction parameter χ and the segmental adsorption energy parameter χ_s. Both a higher χ (poorer solvent) and a higher χ_s (stronger attachments of segments) lead to higher adsorbed amounts. Since dioxane was found to be a poorer solvent than water, especially at high segment densities (see 3.3.2 and 3.3.3) and since water has a higher adsorption affinity for silica than dioxane (*Curthoys*, 1974) so that, probably, χ_s in dioxane is higher than χ_s in water, the results of fig. 4.4 are qualitatively in agreement with theoretically predicted trends (*Scheutjens* and *Fleer*, 1979).

Moreover, we have shown in section 2.6.1 (equation 2.22) that the volume v_1 of the solvent molecule may also play an important role. For water and dioxane, these volumes differ by a factor of 4.75. It is possible that this difference contributes to the differences in adsorbed amounts between both solvents. A more detailed comparison with theoretical results is needed to determine the relative importance of χ, χ_s and v_1. Such a comparison will be made in chapter 6.

4.2.3 *Effect of polydispersity and adsorbent concentration*

In section 2.7 we discussed briefly in what respects the adsorption of poly-disperse polymers differs from the adsorption of monodisperse samples. These ideas have been elaborated in more detail in a recent article (*Cohen Stuart et al.*, 1980). In studying the adsorption of PVP from water and from dioxane we obtained some results which strongly corroborate the ideas presented in this article. Below we discuss these results.

One of the predictions of the model of Cohen Stuart et al. is that the adsorption isotherm for a simple binary mixture of two monodisperse polymers should have three distinct regions: an initial steep rise, a linearly increasing part and a nearly horizontal plateau coinciding with the adsorption plateau of the highest molecular weight fraction. The linear part arises because the larger molecules adsorb preferentially, thereby displacing originally adsorbed smaller ones. This preferential adsorption determines how many small and how many large molecules from a given amount of mixture (of a given composition) can be accomodated on the available surface area. In other words, the available surface area determines how the total amount A^{tot} of polymer in the system, per unit of surface area, is distributed over the surface (A) and the solution (A_*). Since $A_* = cV/S$ (where V is the solution volume and S the available surface area), we find that, at given A, c is inversely proportional to V/S. Accordingly, for a binary mixture, the linear part of the isotherm should have a slope proportional to V/S. Also, isotherms at different V/S should coincide if plotted as $A(A_*)$ instead of as $A(c)$.

In order to check these predictions we used a mixture of the fraction
$K_{90/V}$ (M_v = 525,000) and $K_{12/3}$ (M_v = 3,090) in the weight ratio 1:3. This gives
a bimodal molecular weight distribution comparable to the simple binary mixture
mentioned above. Adsorption isotherms for two different adsorbent concentrations
are shown in fig. 4.5 (solid lines) together with the individual isotherms for
both fractions (dashed lines).
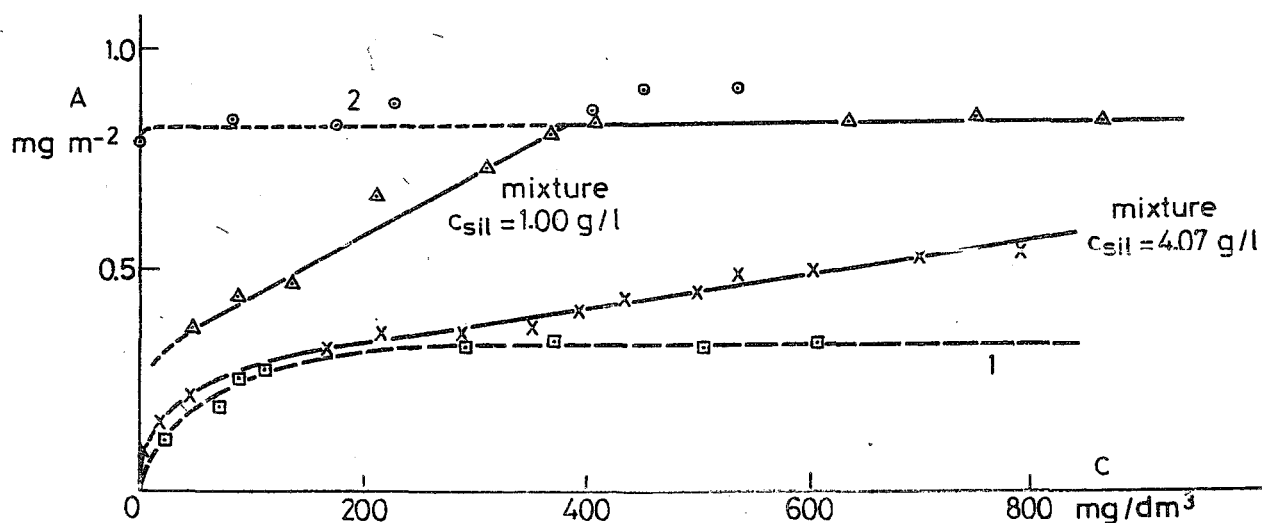
Fig. 4.5. Adsorption isotherms from water of a sample with bimodal molecular
weight distribution, obtained by mixing fractions $K_{90/V}$ and $K_{12/3}$ in a
1:3 ratio, at two silica concentrations.

The isotherms of the mixture clearly show the discontinuous pattern predicted
by the model of Cohen Stuart et al. Moreover, the slopes of the two linear middle
regions differ by a factor of 3.65 which compares favourably to the ratio of
4.07 between the two silica concentrations.

For a continuous distribution, which contains many components of different
M, the slope of the isotherm will change in a continuous manner as longer molecules
displace shorter ones. Therefore, such samples show 'rounded' isotherms,i.e. A
increases only gradually with c. Narrow fractions show a much sharper bend be-
tween the very steep initial rise and the nearly horizontal plateau. These
differences are illustrated in fig. 4.6 where isotherms of the fraction $K_{90/2}$
(M_v = 1,600,000) and the polydisperse sample K_{90} (M_v = 730,000) are given.
The adsorbent concentrations were 3.25 g dm^{-3} and 2.1 g dm^{-3}, respectively.
It is seen that the fractionated sample adsorbs in higher amounts and shows a
much 'sharper' isotherm than the polydisperse sample.

If K_{90} and $K_{90/2}$ had been identical polymer samples, the result would have been reversed because of the higher silica concentration for the latter.
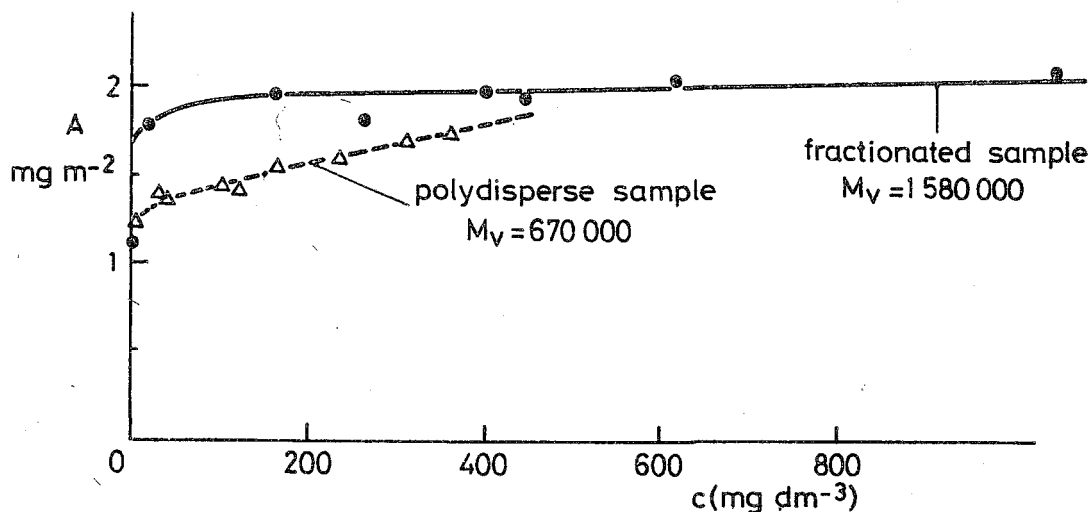
Fig. 4.6. Adsorption isotherms for a polydisperse polymer sample (K_{90}, dashed line) and a fraction thereof ($K_{90/2}$; solid line).

The effect of the surface to volume ratio S/V can also be demonstrated on polydisperse samples. In fig. 4.7a we show adsorption isotherms of the polydisperse sample K_{17} from H_2O at two different silica concentrations in the ratio 5:1 (7500 mg dm^{-3} and 1500 mg dm^{-3}, respectively). At given A, the polymer equilibrium concentrations should here be in the ratio 1:5. We replotted both isotherms as A (A_*) in fig. 4.7b. It can be seen that the curves nearly coincide. Koopal, studying the adsorption of polyvinylalcohol on silver iodide, reported also isotherms at different adsorbent concentrations (*Koopal*, 1978, p. 70). His results depend in the same way on the parameter S/V as ours and lend further support to the ideas presented by Cohen Stuart et al.
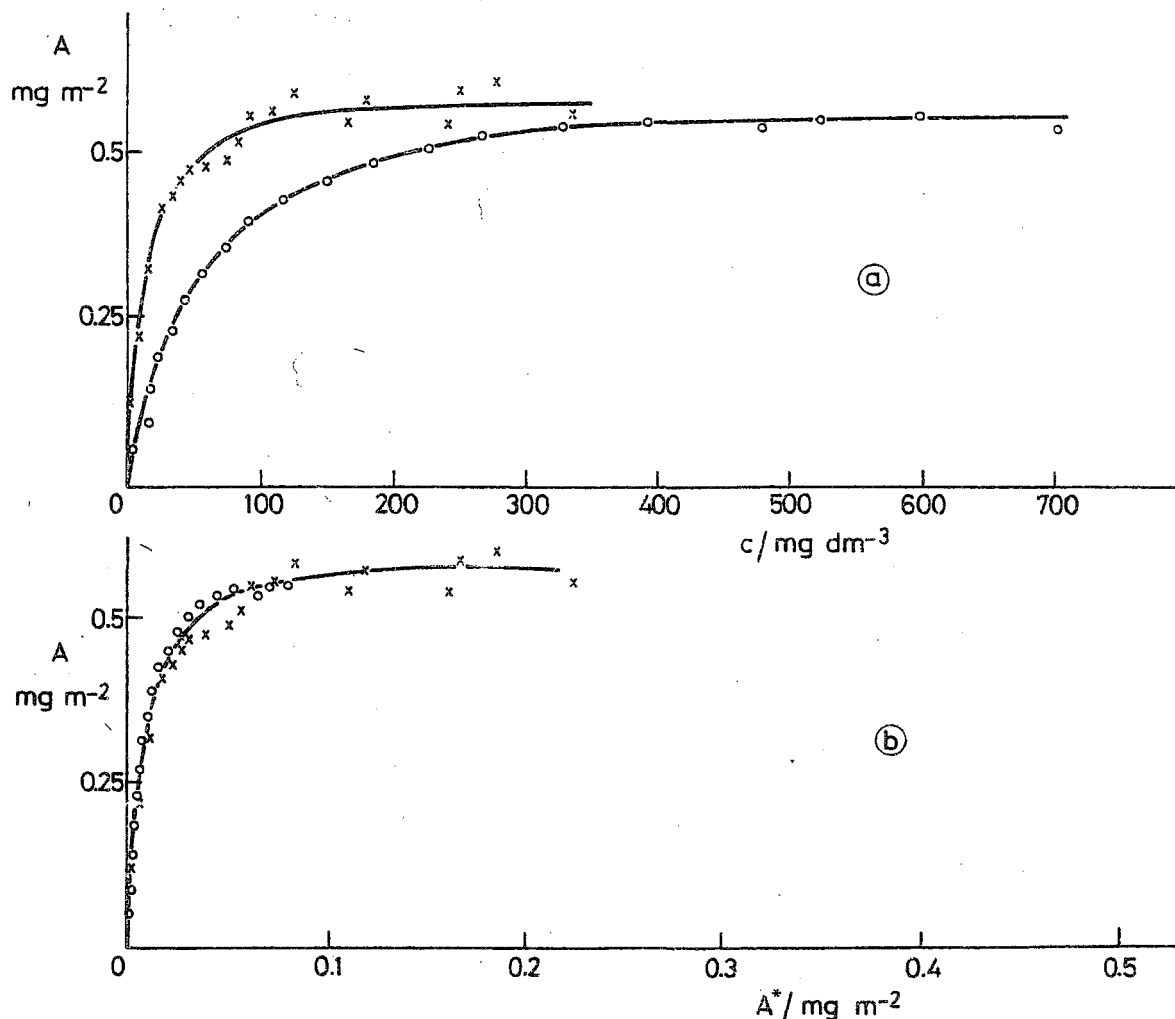
Fig. 4.7. Adsorption isotherms of polydisperse PVP (K_{17}) from H_2O onto silica, at two silica concentrations.

From the results discussed above it can be concluded that an adsorption isotherm of a polydisperse mixture carries information about two things. The composition of the adsorbate mixture, i.e. the molecular weight distribution, *and* the dependence of the adsorption plateau on molecular weight (for monodisperse polymers), A (M), must both be reflected in the isotherm's shape. In their paper, Cohen Stuart et al. presented a method to derive either A (M) (from a known molecular weight distribution) or the molecular weight distribution (if A (M) is known) from experimental isotherms. We attempted to apply this analysis to the adsorption of PVP from water, but the agreement with the independently determined molecular weight distributions (section 3.4.1) and A (M) (see fig. 4.4) was far from satisfactory.

The disagreement probably arises because of the simplicity of the assumptions underlying the applied analysis. First, Cohen Stuart et al. assumed that the plateau of isotherms for monodisperse samples is always completely horizontal, i.e. A is independent of the concentration. In reality however, such a dependence exist, though usually it is weak. Second, the preference of large molecules over smaller ones is certainly less pronounced than was supposed. The fractionation process thus does not cut the molecular weight distribution sharply at some well-defined molecular weight, but the compositions of bulk and surface phase vary rather smoothly with molecular weight. (*Felter et al.*, 1969; *Vander Linden et al.*, 1978b). Hence, the analysis of Cohen Stuart et al., though qualitatively correct, lacks refinement.

We conclude that many important consequences of preferential adsorption may be considered to be well understood. This understanding may serve as a basis for a more refined analysis which appears to be needed if experimental isotherms of polydisperse samples are used to obtain information about the adsorption of monodisperse polymers.

4.2.4 *Effect of pretreatment of silica*

As has been pointed out in section 3.6.2, the hydroxyl (silanol-)group density on the silica surface can be reduced by means of heating. In order to get some information about the importance of these silanol groups in the adsorption process we studied the changes in adsorption behaviour induced by such heating. To this end silica was heated for 16 hours in platinum crucibles in a small cylindrical oven (Heraeus). Temperature was controlled within $\pm$ 3°C).

Due to a sintering process the specific surface area of silica is reduced by heating at temperatures higher than 600°C (see section 3.6.1). Therefore, we determined the specific surface area S_{sp} after a standard heating procedure by BET nitrogen adsorption. The results, including the relative reductions, are summarized in table 4.1. This table also contains values obtained by interpolation between results of *Rubio et al.* (1976), which apply to 24 hours of heating. The relative reduction found by Rubio et al. is considerably larger for the heating temperatures 900 and 1000°C. This may be due to the fact that they heated for a longer time.

Adsorption isotherms for preheated silica samples are given in figs. 4.8 and 4.9. Fig. 4.8 shows that heat treatment up to 600°C does not affect the adsorption from dioxane. However, the amount adsorbed on silica heated at 900°C is severely reduced even when accounting for the reduction in specific surface area.

Table 4.1. Specific surface area of Cab-O-Sil M_s silica as a function of pretreatment temperature. [*] *Rubio et al.* (1976).

$T/^{\circ}C$	(16 hours)		Rubio	(24 hours)[*]
	S_{sp}	%	S_{sp}	%
450	203	100	169	99
600	203	100	165	96
800	173	85	136	80
900	169	83	111	65
1000	164	81	96	56
1050	118	58	92	54
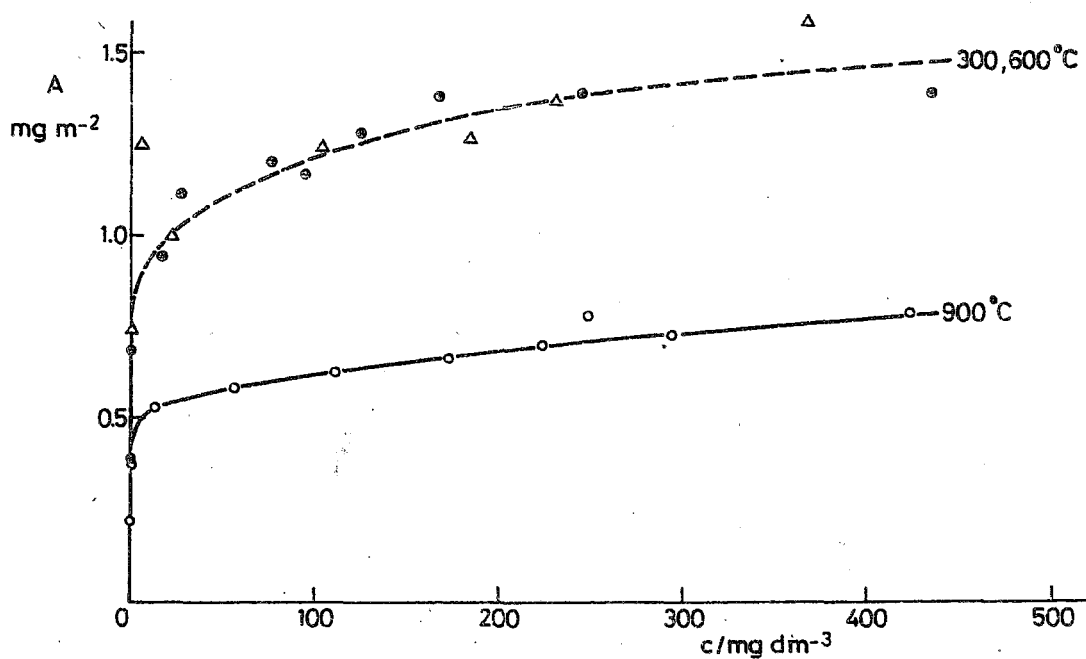
Fig. 4.8. Adsorption isotherms for PVP K_{25} from dioxane onto heated silica. Heating temperatures:

- ⊛ $300^{\circ}C$
- △ $600^{\circ}C$
- ⊙ $900^{\circ}C$

Silica concentration: 2 g dm^{-3}

For the adsorption from water a different behaviour is observed (fig. 4.9). Using our own surface area data, we calculated a slight decrease of the adsor-bance on silica heated at $900^{\circ}C$. However, after heat treatment at $1020^{\circ}C$ the adsorbed amount is considerably increased. If we calculate adsorbances with the specific surface area given by Rubio et al., we find a strong increase in both cases. It appears from these results that PVP adsorbs readily from water on a virtually hydrophobic surface. This is in line with observations of *Glass* (1968) and *Kul'man* (1970) that PVP adsorbs also at the aqueous/air interface.
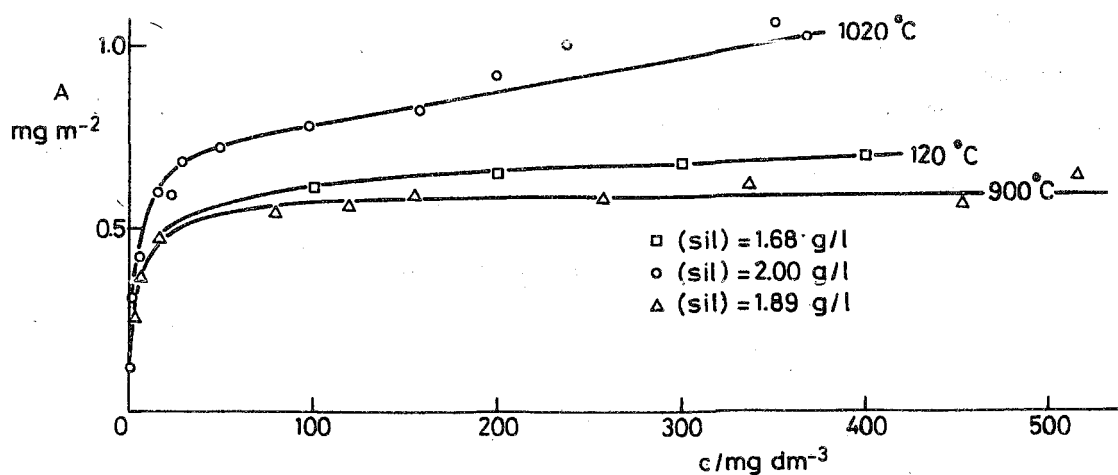
Fig. 4.9. Adsorption isotherms for PVP K_{25} from water onto heated silica.

      Heating temperatures: ◻ $120^{\circ}C$

                                △ $900^{\circ}C$

                                ⊙ $1020^{\circ}C$

Silica concentrations are indicated.

From the results discussed above it appears likely that PVP adsorbs on silica through various mechanisms, depending on the solvent. In dioxane, adsorption is promoted by the presence of silanol groups. Therefore, we conclude that the formation of hydrogen bonds between silanol groups and carbonyl groups of the polymer is the most important mechanism.

On the other hand, in water the adsorbed amount increases as more silanol

groups are removed. This speaks in favour of a hydrophobic interaction between
the polymer and the surface. The adsorption of polyvinyl alcohol (PVA) and poly-
acrylamide (PAAm) on silica are both also increased by pretreatment of the
silica at high temperatures (*Griot* and *Kithener*, 1965; *Tadros*, 1978). This is
also explained as indicative of hydrophobic bonding. However, whereas the adsor-
bance of PVA on a fully hydroxylated ('aged') pyrogenic silica is very low
(*Tadros*, 1978), the adsorption of PVP on such a surface is still appreciable.
In this respect it behaves somewhat like Polyethylene oxide (*Rubio* and *Kithener*,
1976). Probably, the occurrence in the aqueous systems of hydrogen bonds with
the surface cannot be ruled out completely for these polymers.

4.2.5 Influence of pH

In order to check whether the slight changes in pH (maximally about 0.3
units) which were observed during adsorption of PVP from water could affect the
adsorbed amount to any extent, we measured the adsorbed weight at three pH values:
3.3, 6.0 and 9.0. From these results we conclude that even if the pH changes by
0.3 units the differences in adsorbed weight are of the order of 0.6%, which is
less than the measuring accuracy (see fig. 4.10).

Fig. 4.10. Adsorbed weight of PVP K_{90} from water onto silica as a function of pH.

·Usually the pH changes were even less than 0.3. The adsorbed weight is highest at low pH and decreases about 6% over the range from 3 to 6; at higher pH no further reduction in A is observed.
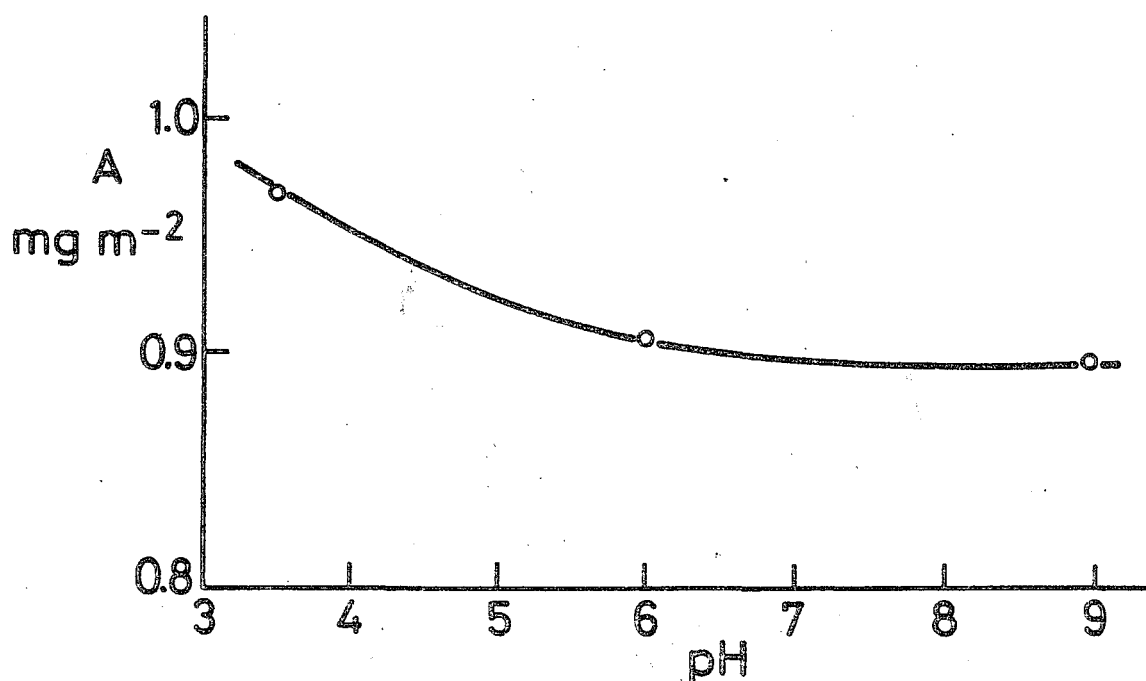
These results show that the adsorption of PVP depends only weakly on the surface charge of the silica. Since the dissociation of silanol groups, occurring at pH > 3 should effectively prohibit the formation of hydrogen bonds between silanol groups and the polymer, we conclude that the adsorption of PVP from water cannot be characterized by many hydrogen bonds. Instead, hydrophobic interactions could play an important role. These interactions are only indirectly influenced by the surface charge. Since the monomer unit is rather polar, it is not likely that its adsorption from water would be very sensitive to changes in the surface charge. Hence, the conclusion that for the adsorption of PVP from water onto silica hydrophobic bonding is important (see section 4.2.4) is further supported by the observed weak pH dependence.

4.3 DESORPTION MEASUREMENTS

4.3.1 *Theoretical introduction*

Each of the theories discussed in chapter 2 predicts that adsorption of a polymer (from dilute solution) occurs only if the adsorption (free) energy χ_s, associated with the exchange of a segment in the bulk solution with a corresponding volume of solvent at the surface, is larger than a certain critical value. We shall denote this value as $\chi_{s,cr}$. The reason for the existence of a $\chi_{s,cr}$ (usually a few tenths of kT) is that the loss in conformational entropy experienced by the adsorbed molecule must be outweighed by a decrease in free energy through the formation of polymer-surface contacts.

As was pointed out in section 2.2.2, χ_s is an *exchange* (free) energy. Segmental attachment to the surface is accompanied by displacement of solvent molecules from the adsorption sites and, hence, χ_s is the energy difference between the polymer/surface and solvent/surface interactions. If the latter interaction is particularly strong, χ_s remains below its critical value, and adsorption is impossible. Hence, solvents may exist which prohibit adsorption (we will call such solvents *displacers*), whereas from other solvents, adsorption occurs ('normal solvents'). It is easy imaginable that by varying the composition of a mixture of a normal solvent and a displacer, we may pass from one type of behaviour to the other. Below we will investigate the relation between the composition of such a mixture and its effect on adsorption from a *dilute* polymer solution.

In chapter 2 we introduced the weighting factor p_i for a step in or into

layer i; p_i may also be regarded as the equilibrium constant for the exchange of a segment in the bulk solution and solvent molecule(s) in i. Since no polymer molecule can be adsorbed without having at least one segment in the first layer, we are interested here in the weighting factor for the first layer, p_1. In terms of the polymer adsorption theory of *Scheutjens* and *Fleer* (1979), for a polymer in an athermal solvent ($\chi = o$), p_1 is written

$$p_1 = (\phi_1^O / \phi_*^O) \exp \chi_s \qquad (4.4)$$

Here, ϕ_1^O and ϕ_*^O are the solvent volume fractions in the first layer and in the bulk solution, respectively.

Adsorption can only occur if p_1 exceeds a certain critical value $p_{1,cr}$; if $p_1 < p_{1,cr}$, no adsorption takes place. Critical conditions, where the segment density in the first layer just vanishes ($\phi_1^O \to 1$) are reached if χ_s is equal to $\chi_{s,cr}$. For the dilute solution ($\phi_*^O \to 1$) this means that

$$p_{1,cr} = \exp \chi_{s,cr} \qquad (4.5)$$

Let us now consider a mixture of a 'normal' solvent and a displacer, D. Again, critical conditions are reached if $p_1 = p_{1,cr}$. However, in this case the reduction of p_1 is not brought about by a decrease in adsorption energy (χ_s) but by a decrease in the factor ϕ_1^O / ϕ_*^O. The cause of this decrease is the strong adsorption of D, so that ϕ_1^D, the volume fraction of D in the first layer, becomes larger than the bulk value ϕ_*^D. The adsorbed amount of D is determined by the exchange free energy χ_s^D; we may write, analogously to (4.4):

$$p_1^D = (\phi_1^O / \phi_*^O) \exp \chi_s^D \qquad (4.6)$$

Since D is a small molecule, it may be regarded as a monomer. This means that we may identify the equilibrium constant p_1^D with ϕ_1^D / ϕ_*^D. Then, eq. (4.6) becomes identical to the Langmuir equation for the adsorption from regular solutions:

$$\phi_1^D / \phi_*^D = (\phi_1^O / \phi_*^O) \exp \chi_s^D \qquad (4.6a)$$

As before, critical conditions are characterized by a vanishing density of polymer segments in the first layer. However, this layer contains now solvent *and* D, so that $\phi_1^O \simeq 1 - \phi_1^D$.

For the dilute polymer solution we may write, analogously $\phi_*^O \simeq 1 - \phi_*^D$. Substituting these expressions into (4.4) we find p_1 in terms of ϕ_1^D, ϕ_*^D and χ_s. The same substitution in (4.6a) gives us ϕ_1^D in terms of ϕ_*^D and χ_s^D, so that we can eliminate ϕ_1^D and write p_1 in terms of ϕ_*^D, χ_s and χ_s^D. Since we have critical conditions, $p_1 = p_{1,cr}$ and we can replace p_1 bij exp $\chi_{s,cr}$ (eq. 4.5). Denoting the volume fraction of D in the bulk solution under critical conditions as $\phi_{*,cr}^D$, we find

$$\phi_{*,cr}^D = \frac{\exp\,(\chi_s - \chi_{s,cr}) - 1}{\exp\,\chi_s^D - 1} = \frac{\exp\,\Delta\chi_s - 1}{\exp\,\chi_s^D - 1} \tag{4.7}$$

Here, we defined $\Delta\chi_s$ as the difference between χ_s and $\chi_{s,cr}$.

Although the derivation of (4.7) was given for a completely athermal mixture (all χ-parameters are zero) it applies equally well to other solvents and displacers. Since the polymer concentration in the first layer vanishes, so does the contribution of the free energy of mixing to p_1, for any χ. A derivation including all interactions between polymer, solvent and displacer can be given but it is found that their contributions vanish under critical conditions.

Inspection of eq. (4.7) brings us to the important conclusion that we may relate a critical volume fraction $\phi_{*,cr}^D$ of substance D to the adsorption energy parameter χ_s^D of D and to the 'residual' adsorption energy parameter $\Delta\chi_s$ of the polymer (both with respect to a given solvent). Measurement of $\phi_{*,cr}^D$ enables us to determine $\Delta\chi_s$ for a given polymer/solvent combination, provided that we know χ_s^D from a separate adsorption experiment.

For the derivation of eq. (4.7) we used the weighting factor p_i as defined in eq. (2.21) without any reference to the bulkiness parameter b defined in section 2.6.1. This implies that $\Delta\chi_s$, as found from eq. (4.7), has the meaning of a residual adsorption energy of a chain portion with the same effective surface area as a *displacer molecule*. In order to derive from this the $\Delta\chi_s$ *per statistical segment* we should specify how many *adsorbed* displacer molecules must be removed when a segment adsorbs in their place. We consider this question in the last chapter (section 6.1.4).

Expression (4.7) was also obtained independently by *Silberberg* (1970), on the basis of his own adsorption theory, but by way of a much lengthier derivation. From a more general expression, he finds (4.7) for the particular case of a completely athermal mixture.

To our knowledge, χ_s or $\Delta\chi_s$ have never been determined experimentally. Eq. (4.7) enables to do so, provided that suitable displacers can be found. We tried to find a number of effective displacers with different adsorption

affinity (i.e. different χ_s^D) in order to see whether a reliable value of $\Delta\chi_s$ could be obtained. In view of the acidic nature of the silica surface we selected substances with basic properties. The experiments and the results obtained will be described in the next two sections.

4.3.2 *Experimental methods*

The critical displacement volume fractions $\phi_{*,cr}^D$ were determined, both in water and in dioxane, for five different substances: N-methylpyrrolidine (NMP), N-ethylmorpholine (NEM), pyridine (PYR), dimethylsulfoxide (DMSO), and N-ethyl-pyrrolidone (NEP). All these substances are completely miscible with water and with dioxane. Some relevant data were given in chapter 3, table 3.1

A desorption experiment was carried out as follows: to a weighed amount of about 200 mg dry silica in a 50 cm^3 bottle, a solution of about 33 mg PVP K_{90} in the required amount of solvent was added, and the mixture was gently shaken by end-over-end rotation for one hour. Next, displacer was added and the sample was rotated overnight. When very little solvent and much displacer was used, the polymer was dissolved in the displacer and then added to the silica together with the required amount of solvent. In all experiments, the final amount of liquid was 10 cm^3. After 16 hours the adsorbent was separated from the supernatant by centrifugation and the adsorbed amount of PVP was determined. In all cases, except with NEP, the following method could be used.

A 1 cm^3 aliquot of the supernatant was evaporated under reduced pressure (ca 1 torr) at 80°C. When completely dry, the PVP was redissolved in a known amount of H_2O and the concentration of the resulting PVP solution was determined spectrophotometrically (see section 4.1). In the presence of strongly basic substances (NMP, PYR) PVP sometimes reacted upon heating to an insoluble, probably slightly cross-linked, product. This reaction could be suppressed by adding some water or ethanol to the samples during the later stages of the evaporation process.

NEP has a very high boiling point, so that it could not be removed by evaporation at 80°C. Due to the similarity between NEP and the monomer unit of PVP, NEP has almost the same UV-spectrum as PVP and therefore it must be separated from the polymer as completely as possible. The following methods proved suitable for the determination of adsorbed amounts from mixtures containing NEP.

From aqueous mixtures, 1 ml of the supernatant was pipetted into a small dialysis tube, which was bent into U-shape. The ends were kept open, and the bag was carefully suspended in a 1 litre beaker with distilled water (see fig. 4.11).
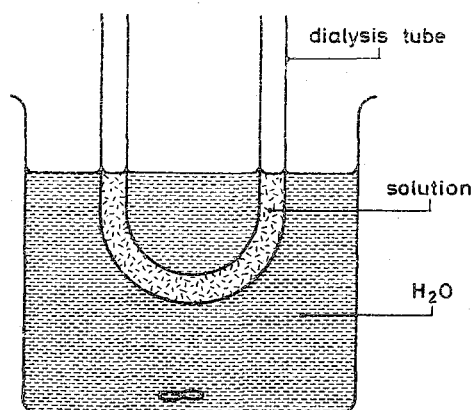
Fig. 4.11. Experimental arrangement for the removal of NEP from aqueous mixtures.

NEP could diffuse through the membrane, whereas PVP was retained. The water was tested for the presence of NEP by measuring the UV-absorbance at 196 nm, and replaced regularly. After three days all low molecular weight substances had been removed and the contents of the bag were quantitatively transferred to a volumetric flask. The PVP concentration was again determined by spectrophoto- metry.

The dialysis method failed to give reliable results in the case of dioxane/ NEP mixtures. Therefore we measured the adsorbed amount directly by a gravimetric method. The silica was recovered by filtration over a previously dried and weighed paper filter. The residue, containing the adsorbed PVP was rinsed thoroughly with distilled water and some acetone (which is a non-solvent for PVP) and dried at 100°C to constant weight. It was checked that the paper filter did not adsorb PVP in measurable amounts and that the filtrate was spectrosco- pically pure water. The adsorbed amount was then calculated as the difference in weight between the dried residue and the bare silica. It was checked that no more NEP could be extracted from the silica when redispersed in H_2O. The reproducibility of the adsorbed amount was found to be within 7%.

The adsorption isotherm of each of the displacers, from dioxane and from water (without PVP) was determined in the following way. Solvent and displacer were mixed in various proportions to cover a suitable concentration range. To 200 mg portions of carefully dried and weighed silica, 10 cm^3 aliquots of these mixtures were added and the samples were shaken for at least 2 hours at room temperature. The silica was removed by centrifugation and the difference in composition of the fluid mixture before and after adsorption was determined either interferometrically (NEP, DMSO, PYR, NEM) or titrimetrically (NMP).

For interferometry, a Zeiss instrument was used with cells of 20 mm path- length. The cells fitted into a thermostatted bath, which was filled with water

in most cases. A temperature of 20 ± 0.1 °C was maintained and the samples were equilibrated at this temperature before any measurement. Readings taken immediately after filling the cell gave reproducible results. After waiting for some time, we found in several cases large deviations, probably due to concentration changes brought about by evaporation. For each series a calibration curve was obtained by diluting a sample with small portions of solvent. In this way, concentration differences of the order of 1% could be measured to within 5% of this difference.

With NMP, the most basic representative of our displacers, the interferometric measurements led to strange results. Adsorption isotherms were poorly reproducible and showed a maximum adsorbed amount as a function of the concentration. We regard this anomaly as an artefact. It may have been caused by dissolution of small amounts of silica in the NMP solution, but we are not sure of this. In order to avoid these problems, we measured the NMP concentration by acid-base titration. We employed a Metrohm titrating potentiograph E 436, equipped with a combined glass/calomel electrode. Dilute hydrochloric acid, about 0.02 N, was the titrant. Solutions were titrated under nitrogen atmosphere in order to avoid interference by CO_2. Both the original solution and the supernatant after adsorption were titrated and the difference in composition (due to adsorption) was calculated from the difference in titrant needed to reach a specified pH. We choose a pH of 6.5 in the steep part of the titration curve for maximum accuracy. This pH may differ from the pH of the exact point of equivalence, so that absolute concentration values carry a systematical error. The error is eliminated by taking the concentration difference. The titration technique led to reproducible results.

4.3.3 *Results and Discussion*

Displacer adsorption isotherms

Adsorption isotherms for each of the displacers from water and from dioxane are given in figs. 4.12 and 4.13, respectively. Adsorbed amounts are plotted as a function of displacer volume fraction ϕ_*^D. In water (fig. 4.12) the weakest adsorption is found for DMSO. This adsorption isotherm has the smallest initial slope: increasingly higher slopes are found for NEP, PYR, NEM and NMP, respectively. A striking feature of fig. 4.12 is that the isotherms seem to reach very different adsorption plateaus. A low plateau is found for DMSO and NEM (about 0.08 mg m^{-2}); intermediate values of about 0.15 mg m^{-2} may be estimated for NMP and NEP. The adsorption of PYR reaches a value of 0.35 mg m^{-2} in the concentration range studied but continues to increase well beyond that value.

In dioxane (fig. 4.13) it is PYR which show the weakest adsorption; the

initial slopes increase in the order PYR, NEP, DMSO and NEM, respectively. The adsorption isotherm for NMP shows a maximum at $\phi_*^D \approx 5 \times 10^{-3}$. Perhaps this is an artefact; its occurrence is difficult to explain. Dissolution of silica, as suggested in connection with interferometry (previous section), is not likely to occur in dioxane.
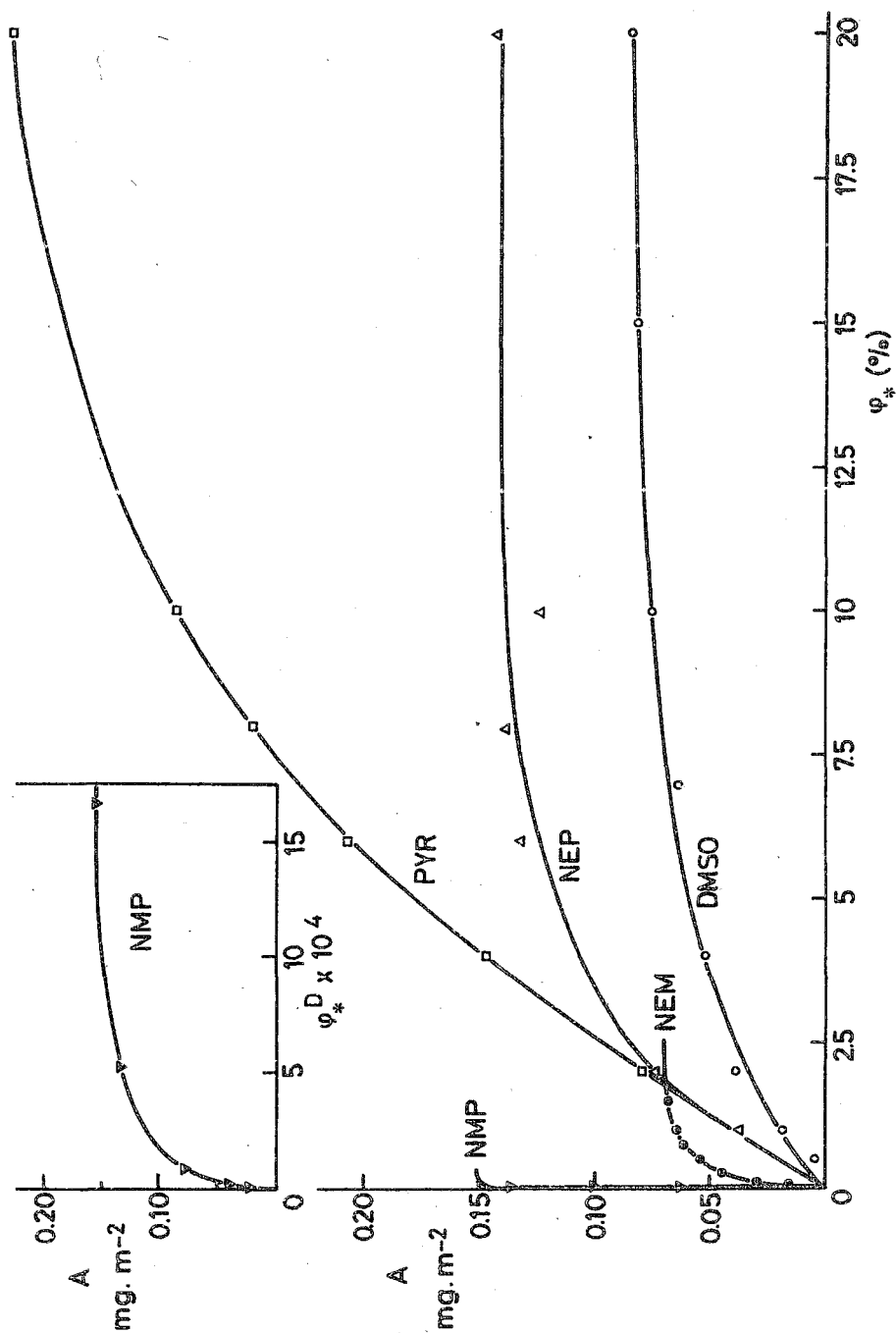
Fig. 4.12. Adsorption isotherms of displacers from water onto silica.

As in the case of water, the adsorption plateaus are widely different. The lowest plateau (about 0.15 mg m^{-2}) is found for PYR and NEP. The adsorption plateau of DMSO is of the order of 0.30 mg m^{-2} and NEM reaches adsorbances of at least 0.60 mg m^{-2}.

In the derivation of eq. (4.7) it was assumed that the displacers can be considered as monomers and adsorb according to a Langmuir equation, eq. (4.6a). We may rewrite this equation in the following way:
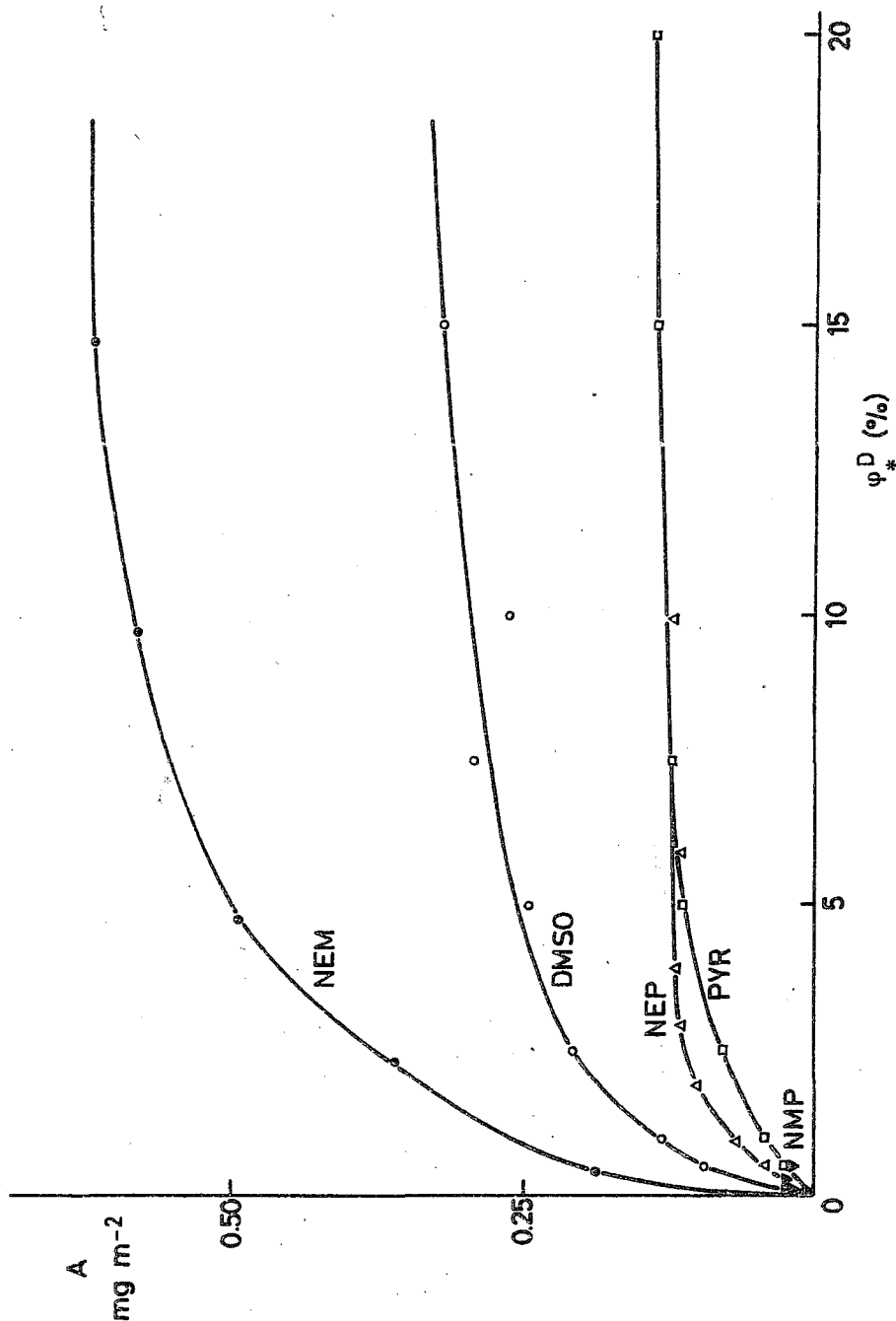
Fig. 4.13. Adsorption isotherms of displacer from dioxane onto silica.

$$\frac{\phi_1^D}{1 - \phi_1^D} = \frac{\phi_*^D}{1 - \phi_*^D} \exp \chi_s^D \qquad\qquad (4.8)$$

The surface coverage ϕ_1^D may be identified with the fraction of the maximum (monolayer) adsorbance A^{mon} which is adsorbed, so that $\phi_1^D = A / A^{mon}$. Values of χ_s^D may be obtained by linearization of the isotherm (4.8), provided that ϕ_*^D is low enough so that A is equal to the experimentally measured surface excess A_{ex} (*Hansen*, 1951). The relevant equation reads:

$$\phi_*^D / A = (A^{mon} \exp \chi_s^D)^{-1} + \phi_*^D (1 - 1 / \exp \chi_s^D) / A^{mon} \qquad (4.9)$$

If we plot ϕ_*^D / A versus ϕ_*^D we find $1/A^{mon}$ and $(\exp \chi_s^D - 1)$ from slope and intercept, taking their sum and their quotient, respectively. Experimental values for A^{mon} and χ_s^D obtained in this way are given in table 4.2. Results for NMP in dioxane were omitted for reasons discussed above.

Table 4.2. A^{mon} and χ_s^D obtained from Langmuir linearization plots.

|	Dioxane					Water				
	NEP	PYR	DMSO	NEM		NEP	PYR	DMSO	NEM	NMP
A^{mon} / mg m^{-2}	0.19	0.16	0.34	0.57		0.17	0.90	0.09	0.07	0.16
χ_s^D	4.0	3.6	4.1	4.8		3.7	1.8	3.4	6.5	9.0

However, application of the Langmuir equation to the results of figs. 4.12 and 4.13 is questionable for the following reasons.

First, the surface of silica is energetically heterogenous. Adsorption may occur on hydrophobic siloxane bonds and on different kinds of silanol groups; the adsorption energy may vary in a wide range. Probably, this is the reason that different substances have a widely different adsorption plateau . The Langmuir equation is unable to describe the adsorption on heterogenous surfaces. In principle, any isotherm can be described if a suitable *distribution* of energies is assumed, but it is beyond the scope of this thesis to carry out such an analysis (see, e.g. *Sacher* and *Morrison*, 1979; *House*, 1978).

Second, in many cases the volume fraction of displacer in the solution, ϕ_*^D is so high that differences between A and A_{ex} cannot be neglected. It is possible to correct for this difference by adding ϕ_*^D to the excess volume fraction

ϕ_{ex}^{D} of D, defined by $\phi_{ex}^{D} = A_{ex}/A^{mon}$. However, this requires an assumption for the value of A^{mon}.

Third, the Langmuir equation is unable to account for differences in volume between solvent molecules and adsorbate molecules. If these volumes are not equal, so that each adsorbate molecule does not displace one single solvent molecule on the surface, the adsorption isotherm must follow another expression which cannot be linearized so easily (Dhar et al, 1973).

For these reasons we do not rely very much on the χ_{s}^{D} values in table 4.3. The order of increasing χ_{s}^{D} in this table is PYR < DMSO < NEP < NEM < NMP for water and PYR < DMSO < NEP < NEM in dioxane. No correlation is found with the order of increasing initial slope of the isotherms which is DMSO < PYR ≃ NEP < NEM < NMP in the case of water and PYR < NEP < DMSO < NEM for dioxane. For Langmuir isotherms, this correlation would be expected.

Displacement isotherms

In order to determine critical displacer volume fractions, $\phi_{*,cr}^{D}$, we plotted adsorbed amounts of PVP as a function of ϕ_{*}^{D}. It was found that a logaritmic scale for ϕ_{*}^{D} was most suitable. Results are shown in figs. 4.14 and 4.15 for water and for dioxane, respectively. We will refer to these curves as 'displacement isotherms'.
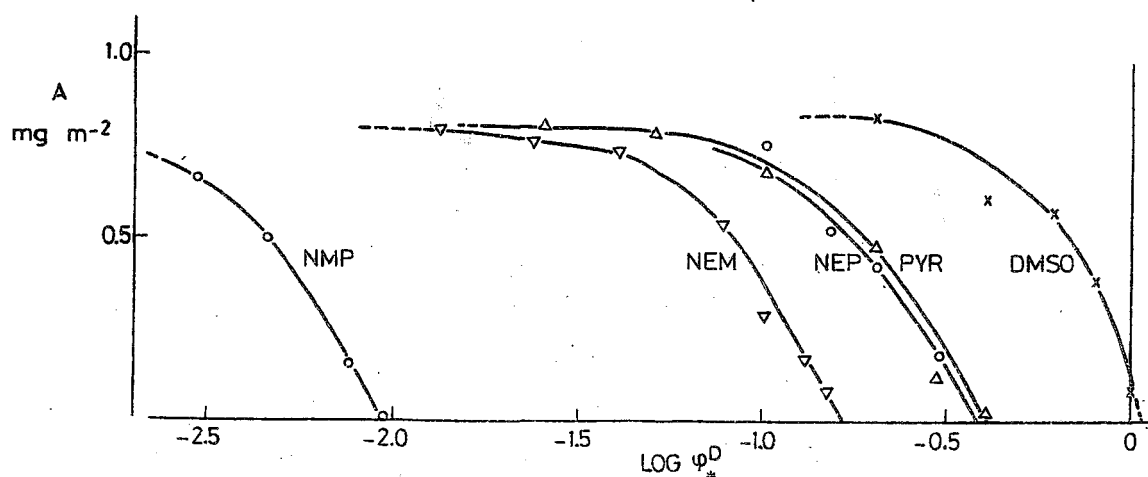
Fig. 4.14. Displacement isotherms of PVP from silica into water/displacer mixtures.

It can be seen that all displacement isotherms have the same general shape, but that they are shifted relative to each other along the log ϕ_*^D axis. The critical desorption concentration $\phi_{*,cr}^D$ is defined as the point of intersection of the isotherm and the line A = o. Values of $\phi_{*,cr}^D$ are tabulated below (table 4.3).
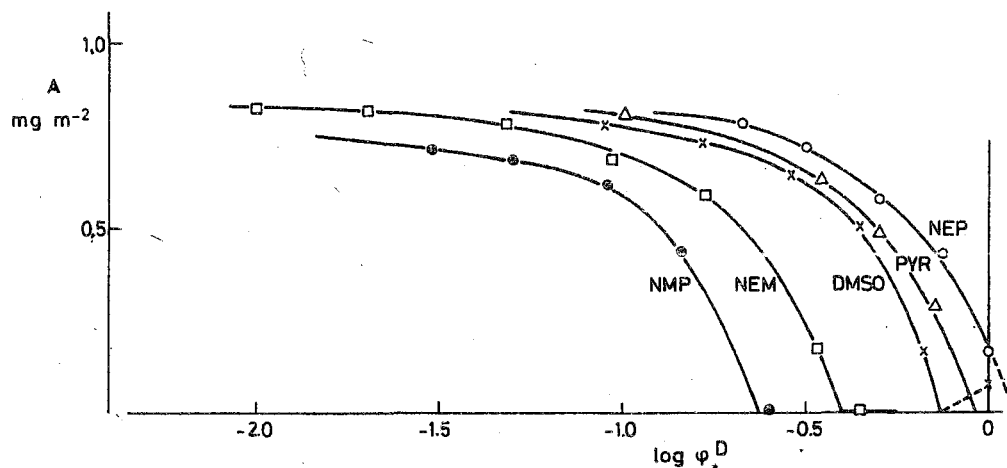
Fig. 4.15. Displacement isotherms of PVP from silica into dioxane/displacer mixtures.

Table 4.3. Critical desorption concentrations and residual adsorption energies for PVP onto silica in the presence of various displacers.

	Dioxane				Water				
	NEP	PYR	DMSO	NEM	NEP	PYR	DMSO	NEM	NMP
$\phi_{*,cr}^D$	1.15	0.91	0.74	0.40	0.35	0.35	1.05	0.16	0.0089
$^a\Delta\chi_s$	4.14	3.56	3.80	3.77	2.70	0.99	3.45	4.68	4.30

^{a} Calculated from χ_s^D values given in table 4.2 according to eq. (4.7).

In a few cases, even $\phi_*^D = 1$ did not bring about complete desorption (NEP/dioxane; DMSO/water). In these cases, $\phi_{*,cr}^D$ was estimated by extrapolation of the displacement isotherms into the (virtual) range $\phi_*^D > 1$. In the mixtures NEP/water and DMSO/dioxane complete desorption was achieved (at a $\phi_{*,cr}^D$ of 0.35 and 0,74, respectively). However, at $\phi_*^D = 1$ (pure DMSO and pure NEP, respectively) there is some adsorbed polymer (A > o). Hence, the displacement isotherms for the NEP/water and DMSI/dioxane systems must have a minimum.

For NEP/water, the adsorbed amount of PVP is indeed found to increase with increasing ϕ_*^D in the range $0.35 < \phi_*^D < 1$. For DMSO/dioxane, this increase is expected in the concentration range $0.8 < \phi_*^D < 1$, but we have no experimental points in this range. Fig. 4.16 illustrates the occurrence of the minimum in the NEP/water displacement isotherm and the common point with the NEP/dioxane isotherm at $\phi_*^D = 1$ (pure NEP).
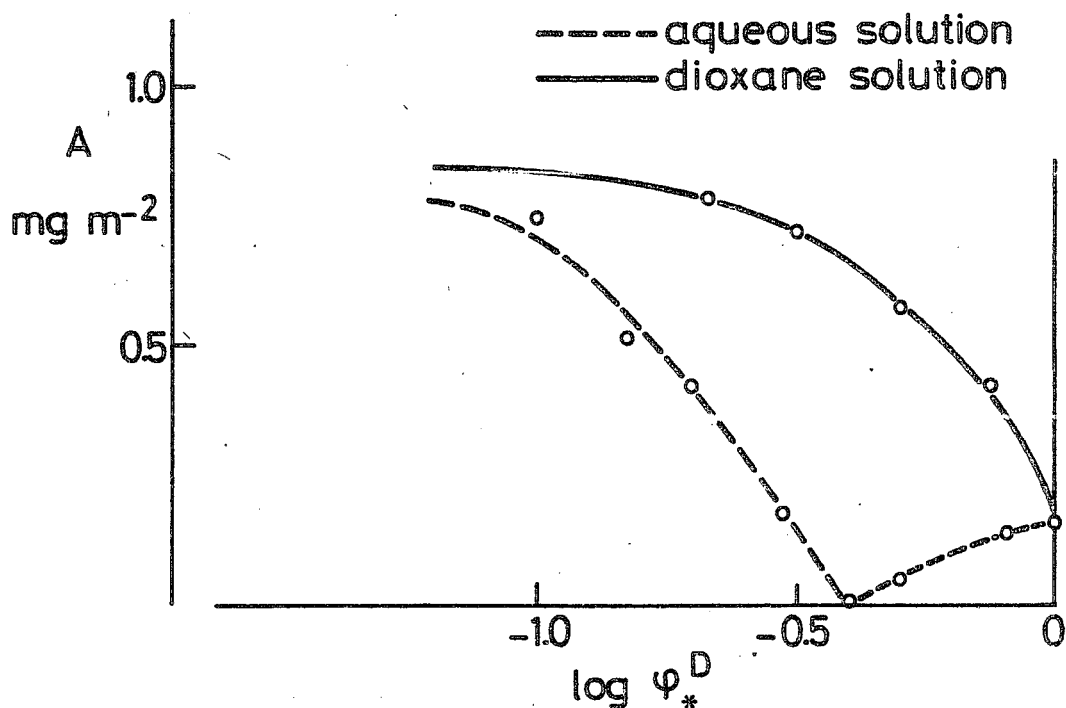
Fig. 4.16. Displacement isotherms of PVP by its monomeric analogue, NEP, in aqueous and in dioxane solution.

From table 4.3 and from fig. 4.14 we see that $\phi_{*,cr}^D$ in water decreases in the order DMSO > PYR $\simeq$ NEP > NEM > NMP. In dioxane, the order is NEP > PYR > DMSO > NEM > NMP.

It is interesting to consider the results obtained with NEP (which is a monomer analogue for PVP) more closely. Regarding the structural similarity between NEP and the monomer unit in PVP it would be plausible to assume a similarity in adsorption behaviour, and hence in adsorption affinity. Let us assume χ_s (PVP) = χ_s^D (NEP). (Such an assumption implies that we disregard

differences between monomer units in a chain and free monomers, with respect to e.g. orientability and rotational freedom). Using this assumption to eliminate χ_s from the displacement relationship (4.7) we obtain

$$\exp(-\chi_{s,cr}) = \{ \phi_{*,cr}^D (\exp \chi_s^D - 1) + 1 \} / \exp \chi_s^D \qquad (4.10)$$

This expression enables us to estimate a $\chi_{s,cr}$-value from $\phi_{*,cr}^D$ and χ_s^D. If χ_s^D is not too small we may approximate (4.10) by

$$\exp(-\chi_{s,cr}) = \phi_{*,cr}^D + \exp(-\chi_s^D) \simeq \phi_{*,cr}^D \qquad (4.11)$$

Since, theoretically, we expect values of 0.1 - 0.3 for $\chi_{s,cr}$, $\phi_{*,cr}^D$ should be in the range 0.74 to 0.90. This is not observed.

In water $\phi_{*,cr}^D$ (NEP) equals 0.35, which implies that χ_s (PVP) < χ_s^D (NEP). This is not easily accounted for. Perhaps it is easier for the hydrophobic ethylgroup of NEP than for the PVP-backbone to approach the hydrophobic parts of the silica surface closely, because the NEP molecule is not subject to the constraints typical for chain structures. In dioxane, the critical volume fraction is larger than 1 ($\phi_{*,cr}^D$ = 1.15) so that here χ_s (PVP) > χ_s^D (NEP). The reason for this difference might be that NEP, being a small molecule, looses more rotational entropy than a monomer unit in a chain. (This effect must also play a role in water, but it is perhaps outweighed by the advantage of closer approach). We estimate a difference between χ_s and χ_s^D of 0.8 kT units in the case of water and of 0.3 kT units in the case of dioxane.

Let us now compare the displacement isotherms with the displacer adsorption isotherm. For the aqueous mixtures we find that the order of increasing displacer strength (decreasing $\phi_{*,cr}^D$) is different from the order of increasing χ_s^D, but agrees very well with the order of increasing initial slope of the displacer isotherm. In dioxane, the correlation between χ_s^D and $\phi_{*.cr}^D$ is also poor, mainly because $\phi_{*,cr}^D$ for NEP is much lower than expected from its χ_s^D. The correlation with initial slopes is also imperfect, since the order of PYR and NEP is reversed; the $\phi_{*,cr}^D$ for PYR is somewhat lower than expected from the initial slope of the isotherm. Still, it seems that the initial slope of the adsorption isotherm is a better measure for the displacer strength than the χ_s^D-value obtained from a linearization plot. In fig. 4.17 we represented the correlation graphically, as a plot of log $\phi_{*,cr}^D$ versus the logaritm of the initial slope. We expressed the initial slope as the number of adsorbed moles per m^2 (Γ_{in}) divided by the mole fraction of adsorbate in the solution (X_{in}). Although there is no theoretical basis for this type of plot it illustrates to some extent the correlation mentioned above.
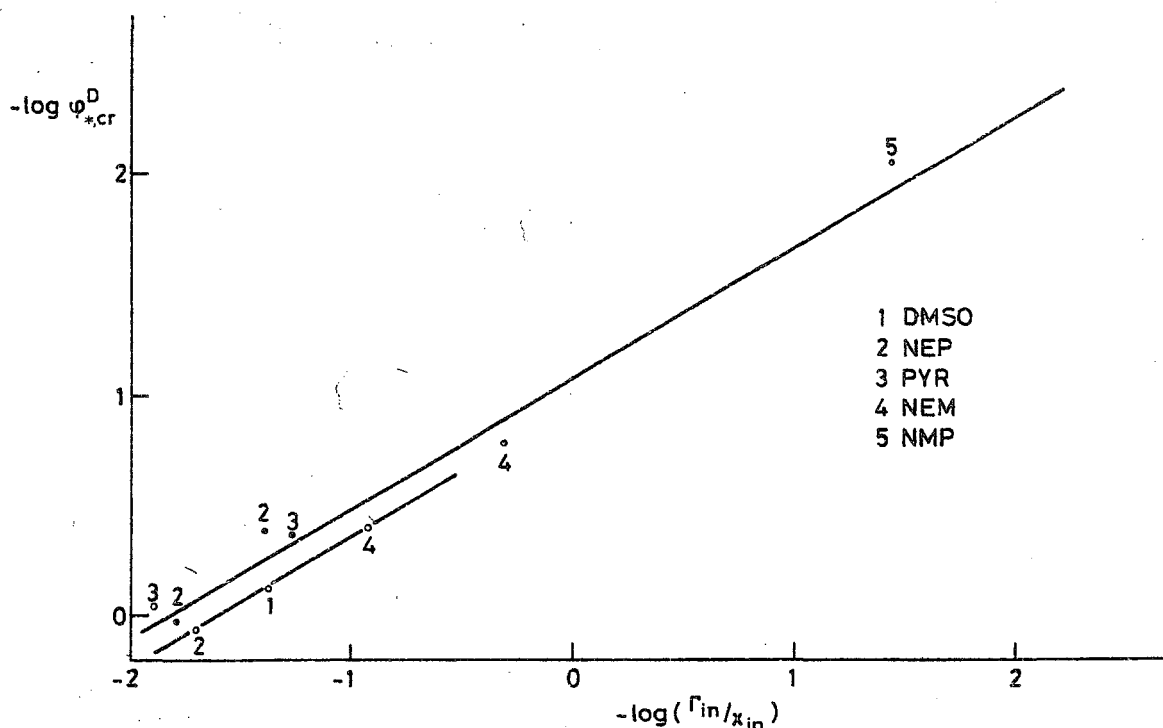
Fig. 4.17. Correlation between critical displacer concentration $\phi^{D}_{*,cr}$ and initial slope of displacer isotherm (Γ_{in}/X_{in}), for adsorption from water (solid circles) and from dioxane (open circles).

Once more these results underline that the simple Langmuir equation is not suitable for the description of the adsorptions·studied here. Therefore, χ_s^D values from the linearization plots can only lead to a rough estimate of $\Delta\chi_s$. Nevertheless, by lack of anything better, we calculated $\Delta\chi_s$ for the polymer (eq. 4.7). The results are also given in table 4.3. In dioxane $\Delta\chi_s$ is reasonably constant; the average value from all displacement experiments is 3.8. In water $\Delta\chi_s$ ranges from 1 to 4.7 around an average value of 3.2.

We conclude that although displacement experiments can be performed with reasonable accuracy, the application of eq. (4.7) is hampered by lack of suffi-ciently accurate χ_s^D values. Since the Langmuir equation is unable to describe the adsorption of molecules of various sizes on a heterogeneous surface, better agreement can perhaps be obtained if solvent and adsorbate molecules have more or less equal volumes and if the surface is energetically more· homogeneous. Nevertheless, it is found that the initial slope of the displacer isotherms (which is probably a better measure for the displacer's adsorption affinity) correlates satisfactorily with the displacer strength. A rough estimate of $\Delta\chi_s$ is obtained on the basis of Langmuir linearization plots. We ·find $\Delta\chi_s$ between 2 and 4 for water and a somewhat better defined value of about 4 for dioxane.

Chapter 5

The fraction of Bound Segments

5.1 INTRODUCTION

In chapter 2.1 we introduced the bound fraction or train fraction p as a
measure of the conformation of adsorbed molecules. A high p is indicative of a
strongly flattened molecule, whereas a low p means that the molecule is more
randomly coiled. The bound fraction alone is not enough to give us a complete
picture of the conformation, because the information contained in p is rather
limited. For example, the same p may be found for a chain with a few long trains
and for one with many short trains.

Nevertheless, p is a useful parameter due to its experimental accessibility.
At least five methods have been devised to determine p: infrared, NMR,and ESR
spectroscopy, microcalorimetry and electrical double layer measurements. Each of
these methods has its specific advantages and restrictions and the results
depend on inherent assumptions. Below we discuss these assumptions briefly.
The very choice of the experimental system (PVP and silica) enabled us to
measure bound fractions with infrared spectroscopy (in dioxane), NMR spectros-
copy (in D_2O) and microcalorimetry (in dioxane and in H_2O). In the following
sections we discuss the principles of the methods, whereas sections 5.3 - 5.6
deal with experimental results.

5.2 PRINCIPLES OF THE VARIOUS MEASURING TECHNIQUES

5.2.1 *Infrared spectroscopy*

Infrared spectroscopy has as yet been applied mainly to the stretching
vibration of carbonyl groups in the polymeric adsorbate (*Fontana et al.*, 1961;
Killman et al., 1972; *Joppien*, 1975; *Korn*, 1978) and to the stretching vibration
of hydroxyl groups on the surface of the adsorbent (*Killmann et al.*, 1972;
Dietz, 1976). These groups are capable of forming a hydrogen bond with each
other. Due to the slight charge transfer from the C = O and O - H bonds to
the newly formed hydrogen bond the strength and, hence, the vibration frequency
of the C = O and O - H bonds decrease. In a few investigations on polystyrene
adsorption (*Herd et al.*, 1971; *Thies et al.*, 1964; *Vander Linden et al.*, 1976)
use is made of the fact that the out-of-plane vibration of phenyl hydrogens
at 698 cm^{-1} shows an intensity increase and a slight upward frequency shift of

4 cm^{-1} upon interaction with an OH (surface) group. Similarly, the ring-stretching vibration in pyridine-rings at 1626 cm^{-1} shifts 5 cm^{-1} downwards upon adsorption and was therefore used to study the adsorption of polyvinyl pyridine (*Herd et al.*, 1971).

Generally, the bound groups show up as perturbed species, producing a new spectral line. Usually the assumption is made that in a train segment all groups are bound, so that the remaining unperturbed spectrum is exclusively due to loops and tails. This is not necessarily true. There may be monomer units close to the surface which do not interact with it through a spectroscopically detectable bond, and these will be counted as contributing to loops or tails. Nevertheless, the position of these units on the surface characterizes them (by definition) as part of a train segment. So we may expect that infrared spectroscopy underestimates p.

The infrared method looks for *specific interactions* between the polymer and the surface. Such interactions are of course easily obscured by comparable interactions with the solvent. Therefore, hardly any frequency shift in the carbonyl stretching vibration is expected if a silanol-carbonyl bond is being formed in a proton-donating solvent (water, alcohols). For the same reason spectral shifts of silanol groups cannot be studied in proton accepting solvents (ketones, ethers, alcohols, water). Consequently, in almost all studies hydrocarbons or chlorinated hydrocarbons were used as solvents. An exception is the investigation by *Morrissey* (1974) who used D$_2$O as the solvent and studied protein bound fractions. However, in this case the observed spectral shifts may have been due to other processes than the formation of a polymer-surface hydrogen bond such as, e.g., penetration of water in the partly uncoiled protein molecule.

The above considerations limit the application of infrared spectroscopy to systems in which (i) the polymer carries a specific group in its chain (C = O, phenyl, pyridine), (ii) these groups interact specifically with the surface, (iii) the solvent does not interfere with these interactions. The last requirement is somewhat relaxed by the use of a spectrometer with high resolving power. Attempts have been made to measure bound fractions of PVP adsorbed from D$_2$O on silica with a Fourier transform infrared spectrometer (*Robb*, 1977a).

5.2.2 *Nuclear Magnetic Relaxation Spectroscopy*

Rather than giving information about specific interactions, magnetic relaxation spectroscopy measures differences in mobility between directly

adsorbed segments (trains) and indirectly adsorbed chain parts (loops and tails).
In the NMR relaxation experiment the sample under investigation, containing
magnetic nuclei (e.g. hydrogen, fluorine, carbon-13), is placed between the poles
of a strong magnet. Under these conditions the sample acquires a net macroscopic
magnetization aligned with the external field H_o. By means of a suitable radio-
frequency pulse the sample's magnetization is disturbed so that it is no longer
aligned with H_o but has also components perpendicular to H_o: the transverse
magnetization. It is this transverse magnetization which is usually measured.
A relaxation process with a characteristic time T_{II}, called the transverse or
spin-spin relaxation time, reduces the transverse magnetization to zero in the
course of time. The characteristic time for the relaxation of the longitudinal
component towards its original value is T_I, the longitudinal, or spin-lattice
relaxation time.

The origin of all relaxation mechanisms is the interaction of the magnetic
nuclei with each other and with their surroundings, in general: with local
magnetic and electric fields. Due to the thermal motion in liquids these fields
fluctuate in time. Since these fluctuations are irregular, they contain Fourier
components in a range of frequencies. Almost always the time scale for irregular
motion can be expressed in a correlation time τ_c. For instance, the rotational
Brownian motion of a small molecule with two protons (e.g. water) is approxi-
mately given by (*Carrington* and *Mc Lachlan*, 1967, p. 189):

$$\tau_c = 4 \pi \eta a_H^3 / 3 kT \qquad\qquad (5.1)$$

where η is the viscosity of the liquid and a_H is the distance between the two
protons in the molecule. Hence, the interproton vector of a rotating water
molecule, in the external field H_o, changes its direction with respect to H_o
with a characteristic frequency τ_c^{-1}, the value of which is found from (5.1).
The magnetic dipolar interaction between the protons is modulated with the
same frequency. An effective (fast) *longitudinal* relaxation is obtained if this
frequency is of the same order as the NMR resonance or *Larmor* frequency ω_o,
since then the frequency components of the random motion are 'tuned' to act
in the same way as the original, disturbing pulse. The Larmor frequency, and
thus the conditions under which T_I is in its minimum, depend on the type of
nucleus and on the strength of the static magnetic field:

$$\omega_o = g_N \beta_N H_o / 2 \pi h \qquad\qquad (5.2)$$

Here, g_N is a dimensionless constant, β_N is the nuclear magneton (radians s^{-1}
Tesla^{-1}) and h is Planck's constant. For protons in a field of 1.4 Tesla,

$\omega_o \simeq 60$ MHz, which means that for effective *longitudinal* relaxation, $\tau_c \simeq 17$ ns.

Transverse relaxation, on the other hand, is effectively accelerated by frequency components of the order of ω_o *and* by static components ($\tau_c^{-1} \simeq 0$). Local deviations from H_o, leading to subtle differences in the local Larmor frequency are sufficient to destroy the overall phase coherency needed to observe a net transverse magnetization. The longer these deviations persist, the more effective they are. Therefore, if the molecular motions slow down, and τ_c^{-1} decreases, T_{II} decreases monotonously, reaching very low values in the case of solids.

For a polymer molecule at the solid/liquid interface it is expected that the train segments have very long reorientational correlation times. The loops, and certainly the tails, will be able to move faster. Therefore, different T_{II}'s should be measurable. There exist a number of relaxation experiments which can detect fast and slowly relaxing components (see section 5.4).

It has been observed in partially crystalline polymers (*Wilson* and *Pake*, 1957) that two distinct relaxations occur, one characteristic of the amorphous region and one of the crystalline region. If the same applies to adsorbed polymers, i.e. if the relaxation times of loops and tails on one hand, and those of trains on the other hand differ sufficiently, it should be possible to estimate p from relaxation measurements. However, it is also plausible to assume that small loops, with inherent low mobilities, relax fast enough to be counted as trains. Hence, NMR probably overestimates p.

As *Abragam* (1961, p. 83-84) has shown the minimum number of protons which is needed to exceed the noise level by a factor of two, at room temperature and in a magnetic field of 1 Tesla, is of the order of 10^{18} to 10^{19}. Consequently, the application of even proton NMR to surface phenomena is limited to adsorbents with high specific surface areas. Most other nuclei have lower sensitivity, so that the required number is even higher. Thus there is virtually no alternative for protons (except perhaps fluorine). Also, the presence of protons in solvents and non-adsorbed molecules must be rigorously avoided so that deuterated solvents can only be used if the isotopic purity is extremely good. Exchange reactions should be avoided. In view of all these inherent difficulties it is not surprising that detailed magnetic relaxation studies on adsorbed polymers have not been published as yet.

5.2.3 *Electron Spin Resonance*

The relaxation of the electron magnetization can be described in a scheme comparable to that for NMR. However, direct observation of the relaxation phenomenon is not possible in this case. Rather, it is the *resonance spectrum* which

is measured and this is composed of two components, one associated with mobile segments, showing narrow spectral lines, and one associated with immobile, fast relaxing spins, giving rise to a spectrum of broad lines. The experimental spectrum can be split up into these components by means of a fitting procedure and the bound fraction is calculated from the relative contributions of the components to the measured spectrum.

Most polymers do not contain the unpaired electrons which give rise to an ESR spectrum. Hence, a suitable spin-label must be attached to them, such that the labelling does not affect the adsorption behaviour of the polymer chain. It should be checked if this latter requirement is fulfilled, otherwise the results have no bearing upon the behaviour of the corresponding unlabelled polymer. Also, the labels should be distributed randomly along the chain.

From a sensitivity point of view the ESR technique is superior to NMR by approximately three orders of magnitude. It is certainly not restricted to high surface area adsorbents and in practice the required number of labels per polymer molecule is also small. Interference by solvent signals is usually absent so that good spectra are easily obtained.

5.2.4 Microcalorimetry

The heat evolved when a polymer adsorbs onto a solid surface may be considered to arise from essentially two contributions. One is the heat associated with the breaking of solvent-surface and solvent-polymer contacts and the concomitant formation of polymer-surface and solvent-solvent contacts in their place. We call this contribution ΔH_{tr} and we expect that it is proportional to the number of contacts n_{tr} between segments and the surface, at least if we deal with a homopolymer and a homogeneous surface.

The other contribution stems from polymer-solvent interactions. It is associated with the increase in segment density near the surface which is accompanied by the replacement of polymer-solvent contacts by polymer-polymer contacts, and therefore it should depend only on the difference in concentration between the adsorbed layer and the bulk solution. We call this second contribution ΔH_{mix}. Then:

$$\Delta H_{ads} = \Delta H_{tr} + \Delta H_{mix} = n_{tr} \, \Delta h_{tr} + \Delta H_{mix} \qquad (5.3)$$

where Δh_{tr} is the heat evolved if one contact between the surface and a segment is formed.

If it is assumed, as in the work of Killmann, e.g. (*Killmann et al.*, 1972) that ΔH_{mix} makes a negligible contribution, the measured heat of adsorption is

proportional to the adsorbance in trains, A_{tr}. For absolute values, we need an estimate of Δh_{tr}, which calls for some calibration procedure. Killmann calibrates his calorimetric data on the basis of bound fractions from infrared spectroscopy, thus giving up the independency of the calorimetric method. An independent method has not yet been proposed and, hence, absolute p-values have not yet been obtained from microcalorimetry. In chapter 6 we attempt to calibrate p-values independently, on the basis of heats of wetting and an estimate of the monolayer capacity.

The heat of adsorption is usually measured from the small temperature changes which develop immediately after mixing the adsorbate and the adsorbent. Such changes are only detectable if the total heat of adsorption is produced in a short time, i.e. if equilibrium is rapidly attained, typically within the first few minutes after mixing. For polymers, especially if their molecular weights are high, the completion of the adsorption process may take longer times, so that part of the heat of adsorption escapes detection. In such a case the results are not reliable because a molecular weight dependency is observed which is not due to equilibrium bound fractions.

5.2.5 *Electrical double layer capacitance*

As a rule, interfaces between solids and aqueous solutions carry a charge, which in many cases can be determined by titration with potential determining ions. Adsorbed molecules, even when uncharged, affect this surface charge so that a different titration curve is obtained. In the presence of sufficient neutral electrolyte (10^{-1} M) the electrical phenomena are virtually limited to a very thin layer adjacent to the solid surface (the *Stern layer*) and the titration curve exclusively reflects the number of segments which reside there: the trains. So far, the method has been applied to silver iodide on which polyvinyl alcohol was adsorbed (*Koopal* and *Lyklema*, 1975). Suitable calibration on the basis of results obtained with low molecular weight substances enabled these authors to calculate the surface occupancy θ. In order to derive absolute p-values, the monolayer capacity has to be known.

Through the work of Koopal and Lyklema, the electrical double layer technique is now well developed and it is to be regretted that in its application it is limited to aqueous systems and to surfaces with very well-characterized electrical double layer properties.

5.3 INFRARED MEASUREMENTS

5.3.1 *Experimental*

A series of PVP solutions of suitably chosen concentrations in dioxane were made up. In order to prevent penetration of moisture into the solutions, all preparations were made in a glove box filled with dried air. From each solution two 5 ml aliquots were pipetted into a sample bottle and a reference bottle, respectively, after which 5 ml of a silica sol was added to the sample bottle and 5 ml of pure dioxane was brought into the reference bottle. These volumes were pipetted carefully in order to match the total polymer concentration on a total volume basis in the sample and in the reference bottle as accurately as possible. The order in which components were added was found to have no measurable effect on the results. The bottles were closed and shaken manually. For the purpose of equilibration, all bottles were rotated slowly overnight.

All infrared spectra were recorded on a Hitachi Grating Infrared spectrometer model EPI – G 3, which a resolution of 2 cm^{-1} at 1000 cm^{-1} according to the manufacturer's specifications. The cells used were provided with calcium fluoride windows. The sample was brought into a demountable cell with a fixed path length of approximately 0.5 mm. The reference was placed into a cell with adjustable path length. Prior to each measurement the reference's path length was adjusted by filling both cells with pure dioxane and nulling any solvent signal.

Due to the formation of the carbonyl-silanol hydrogen bond in the sample, part of the free carbonyl stretching vibration band at the wave number v_o (v_o in dioxane is 1690 cm^{-1}, see table 5.1) disappears and a different band at a lower frequency emerges. This leads to a difference spectrum with a (negative) adsorbance - E at the frequency v_o. This is illustrated in fig. 5.1. According to Lambert Beer's law, the reduction in absorbance of the free carbonyls must be equal to $p\,c_A\,\Delta\,\varepsilon_o$, where c_A is the concentration of adsorbed polymer molecules, Δ is the path length and ε_o is the adsorption coefficient of free carbonyl groups. As can be seen in fig. 5.1 the absorbance of these free carbonyls is just equal to $E + E_A$, where E_A is the absorbance due to bound carbonyls at v_o. Hence,

$$p = \frac{E + E_A}{c_A\,\Delta\,\varepsilon_o} \qquad\qquad (5.4)$$

Since we have also $E_A' = p\, c_A\, \Delta\, \varepsilon_A$, we find that

$$p = \frac{E}{c_A\, \Delta\, (\varepsilon_o - \varepsilon_A)} \qquad\qquad (5.5)$$

This expression was also derived by *Morrissey* (1974) and enables us to determine p from E, c_A and Δ, once ε_o and ε_A are known.
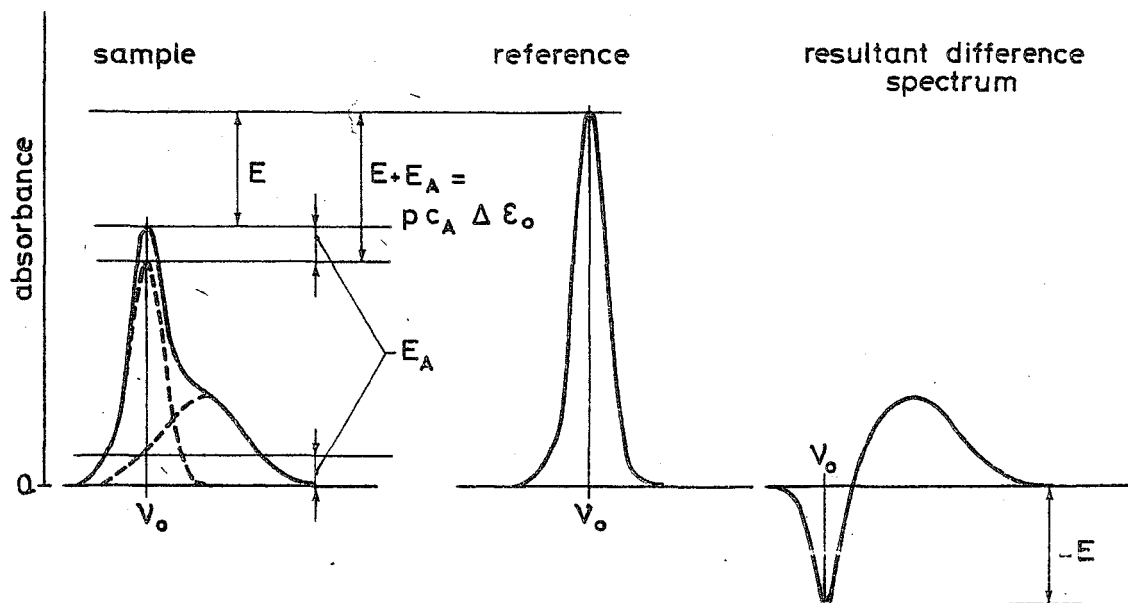

Fig. 5.1. Schematic drawing of the infrared spectra of sample and reference, respectively, and the resultant difference spectrum. The meaning of the absorptions E, -E and E_A (all measured at ν_o) are indicated.

The addition of the silica sol to the polymer solution always brought about strong flocculation, especially in the case of a high molecular weight PVP. As a result, the polymer was distributed inhomogeneously over the dispersion volume and it was difficult to bring a reproducible and representative amount of polymer into the light beam of the spectrometer. Due to this effect, the E-values obtained in the case of K_{90} were rather difficult to reproduce.

After taking spectra we determined the concentration of the adsorbed polymer, c_A, by centrifuging a 1.5 ml portion of the dispersion and determining the polymer concentration in the supernatant (see section 4.1). The path length Δ through the sample cell was measured by the standard method of interference of beams reflected at both walls of the cell. Due to this interference the transmittance of an empty cell is a periodic function of the radiation frequency. The number of maxima N_m occuring in a scan from wavenumber ν_1 to wavenumber ν_2 is related to Δ through:

$$\Delta = \frac{N_m}{2(\nu_1 - \nu_2)} \qquad\qquad (5.6)$$

The adsorption coefficient for the free carbonyl, ε_o, was measured from a number of spectra of PVP solutions (without silica) of known concentrations c, and applying Lambert-Beer's law:

$$E_o = \varepsilon_o \Delta c \qquad\qquad (5.7)$$

From a plot of E_o versus c, at known Δ, we determined ε_o (see fig. 5.2) as (5.06 ± 0.1) 10^{-3} cm^{-1} dm^3 mg^{-1}.
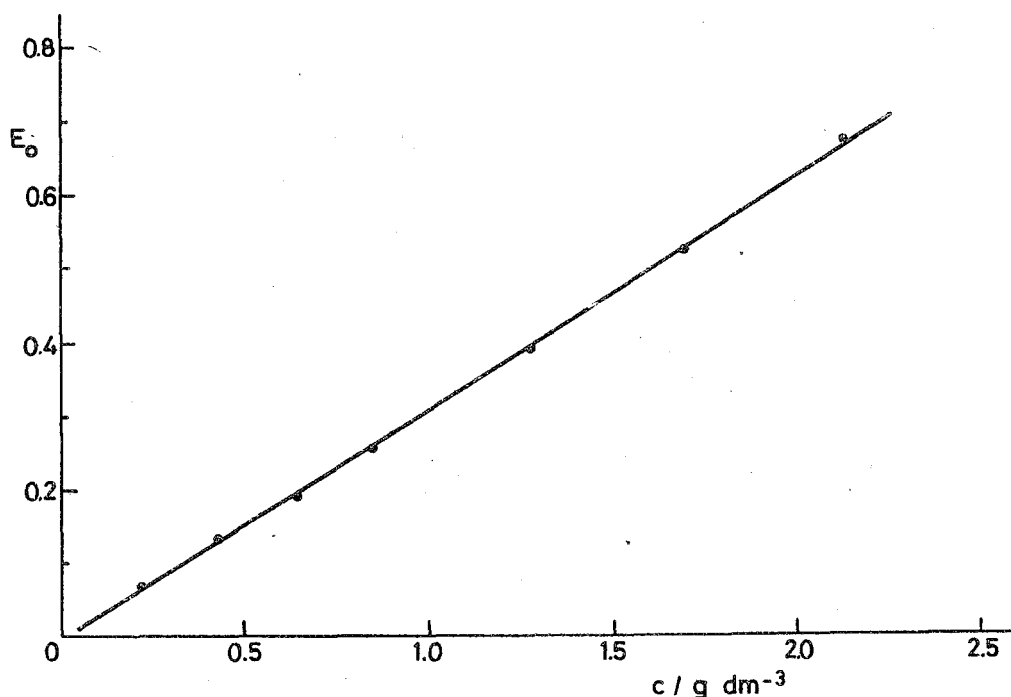
Fig. 5.2. Absorption of PVP in dioxane at 1690 cm^{-1} versus concentration. From the slope, ε_o is calculated.

The determination of the absorption coefficient ε_A for the bound carbonyl is more difficult. In principle, it requires removing the contribution of free carbonyls from the spectrum, and measuring the remaining intensity E_A at ν_o. As is easily seen from figure 5.1, ε_A can be found from

$$\varepsilon_A / \varepsilon_o = E_A / (E + E_A) \qquad\qquad (5.8)$$

Such a "pure bound carbonyl" spectrum can be obtained by diluting the reference solution (by a factor p c_A/c) until the contribution of free carbonyl vanishes.

The criterion for this condition is the shape of the difference spectrum: if a 'pure bound carbonyl spectrum' is associated with a single type of vibration it is expected to give rise to a single, more or less Gaussian peak. Although peak shape does not seem to be a very solid criterion, we found that it works reasonably well in practice. The value of $E/(E + E_A)$ was measured for a number of samples and the average value was used.

5.3.2 *Results and discussion*

A typical infrared spectrum of PVP in dioxane, in the range 1850 cm^{-1} to 1600 cm^{-1} was given in chapter 3, fig. 3.2. The carbonyl stretching vibration gives rise to a symmetrical and relatively sharp absorption peak, with its maximum at 1690 cm^{-1}. For comparison, the peak positions of this band in a number of other solvents are collected in table 5.1. Some were measured in this study, others were taken from the literature.

Table 5.1. Frequency of carbonyl stretching vibration of PVP in a number of solvents.

Solvent	Wavenumber/cm^{-1}	ref.
1,4 dioxane	1690	this work
1,2 dichloroethane	1683	Lety-Sistel (1975)
chloroform	1675	Lety-Sistel (1975)
chloroform	1678	this work
ethanol	1666	Lety-Sistel (1975)
methanol	1658	this work
trifluoroethanol	1663	Lety-Sistel (1975)
D_2O	1645	this work
Solid PVP on KBr disc	1670	this work

It is seen that in dioxane the maximum lies at the highest frequency and the carbonyl seems to be essentially non-interacting. In proton-donating solvents, the peak maximum lies appreciably lower. In the chlorinated solvents, the maximum lies a little lower than in dioxane. Probably the strongly electronegative chlorine atom attracts the electrons from the carbonyl group, thereby slightly weakening this bond.

An example of a difference spectrum obtained from adsorbed PVP is shown

in fig. 5.3. A strong negative absorption at v_o = 1690 cm^{-1} due to the disappearing of free carbonyls in the sample cell is seen. The peak transmission Tr at v_o is converted to the absorbance E according to E = - log Tr.
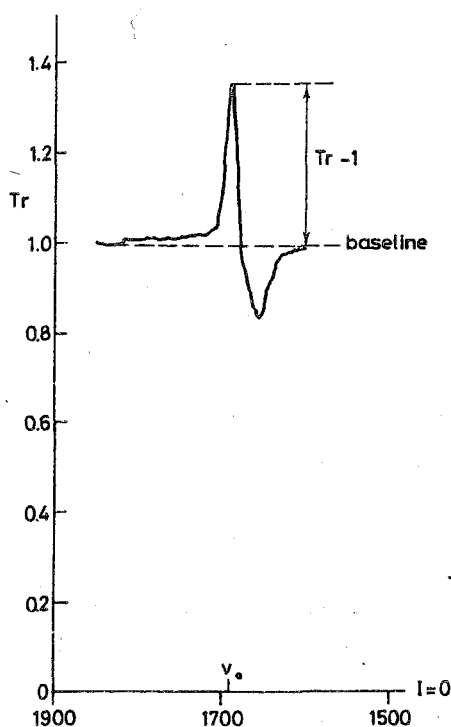

Fig. 5.3. (Transmission) difference spectrum obtained with adsorbed PVP.
The arrow indicates the transmission excess at v_o due to hydrogen bond formation.

Three consecutive dilutions of the reference solution give rise to the spectra in fig. 5.4. In spectrum a, the concentrations of free carbonyls in the sample and reference cell are not yet fully matched, so that a small negative absorption remains at v_o. In spectrum b compensation is complete, so that only a spectrum of bound carbonyls is recorded. Contrary to expectation, this spectrum has not one but two bands, at 1677 and 1655 cm^{-1}, respectively. In spectrum c, the concentration in the reference cell becomes too low and a positive absorption at v_o begins to distort the spectrum of the bound carbonyl.

As was pointed out before, the point where exact compensation is found has to be judged from the peak shape. It is therefore somewhat arbitrary. Spectrum b was assumed to correspond to exact matching because the transmission changes smoothly in the range 1700 to 1680 cm^{-1} and shows no traces of residual absorption at 1690 cm^{-1}. We read the absorbance E_A from the measured transmission Tr_A, indicated in spectrum 5.4b.
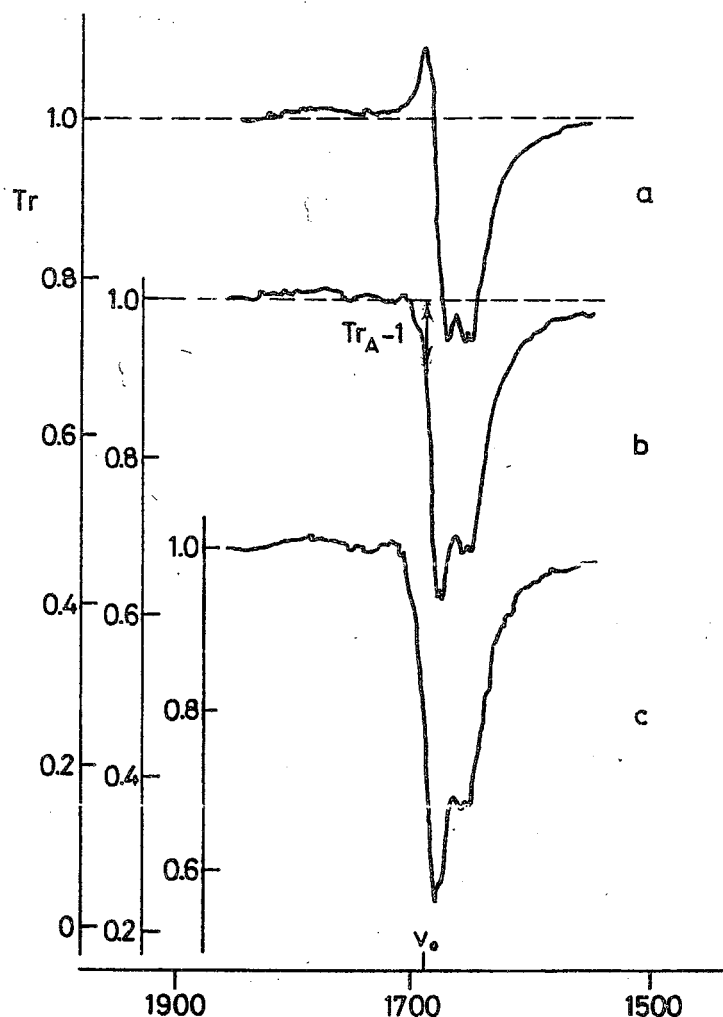
Fig. 5.4. Difference spectra obtained at various dilutions of the reference
solution. Spectrum b corresponds to the point where the absorption
of free carbonyls in the sample and reference are exactly matched,
so that the residual absorption at ν_o equals E_A. Spectra a and c
correspond to concentrations in the reference cell which are too
high and too law, respectively.

As mentioned above, the bound carbonyl spectrum (fig. 5.4b) deviates from
a single Gaussian peak in that two bands are observed. In addition, the band
around 1655 cm^{-1} seems to show some fine structure in which two lines can be
distinguished. In order to convince ourselves of the reality of this multiplet,
we carried out the compensation experiment repeatedly. It turned out that the
doublet structure of the bound carbonyl spectrum is a recurring phenomenon and
even the fine structure of the lowest frequency band was confirmed. Recently,
Korn (1978) has reported a similar doublet structure of the bound carbonyl ·
spectrum of polyvinyl acetate adsorbed from carbontetrachloride onto silica.

Apparently this phenomenon is not a specific feature of PVP. Rather, it may be a property of the silica and an indication that at least two distinct types of bonds between carbonyls and silica surface groups are formed.

We determined ε_A from a number of compensated spectra (eq. 5.8). The results are summarized in table 5.2.

Table 5.2. Determination of ε_A from a number of compensated spectra.

			experiment number			
	1	2	3	4	5	average
E	0.0412	0.0565	0.0947	0.0947	0.1404	
E_A	0.0057	0.0092	0.0110	0.0150	0.0246	
$\varepsilon_A/\varepsilon_o$	0.122	0.140	0.104	0.137	0.149	0.130 ± 0.017

The accuracy of the p-value is determined by a number of factors. Disregarding possible systematical errors, we may write for the error dp in p, on the basis of eq. (5.5):

$$(dp/p)^2 = (dE/E)^2 + (d\Delta/\Delta)^2 + (d\ c_A/c_A)^2 + \{\ d\ (\varepsilon_o - \varepsilon_A)/(\varepsilon_o - \varepsilon_A)\}^2 \qquad (5.9)$$

where dE, dΔ, d c_A and d $(\varepsilon_o - \varepsilon_A)$ are the absolute errors in E, Δ, c_A and $(\varepsilon_o - \varepsilon_A)$, respectively. For each of these contributions we estimated the error, on the basis of known instrument specifications and reading errors.

It turns out that at low amount of polymer, dE constitutes a dominant contribution of about 9%. The optical path length can be determined within 1%, concentration errors can be reduced to 2% by careful handling of samples and although ε_A could not be determined better than within 14%, the difference $\varepsilon_o - \varepsilon_A$ is dominated by ε_o so that the inaccuracy of $\varepsilon_o - \varepsilon_A$ is only 3.5%. In total, the error in p may be 10% at low adsorbed amount and somewhat smaller (7%) at higher polymer concentrations. However, systematical errors may sometimes be the cause of a poorer accuracy. We mentioned above the inhomogeneous distribution of polymer in the infrared cell due to flocculation, which gave rise to considerable irreproducibility. Also, contamination of samples with UV-active substances during the determination of the supernatant concentration (see chapter 4.1) may lead to serious errors in the value of c_A. In conclusion, we expect that the experimental p-values will have an uncertainty of about 20% with regard to the mean value.

Fig. 5.5 shows the p-values obtained from a number of measurements, as a

function of the adsorbed weight A. A systematic effect of the molecular weight
was not detected. In view of the accuracy limits discussed above, one single
line was drawn to represent all the results obtained for different molecular
weights and different adsorbed amounts. As would be expected, p is a decreasing
function of A, being about 0.5 at low A, where the adsorbed molecules are
virtually isolated, and reaching a value of about 0.25 at high A, where
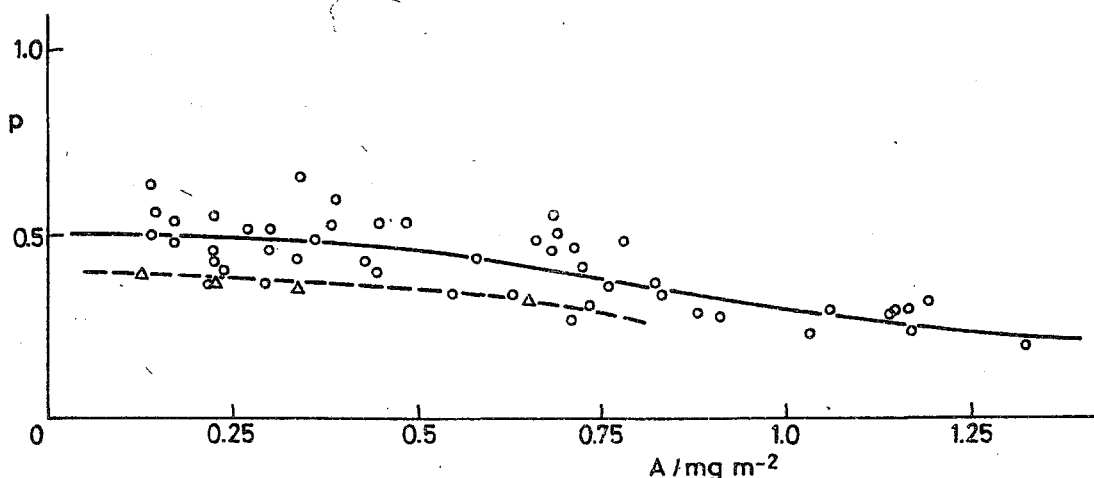competition for surface sites takes place.

Fig. 5.5. Infrared bound fractions as a function of the adsorbed amount:
    o   with normal silica, dried at 120° C;
    Δ with silica heated at 900° C.

In order to verify, whether it were really the surface silanols which were
responsible for the formation of bound carbonyls, we also adsorbed PVP onto a
silica from which all hydroxyl groups are removed by reaction with an organo-
silicon halide (Aerosil R 972, Degussa, BRD). Although the polymer did adsorb
weakly (about 1 mg m^{-2} at 800 ppm) the difference spectrum showed only a very
small peak at ν_o, indicating a bound carbonyl fraction of about 2%. We conclude
that silanols are indeed involved in the formation of hydrogen bonds with the
carbonyls.

Results obtained with silica heated at 900° C prior to adsorption were not
very different from those with normal silica (see fig. 5.5). The bound carbonyl
spectra were identical, and the p-values were only slightly lower. Thus, most
of the surface groups active in the interaction with polymer (in dixoane solution)
were still present on this heated silica. *Korn* (1978) studied the effect of
heating on the adsorption of polybutylmethacrylate from carbontetrachloride onto

silica. He found that p was even slightly higher on the heated silica, and he concluded that the heating process produced some unstable siloxane bridges which were also able to interact with polymer carbonyls. It is as yet difficult to say whether such an interaction occurs also in the system PVP/dioxane.

In connection to this, we refer also to the conclusions of *Hair* (1977) who found that hydrogen bonding occurs mainly with the isolated silanol groups which do not form hydrogen bonds with neighbouring silanols. These groups are also the most stable ones as they do not disappear on heating even up to 900° C. *Mills* and *Hockey* (1975) arrive at essentially the same conclusion in a study of the adsorption of fatty acid methyl esters on silica.

5.4 NUCLEAR MAGNETIC RELAXATION EXPERIMENTS

5.4.1 *Experimental*

As has been pointed out in section 5.2.2, the application of NMR to polymer adsorption is hampered by lack of sensitivity and by the fact that the most sensitive nucleus, the proton, is often present in both polymer and solvent and sometimes even in the adsorbent. The success of the experiment therefore critically depends on sample preparation. After many unsuccesful attemps we succeeded in preparing a single sample which proved suitable for the experiments. The preparation procedure was the following.

Carefully dried silica (100 mg) was dispersed in 10 ml D_2O with an isotopic purity of 99.8 %. About 25 mg of dried PVP were dissolved in 10 ml of the same solvent. The solution and the (stable) sol were brought together in a screw-capped polypropylene centrifuge tube and agitated for approximately one hour. By gentle centrifuging at about 8000 g (Beckman J 21-B centrifuge, 5000 rpm) during 90 minutes the polymer coated silica was concentrated at the bottom of the tube, after which the supernatant was decanted immediately. To eliminate solvent-protons and non-adsorbed PVP, highly pure D_2O (100.0 %, Bio-Rad) was added to the residue which was then allowed to repeptise by gentle agitation during 3 hours. After centrifugation for 45 minutes at 8000 g the supernatant was again discarded. This treatment was repeated twice. Then, a few drops of D_2O 100.0 % were added and the silica was redispersed quickly by ultrasonic vibration. The dispersion was then transferred to a 5 mm NMR sample tube with a Pasteur pipette. The tube was capped and sealed airtight with epoxy resin. Removal of solvent protons was checked by recording a high resolution NMR spectrum on a Hitachi Perkin Elmer R-24 B High Resolution NMR spectrometer (fig. 5.6).
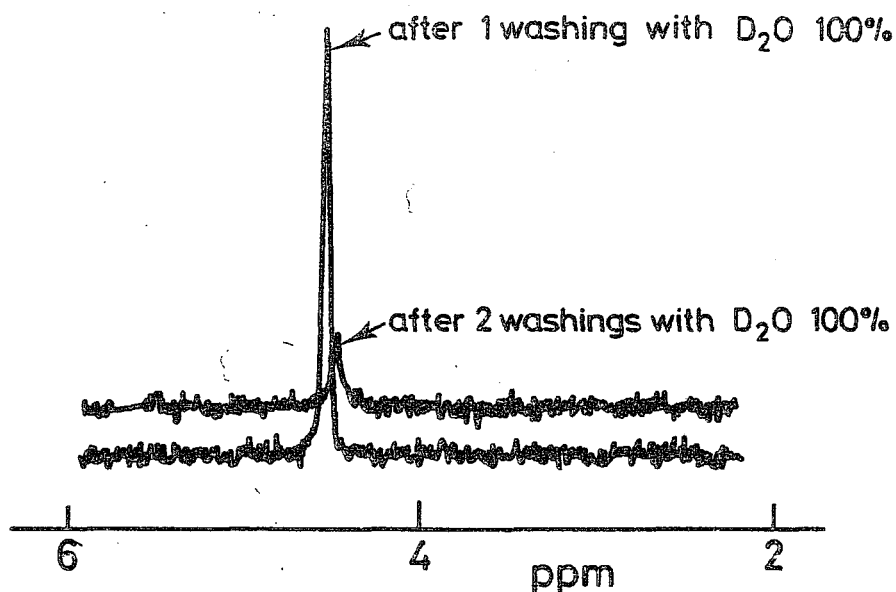
Fig. 5.6. High resolution spectra of a silica dispersion with adsorbed PVP in
D_2O, after two consecutive washings with high purity D_2O. It is seen
that after the second washing the proton content is strongly reduced.

It should be noted that the sample which was used in the experiments
was, in spite of many precautions, slightly flocculated.

Relaxation spectra were recorded on a specially designed spectrometer[*].
The equipment consists of a powerful 2.5 kW emitter capable of producing a 90°
pulse for protons within 5. 10^{-7}s. The RF-probe, based on a design of *Ellett*
(1971) was constructed such that no non-metallic material was used in the
vicinity of the detecting coil. High pulse suppression was achieved by careful
matching of the detector and transmitter circuits and extra broad banding of
the receiver. Spectral accumulations were made using a Datalab high speed data
aquisition system. The network of spectrometer components is shown in fig. 5.7.
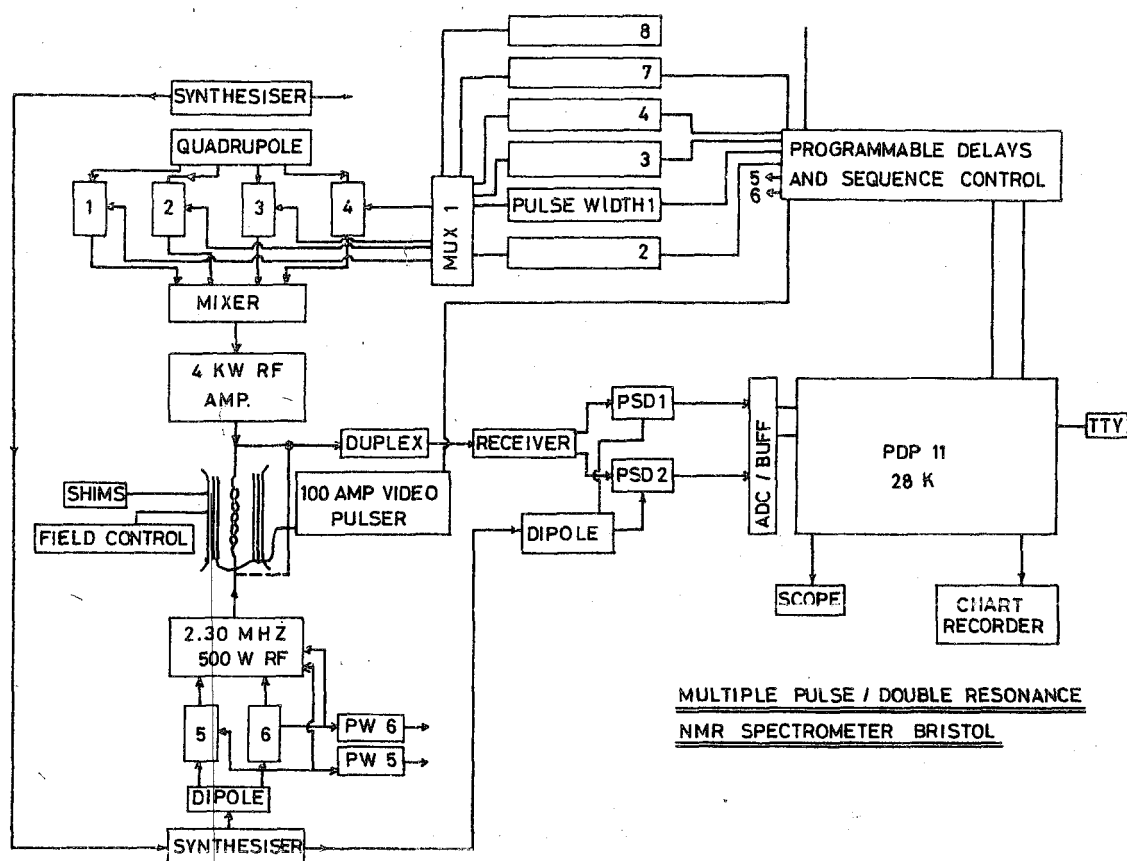
Fig. 5.7. Scheme of NMR spectrometer components.

5.4.2 *Results and discussion*

The sample which was used in the experiment had been prepared with K_{90}. Three relaxation spectra were recorded, each with different pulse sequences. These sequences are characterized by essentially three quantities: the pulse length, the pulse phase and the time lag between pulses, t_i. The pulse length t_p determines the angle β through which the magnetization is rotated away from alignment along the static field:

$$\beta = \gamma H_1 t_p \qquad (5.10)$$

where H_1 is the strength of the (rotating) magnetic field produced by the pulse and γ is a magnetic constant. If $\beta = 90^\circ$, the transverse component of the magnetization is maximal, and if $\beta = 180^\circ$, the magnetization is just opposite to the static field. It is β, rather than t_p which is the quantity of interest; therefore pulse sequences are usually described in terms of β. The pulse phase determines the axis around which the magnetization rotates away from the static field. A pulse which is in phase with the detector is called an x-pulse; a 90°

phase lag corresponds to a y-pulse. The interval t_i between pulses is chosen
in accordance with the time scale of the ralaxation process under investigation.

The first spectrum, shown in fig. 5.8 is a so called Bloch-decay, obtained
by measuring the decay of the magnetization after each of a series of alter-
nating 90°, x and 90°, -x pulses. The result was obtained by averaging 2350
of such spectra to ascertain a reasonable degree of noise reduction. As can be
seen, the spectrum has two discrete regions. At the onset, there is a fast decay,
which is probably Gaussian with a decay time of about 16 μs. This fast decay
is followed by a long one, characterized by a decay time about ten times as
long. It seems that two components are present, as expected. However, two more
spectra were recorded in order to check this conclusion more rigorously, and to
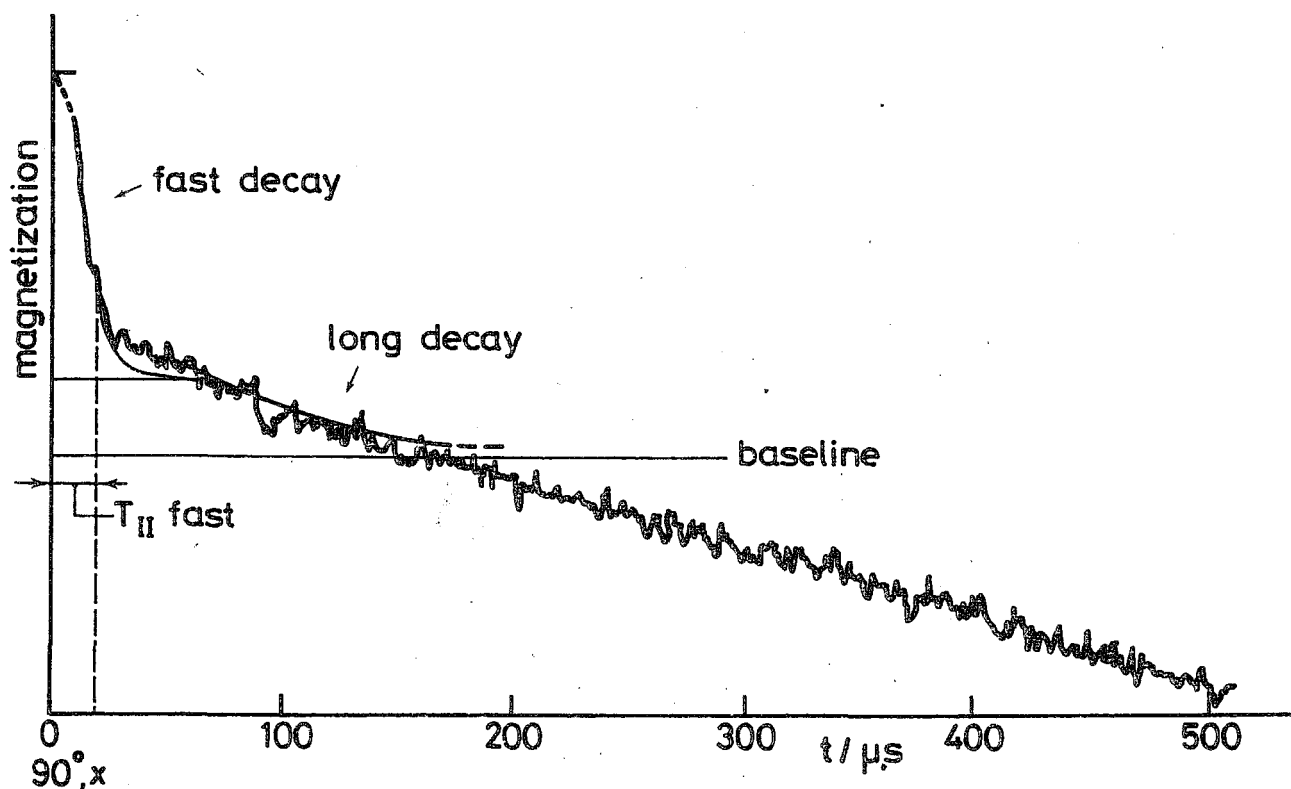measure p.

Fig. 5.8. Bloch decay of adsorbed polymer. Two components can be seen, indicative
of mobile chain parts (tails and loops) and immobile parts (trains),
respectively. The decrease in signal height at times longer than 200
μs is probably due to a background signal.

Fig. 5.9 gives the decay after a 90°, $x - t_i - 90^{\circ}$, y pulse sequence.
The number of scans was 11,170. This sequence preferentially refocuses the fast
component and produces an 'echo' at 2 t_i. Since t_i was chosen to be 20 μs, the
echo is expected at 40 μs. Such an echo is indeed clearly observed, thus esta-
blishing beyond doubt the existence of a fast relaxing component. For a random
distribution of molecular orientations the echo is expected to be Gaussian in
shape. A fit of the experimental curve to a Gaussian peak gives a characteristic
decay time T_{II} = 15.7 μs which agrees well with the decay time of 16 μs for the
fast component which was seen in the Bloch decay.
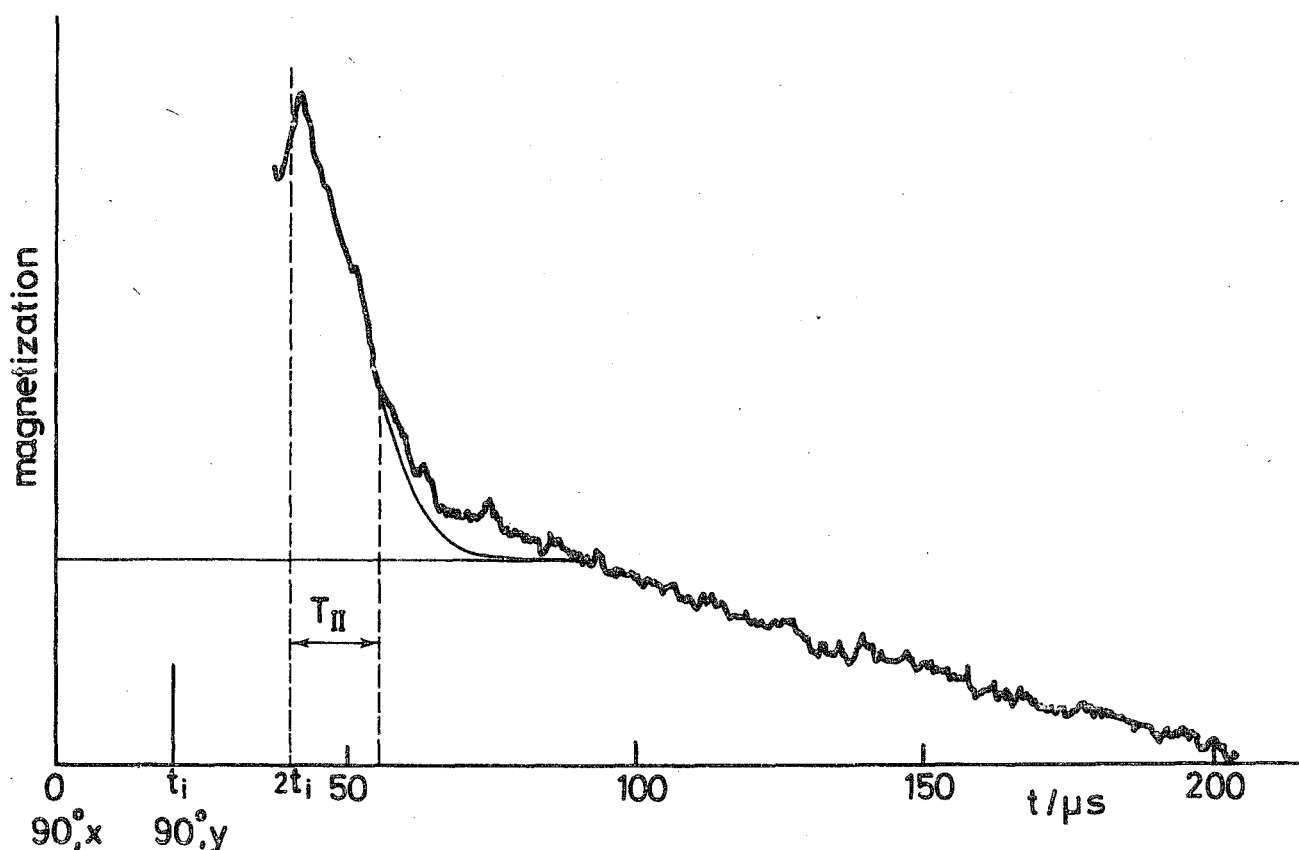
Fig. 5.9. The 'solid echo' due to train segments of adsorbed PVP. 90°, x and
90°, y pulses are indicated at 0 and at 20 μs, respectively. A
Gaussian was fitted to the peak shape, which gave T_{II} = 15.7 μs.

The third spectrum shown in fig. 5.10 is from a 90°, $x - t_i - 180^{\circ}$, y
experiment, also with t_i = 20 μs. Such a sequence gives also rise to an echo after
the 180°, y pulse and is commonly referred to as a conventional spin echo experiment.

The signal between the 90°, x and the 180°, y pulse is the total magnetization M^O, corresponding to the total number of protons in the sample. Since free polymer molecules were removed in the preparation procedure, the signal height M^O is proportional to the total weight of adsorbed polymer. The signal following the 180°, y pulse (the echo) is insensitive to the fast component which showed up in the previous spectrum. It contains only the components in more mobile parts of the polymer chains which relax more slowly, and therefore its value at 40 µs is proportional to M^O (1-p).

In order to find the signal heights we must know what the common baseline is for the whole spectrum 5.10. Since we cannot record the spectrum to full relaxation we cannot find this baseline directly. However, from theoretical considerations we know that at longer times the echo must decay exponentially. The point A where exponential behaviour starts is indicated in fig. 5.10. A method of *Swinbourne* (1960) to find the baseline corresponding to any exponential decay can then be applied to this exponential part of the curve. We draw the fitted line in the spectrum, as well as the corresponding baseline. The spectral intensities at 15 and at 40 µs, counted from this baseline, now correspond with the total amount of polymer and the mobile fraction, respectively. We find p = 0.75. Hence, a relatively large fraction of segments are immobilized in the adsorbed state. However, at 40 µs the spectrum of the mobile component probably contains a slight contribution from the fast decay. This can be estimated to amount to approximately 6%. Correcting for it we find p ≃ 0.80.

It is interesting to note that for the mobile conponent a transverse relaxation time of 84 µs is found. This implies that the narrowest spectral line for this sample would have a width of about 4 kHz which is, in terms of a conventional high-resolution experiment, undetectably wide. Thus it is not surprising that *Miyamoto* and *Cantow* (1972) were unable to detect a high resolution spectrum for adsorbed polymer.
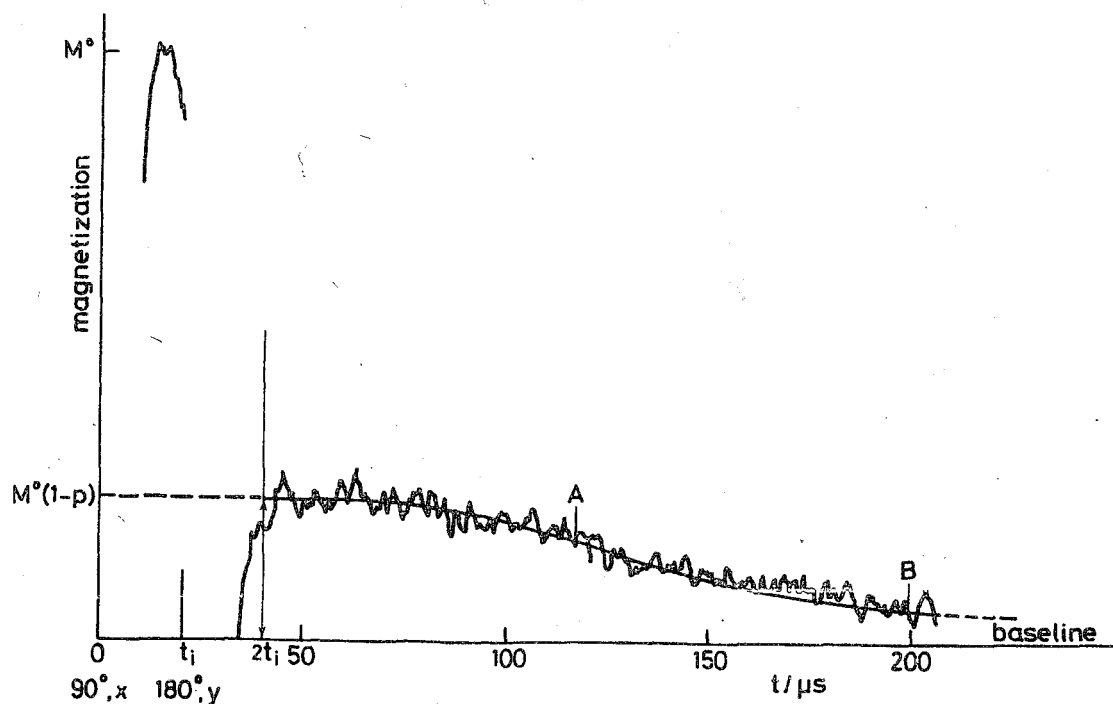
Fig. 5.10. Conventional spin echo experiment showing total magnetization (M^o) and mobile component echo $(M^o(1-p))$. The baseline was reconstructed assuming the decay of the echo to be exponential between A and B. 90°, x and 180°, y pulses are indicated at 0 and 20 µs, respectively.

5.5 ELECTRON SPIN RESONANCE: A DISCUSSION OF EXPERIMENTAL RESULTS FROM THE LITERATURE

A number of electron spin resonance (ESR) results have been published by Robb and coworkers (*Fox et al.*, 1974; *Clark et al.*, 1976; *Robb et al.*, 1974). These studies shed some light upon the conformation of PVP adsorbed from aqueous solutions onto pyrogenic silica. For their experiment, the investigators employed a copolymer of alkylamine (3%) and vinyl pyrrolidone, which was labelled with a nitroxide group by reacting the amine group with 4,4,6,6-tetramethyl piperidino-oxylisocyanate. The distribution of spin labels along the chain obtained in this way is presumably random. Samples were prepared by adsorbing this polymer from water onto silica and subsequent removal of the excess polymer in the solution.

In a separate experiment it was checked that the spin label itself does not adsorb in measurable amounts from the aqueous solution (*Robb* and *Smith*, 1977). Although this observation does not exclude the possibility that the copolymer adsorbs in a way different from a pure PVP chain, the difference is probably small. Robb and Smith claim that their results are also applicable to the adsorption of PVP homopolymer from water onto silica, so that we can compare these data with our NMR and IR results.

The ESR spectrum could be decomposed into two components. One exists of broad lines and corresponds to spins of low mobility and a relatively long correlation time (τ_c of the order of 10^{-8} s) and the other has narrow lines and stems from spins with a mobility comparable to that of the unadsorbed polymer molecule ($\tau_c \simeq 8 \times 10^{-10}$ s). (Note that in the NMR experiment the mobility of loops and tails was still far from the mobility of free molecules).

The main findings of Robb et al. are the following. PVP assumes a conformation with a relatively small number of mobile segments. The p-value decreases with increasing adsorbed amount from about 0.9 to about 0.6. Addition of salt (0.1 N CaCl) has a negligible effect. Equilibrium is rapidly established: spectra were taken repeatedly starting 2 minutes after mixing polymer and adsorbent, but no changes could be detected in the course of time.

We plotted the ESR p-values as a function of the adsorbed weight in fig. 5.11. The curve shape is rather similar to the one obtained from infrared spectroscopy (fig. 5.5) but all p-values lie appreciably higher. The NMR result, $p \simeq 0.8$ compares reasonably with the ESR results. It seems that both NMR and ESR detect a large immobile component. The agreement is not perfect, though, because the molecular weight of the polymer in the NMR experiment (K_{90}) was relatively high and the adsorbed amount would be expected to be close to 1 mg m^{-2}. The adsorbed amounts in Robb's experiment are at most 0.75 mg m^{-2}, but from an extrapolation in fig. 5.11 we estimate p (ESR) for A = 1.0 mg m^{-2} between 0.4 and 0.5, which is only half the value calculated from the NMR experiment. Some flocculation of the sample (see section 5.4.1) could possibly account for part of the difference.
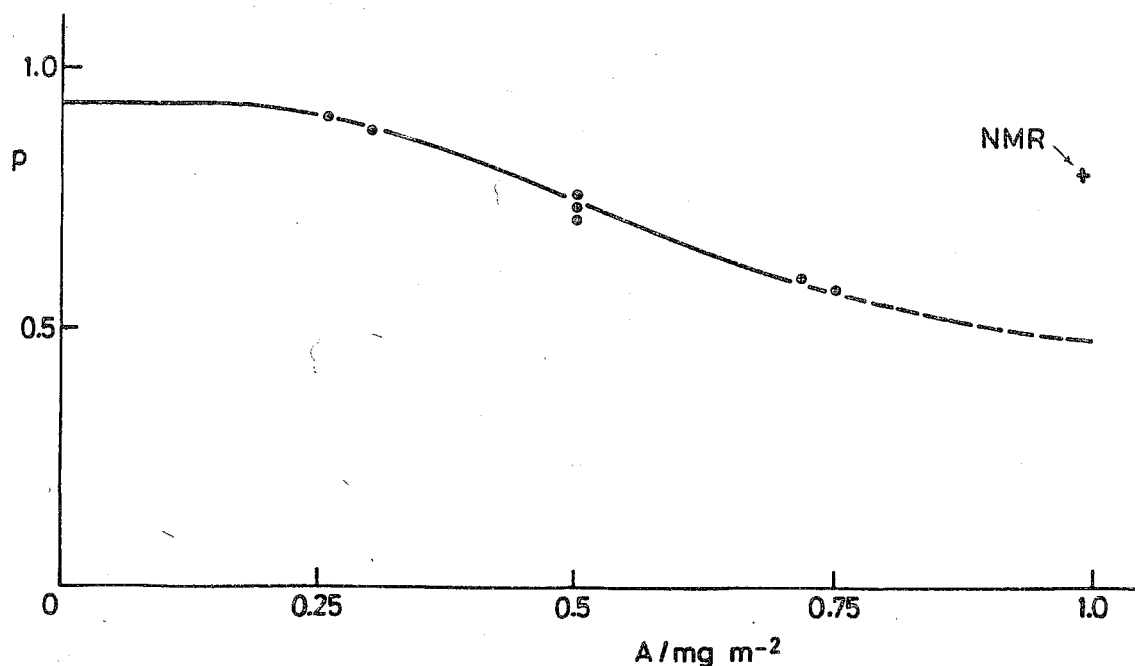
Fig. 5.11. Bound fractions measured with ESR as a function of adsorbed amount. The data were taken from *Robb* and *Smith* (1974).

5.6 MICROCALORIMETRY

5.6.1 *Experimental*

Heats of adsorption were measured in an LKB 10700 microcalorimeter of the batch (conduction) type equipped with two 18 carat gold vessels. Each vessel is divided into two compartments, a big one and a small one, the contents of which can be mixed by rotating the calorimeter block. The temperature difference ΔT between the sample and the reference vessel is determined by means of sensitive thermopiles. The resultant thermovoltage is measured with a Keithley 150 B Microvolt Ammeter, and recorded versus time. The total heat evolved is proportional to the voltage-time integral. The design and mode of operation of this calorimeter has been extensively discussed by *Wadsö* (1968). Calibration of the instrument was carried out by heating one of both cells. This was accomplished applying a known current through a calibrated resistor during a predetermined time.

Adsorption enthalpies were measured in the following way. The small compartments of both cells were filled with 2 ml of a polymer solution. The big compartment of the sample cell was fitted with 4 ml of a silica sol, that of the

reference cell with 4 ml of solvent. Hence, upon rotation, adsorption takes place in the sample cell, whereas in the reference cell the polymer solution is merely diluted. The actual experiment was performed after allowing the system to reach thermal equilibrium. Usually this took 1.5 to 3 hours. The measurement itself was completed in 15 to 20 minutes. It was checked that dilution of silica alone did not give rise to detectable heat effects. Heats of dilution of the polymer were measured by mixing polymer solution and solvent in the sample cell, with only pure solvent in the reference cell.

Heats of wetting of dry silica were determined in a Tronac 450 adiabatic calorimeter. A glass bulb filled with dried silica was broken in a Dewar flask containing the wetting fluid. The resultant temperature jump was measured by means of a temperature-sensitive resistor and calibration was again achieved by means of a heating current through a calibrated resistor.

5.6.2 Results and discussion

In fig. 5.12 we reproduce a typical recording of a microcalorimetric experiment. The shaded area is proportional to the amount of heat evolved. The experiment is followed by a calibration (curve b). Reasonably accurate areas could be obtained by cutting and weighing of the recorder graphs.
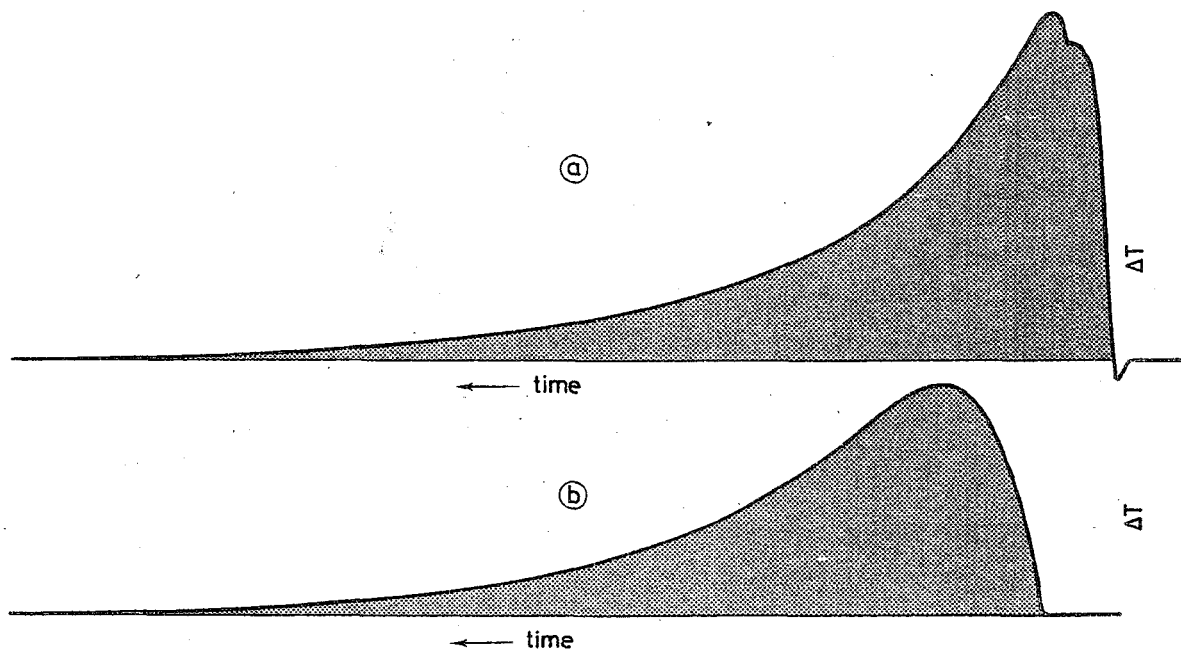
Fig. 5.12. Typical recording of a calorimetric experiment (thermovoltage as a function of time). Curve (a): measurement. Curve (b): calibration.

For heats evolved rapidly after mixing, the detection level is about 0.5 mJ and the inaccuracy is of the same order of magnitude. As we only measured heats of adsorption larger than 6 mJ the results were reasonably accurate. In fig. 5.13, the heat of adsorption ΔH_{ads} is plotted as a function of the adsorbed amount A for both water (a) and dioxane (b), and for two different PVP samples (K_{12} and K_{90}).
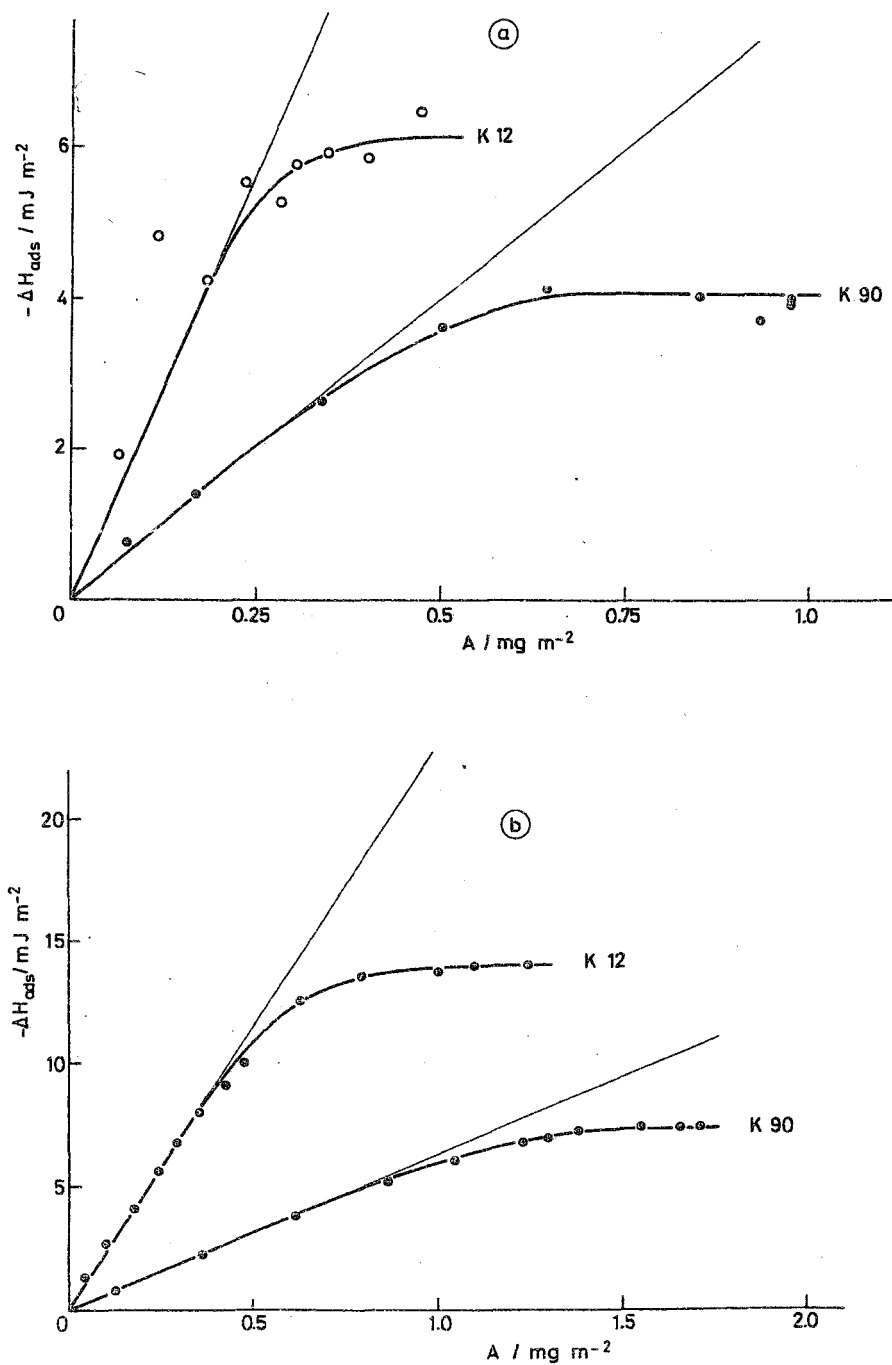
Fig. 5.13. Heats of adsorption of PVP as a function of the adsorbed weight for two different polymer samples (K_{12} and K_{90}).
(a) from aqueous solution
(b) from dioxane

All curves show an initial linear part at low A and reach a limiting value at higher A. The heats found in dioxane are higher than those in water, but in both systems the plateau level and the slope of the initial part decrease with increasing molecular weight. Similar results were obtained by *Killman, Strasser* and *Winter* (1972) for the adsorption of poly ethylene oxide from carbon tetrachloride onto silica. For reasons to be explained below the molecular weight dependency was not expected (see chapter 2). We therefore thought it useful to explore this phenomenon a little further and we measured the plateau value of ΔH_{ads} as a function of molecular weight. The results are plotted in fig. 5.14. The systematic decrease of ΔH_{ads} with M_v is obvious.
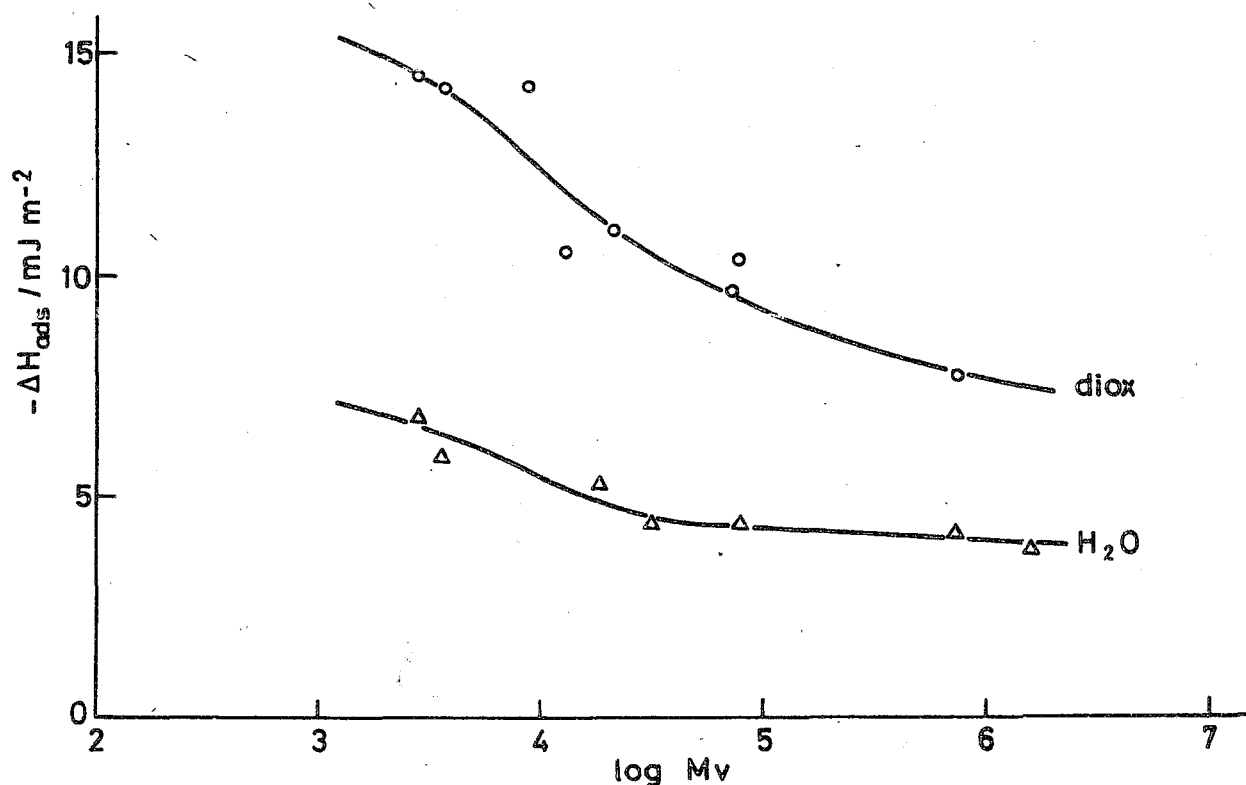
Fig. 5.14. Heats of adsorption of PVP at the plateau adsorbed amount, as a function of molecular weight (M_v), from water and from dioxane.

For the adsorption of PVP from water and from dioxane on silica heated to 922° C we measured almost the same ΔH_{ads} as on unheated silica. However, on the hydrophobic silica Aerosil R 972, PVP adsorbed from dioxane almost without a detectable heat effect. We conclude that silanol groups are required to produce heat effects in adsorption onto silica, and that the silica surface heated to about 900° C can still fulfil this requirement.

As was argued in section 5.2.4, ΔH_{ads} may contain a contribution related to the heat of mixing, ΔH_{mix} (eq. 5.4). Since from theoretical considerations it is not expected that the surface occupancy θ, and thus n_{tr}, depends on the molecular weight, it might be that this second term ΔH_{mix} accounts for the observed molecular weight dependency in ΔH_{ads}. As is clear from the results, such an explanation is only acceptable if ΔH_{mix} has the same sign for both water and dioxane.

We measured ΔH_{mix} as a function of the polymer volume fractions ϕ before dilution. We write for ΔH_{mix} a modified Tompa expression (*Murakami et al.*, 1975)

$$\Delta H_{mix} / RT\, n_+^o = \phi\phi' \{ \kappa_1 + \kappa_2 \ (\phi + \phi') / 2 \} \tag{5.10}$$

where n_+^o is the number of moles of solvent added to the polymer solution, ϕ' is the volume fraction of polymer after dilution and κ_1 and κ_2 are constants. However, for sufficiently dilute solutions the first term of the right hand side of (5.10) will be dominant, so that we can estimate κ_1 accurately enough by plotting ΔH_{mix} against $\phi\phi'\, n_+^o$. In fig. 5.15 this was done for PVP K_{12} in water. From the slope of this curve a value of 0.304 RT mol^{-1} for κ_1 is derived. For other PVP samples in water, dioxane and methanol, the same procedure leads to the κ_1 values summarized in table 5.3.
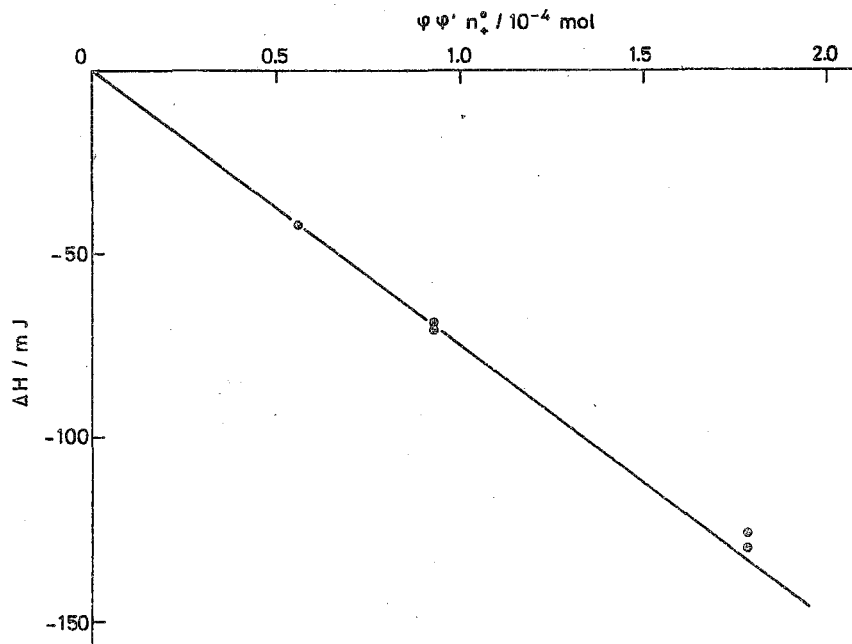
Fig. 5.15. Heat of dilution of a function of concentration. From the slope of the curve, κ_1 is obtained.

Table 5.3. Heat of dilution parameter κ_1 for a number of PVP samples, in various solvents.

Polymer sample	M_v (g mol^{-1})	κ_1 / RT (mol^{-1})		
		H_2O	dioxane	methanol
K_{12}	3590	-0.304		-0.264
K_{17}	8875	-0.207		
K_{25}	28100	-0.121	+0.238	
K_{30}	43200	-0.092		
K_{90}	731000	-0.082		-0.043

As can be seen, dilution in the proton-donating solvents water and methanol is exothermic ($\kappa_1 < 0$) whereas in dioxane it is endothermic ($\kappa_1 > 0$). Thus, the mixing contribution cannot account for the molecular weight dependency in ΔH_{ads}. Furthermore, we find a surprising molecular weight dependency of κ_1 in water: the heat of dilution drops sharply at low M_v until at molecular weights of about 80,000 a constant value is attained (see also fig. 5.16). In methanol, there is also a substantical decrease between κ_1 for K_{12} and for K_{90}, so that we do not believe that it is a specific feature of the aqueous solution.
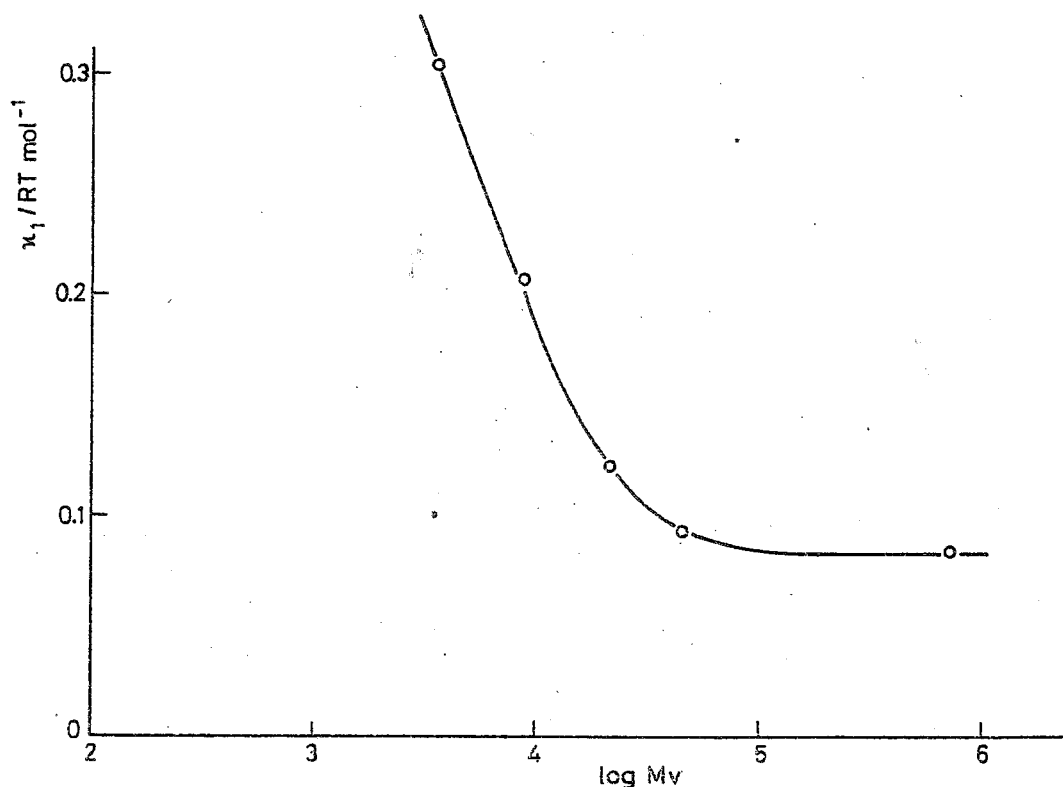
Fig. 5.16. Molecular weight dependence of the heat of dilution parameter κ_1; PVP in aqueous solution.

Heats of wetting were determined for water, dioxane and NEP. These are tabulated below (table 5.4). For the sake of comparison a few literature values are also included. As can be seen, for water the agreement is fairly good, but our value for dioxane is probably less reliable.

Table 5.4. Heats of wetting of pyrogenic silica.

Wetting fluid	$- \Delta H / J\ m^{-2}$	
	this work	literature data
H_2O	0.142	0.142 (Killmann et al., 1972)
dioxane	0.131	0.146 (Killmann et al., 1972)
		0.146 (Curthoys et al., 1974)
NEP	0.170	-

*Korn* (1978) compares enthalpies of hydrogen bond formation obtained on the basis of the spectral shift relations as suggested by *Hair* (1977) and *Hertl* (1968) with those calculated from measured adsorption enthalpies. For this calculations, heats of wetting and infrared bound fractions were used. In the case of mono-functional, low molecular weight adsorbates (for which p = 1) he found very good agreement. Hence, the binding enthalpies for these adsorbates can, in principle, derived from gas phase adsorption and wetting data. However, in the case of polymers, the measured enthalpies were systematically lower than those expected from the spectral shift (*Korn*, 1978, p. 70). For high polymers, the differences found were of the order of 12 kJ per mole of monomer units, which is about 25%. This observations appears to be in line with the decrease of ΔH_{ads} with molecular weight observed in this study.

One explanation was already suggested: the contribution ΔH_{mix} is not negligible, so that the total enthalpy does not exclusively reflect the process in the layer immediately adjacent to the solid surface. This explanation was rejected since it is inconsistent with the fact that the heats of dilution in water and dioxane have opposite signs.

A different explanation is that the heat effect is incomplete, because the adsorption process is slow. As has been argued in the introductory section (5.2.4) the microcalorimeter is not able to detect heats which evolve too slowly to give rise to a measurable temperature difference. With increasing molecular weight, the adsorption process might slow down so that the heat effect

is smeared out over longer times. As a result, part of the heat effect escapes detection. This explanation agrees with the experimental data presented by *Killmann et al.* (1972) and *Korn* (1978) and with our results. It leads to the conclusion that microcalorimetry has important limitations as a method to study the adsorption of heigh polymers. For short chains, however, it can be a useful technique.

In chapter 6 we compare the results for low molecular weight PVP (K_{12}) with theoretical results. In this chapter, we also develop a way to calibrate the calorimetric data in units of surface occupancy.

Chapter 6

Comparison of experimental and theoretical results.

6.1 CHOICE OF THE PARAMETERS

In this chapter we want to compare numerical results from the modified Scheutjens-Fleer theory, which was described in chapter 2, section 2.6, with the experimental data obtained in our study of the PVP/silica system. For the calculations we need the following input variables: the lattice type (from which we find the coordination number Z and the fraction of neighbouring sites in the same layer), the bulkiness parameter b, the number of segments per chain r, the energy parameters χ and χ_s and the concentration. In order to convert the results to experimentally measurable quantities, we must also estimate the monolayer capacity A^{mon}. In the following subsection we briefly comment on the choices which were made for all these quantities.

6.1.1 *Lattice type*

Although an adsorbed polymer may, in a sense, be regarded as an anisotropic solution, the anisotropy cannot be a consequence of the lattice type which is chosen to describe the solution. Since the lattice is merely a tool to describe a particular physical situation, it would be illogical if this tool had an effect on this situation. Therefore we require that in our lattice the *a priori* probabilities for steps in three orthogonal (i.e. x-, y-,and z-) directions are all equal. Steps in a givenplane (e.g. parallel to the adsorbing wall) are then twices as probable as steps perpendicular to that wall.

The lattice which meets this requirement is the simple cubic lattice with Z = 6, so that we prefer this lattice for our description of the solution adjacent to the solid/liquid interface. Both Roe (1974) and Scheutjens and Fleer (1979) varied the lattice type but they found that the results do not depend very critically on the lattice type chosen.

6.1.2 *The bulkiness parameter b*

As was pointed out in section 2.6.1, we shall define a segment on the basis of the thickness d of the chain (eq. 2.23). We can estimate d^2 from the volume of the PVP chain, which is $L\,d^2 = Pv_{mon}$. Here, L is the length of the fully stretched chain. Inserting eq. 2.9, written in the form: $L = 0.253\,P$ (nm), we obtain $d^2 = 3.95\,v_{mon}$, or

$$P/r = 7.85 \sqrt{v_{mon}} \qquad (nm) \qquad\qquad (6.1)$$

Here, d is expressed in nm and v_{mon} in nm^3. With $v_{mon} = 0.156 \ nm^3$ (*Brandrup* and *Immergut*, 1975) we find $P/r = 3.1$ and $d = 0.784$ nm. Since the same value for d was found from estimates of the monolayer thickness with the help of molecular models, we regard this as a reliable value.

In order to check whether the flexibility is reasonably accounted for with the above choice for P/r, we calculate P/r also on the basis of chain flexibility data, from eqns. (2.26) and (2.30). Concerning eq. (2.26) we assume that the flexibility of PVP can be reasonably compared to that of polystyrene, for which Tonelli (see Flory, 1969, p. 236) estimated $Z_p = 1.62$. With $Z = 6$, this leads to $P/r = 3.7$. Eq. (2.30) contains the characteristic ratio C, for which values were given in section 3.3.5. It was concluded there that in a number of theta solvents PVP behaves as a flexible chain. For these solvents, $C = 7.1$, which leads to $P/r = 3.8$. However, in other solvents the chain stiffens somewhat, giving $C = 10$, and $P/r = 5.3$.

We conclude that the isotropic statistical segments found from the application of (6.1) are only slightly shorter than those estimated from the flexibility of PVP. Hence, the statical segments that we shall use in our model are reasonably consistent with the conformational properties of the PVP chain. In connection to this, we mention that *Boyer* and *Miller* (1977) found a strong correlation between the cross-sectional area (d^2) and the flexibility (expressed in C) for a large number of different polymer chains. Hence, d^2 is a good measure for the flexibility of a given polymer.

We can now calculate the bulkiness parameter b from eq. (2.22). Inserting $v_1 \ (H_2O) = 3.0 \ x \ 10^{-2} \ nm^3$ and $v_1 \ (diox) = 1.4 \ x \ 10^{-1} \ nm^3$ we find

$$b(diox) = 3.6 \qquad\qquad (6.2\ a)$$
$$b(H_2O) = 17.1 \qquad\qquad (6.2\ b)$$

The number of statistical segments for a chain of molecular weight M follows from $r = P/3.1 = M/3.1 \ M_o$ or

$$r = M/347 \qquad\qquad (6.3)$$

6.1.3 *Polymer solvent interaction parameter* χ

From the results presented in section 3.3.3 it turns out that the polymer-solvent interaction parameter χ depends on concentration. For H_2O it decreases with increasing volume fraction of polymer, whereas for dioxane it increases.

In section 3.3.4 we discussed the possibility to incorporate this concentration dependency into the lattice theory and we conclude that such an incorporation is only justified if χ represents purely local interactions. We cannot be sure that this is the case. Also, the values of χ at high ϕ are subject to experimental uncertainty. Therefore we use the value of χ for the dilute solution throughout the calculations. For water, this leads to $\chi = 0.48$, for dioxane to $\chi = 0.49$.

6.1.4 *Adsorption energy parameter* χ_s

In section 4.3 we described a method to assess the adsorption energy parameter $\Delta\chi_s$ by means of displacement studies. We also concluded that the number obtained from these experiments is the residual adsorption energy per displacer molecule, and that $\Delta\chi_s$ *per segment* is found by considering the average number of displacer molecules that occupy the same area as a polymer segment.

For a homogeneous surface this would lead to the conclusion that the experimental $\Delta\chi_s$ value must be multiplied by the ratio f between the surface areas occupied by a segment and a displacer molecule, respectively. For the segment we estimated, on the basis of a molecular model, an area d^2. It would be logical to estimate the effective area for the displacer molecules also from such a model, but it turns out that the outcome is not consistent with the experimentally determined monolayer capacities (see section 4.3.3). Therefore we prefer to take these experimental values of A^{mon} as our basis and we find that the effective area per molecule must be $M_D/N_{AV} A^{mon}$ where M_D is the molecular weight of the displacer (table 3.1), N_{AV} is Avogadso's number and A^{mon} is the displacer's monolayer capacity as obtained from a Langmuir plot. A discussion of the reliability of A^{mon} values was given in section 4.3.3; values are tabulated in table 4.2. We find that

$$f = d^2 A^{mon} N_{AV} / M \tag{6.4}$$

The value for $\Delta\chi_s$ per segment is found by multiplying the values tabulated in table 4.3. For d^2 we use 0.61 nm^2 (section 6.1.2). The values for f are given in table 6.1, together with the values of $\Delta\chi_s$ per segment.

Table 6.1. Conversion factor f and residual adsorption energy $\Delta\chi_s$ per segment.

	water		dioxane	
	f	$\Delta\chi_s$ (per segment)	f	$\Delta\chi_s$ (per segment)
PYR	4.17	4.13	0.74	2.82
NEP	0.55	1.49	0.62	2.55
NEM	0.22	1.04	1.81	6.84
NMP	0.69	2.96		
DMSO	0.42	1.46	1.61	6.06

As is seen from table 6.1 the spread in the values is considerable. We pointed out in section 4.3.3 that the data for both χ_s^D and A^{mon} are not very reliable for a number of reasons. Therefore we should not be surprised that the results of the displacement experiments do not lead to a well defined value for $\Delta\chi_s$. Hence, we regard χ_s more or less as an adjustable parameter whose value must be somewhere in the range covered by the experimental values. It turned out that a reasonable fit could be obtained with the following choices

$$\chi_s \text{ (dioxane)} = 4$$
$$\chi_s \text{ (water)} = 2.5$$

6.1.5 *Concentration*

In the plateau region of the adsorption isotherm, the adsorbed amount and the conformation depend only weakly on the concentration c. Therefore, the choice of c is not very critical. We used adsorbed amounts at c $\simeq$ 800 mg dm^{-3} to establish the molecular weight dependency (see fig. 4.4). This concentration corresponds to a volume fraction of about 6 x 10^{-4} if the specific volume V_2 of PVP is taken into account. Thus for all calculations $\phi_* = 6$ x 10^{-4} was chosen.

6.1.6 *Monolayer capacity*

Theoretical results are expressed in numbers of monolayers (see section 2.3). In order to compare them with experimental results we need to know the monolayer capacity A^{mon}. In a fully packed monolayer we have one segment with volume d^3 and weight d^3/V_2 on each surface site with area d^2. The weight of polymer per unit area in a compact monolayer is then

$$A^{mon} = d / V_2 \qquad\qquad (6.5)$$

Using $V_2 = 0.78 \times 10^{-6}$ m^3 g^{-1} (*Brandrup* and *Immergut*, 1975) and d = 0.784 nm we find A^{mon} = 1.02 mg m^{-2}.

6.2 RESULTS AND DISCUSSION

For the calculations the original programme for the Scheutjens-Fleer theory, written in Algol by *Scheutjens* (1979), was modified by introducing the bulkiness parameter b (see 2.6.3). All calculations were carried out on a DEC-10 computer.

6.2.1 *Adsorbed amount*

In fig. 6.1 we compare experimental and theoretical results for the adsorbed amount A as a function of molecular weight M. Both log M and log r (related through r = M/347) are indicated on the horizontal axis; the vertical axis displays both Γ and A (related through A = 1.02 Γ).
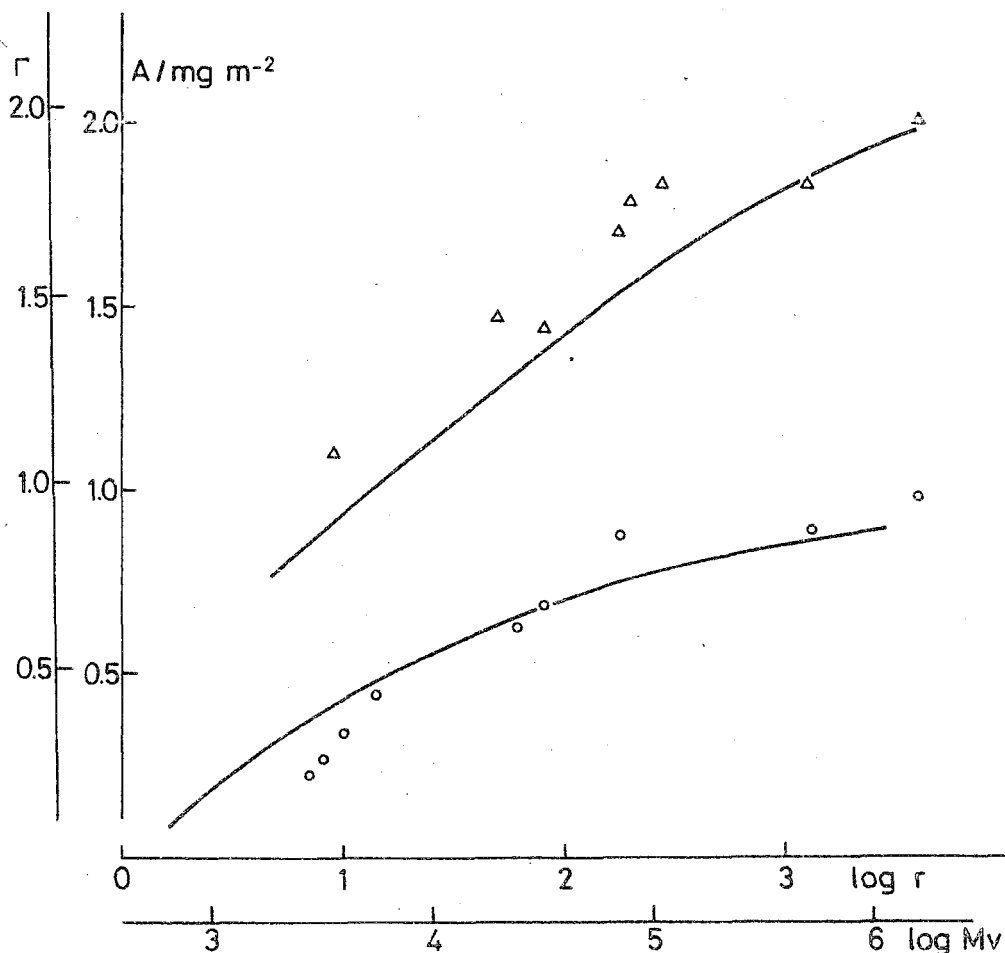

Fig. 6.1. Adsorbed amount as a function of chain length. The ordinate gives both the adsorbed weight A and the adsorbance Γ, and the abscissa gives both r and M on a logaritmic scale. Solid curves are theoretically calculated. Experimental points are indicated for dioxane (triangles) and water (circles).

Since the experimental points deviate by no more than 10 to 20 % from the theoretical curve over the whole molecular weight range, we conclude that the agreement is fairly good. Also the slopes of the theoretical curves give a very good representation of the experimental trend. By far the most important factor determining the difference in behaviour between dioxane and water is the bulkiness. This is to be expected, because differences in the energy parameter between both systems are only small and yet a large difference in adsorbed amount is observed. Hence, only a difference in bulkiness can account for the experimental facts. We conclude that the incorporation of the volume properties of polymer and solvent   is an essential step. It brings the theory into much closer agreement with experimental results, and gives an explanation of solvent effects not included in χ.

The experimental points on the low molecular weight end of the curve for water indicate a somewhat stronger decrease of A with decreasing M than calculated from theory. We have no straightforward explanation for this. It may be due to the fact that for short chains the conformational entropy is not adequately described by a single parameter Z_p (Flory, 1969). Another reason may be a poorer fractionation of the lower molecular weights, so that poly-dispersity effects would play a role.

For the higher molecular weights, where $M_w/M_n \simeq 1.5$, polydispersity effects are not expected to be important for the case that $S/V \simeq 650$ (*Cohen Stuart et al.*, 1980). Hence, despite the far from perfect fractionation technique, the dependency of the adsorbed amount on M_v can be fairly well described by the theory.

6.2.2 *Bound fraction*

Although we found in section 2.6.3 that the conformation of the macromolecules at the interface depends hardly on the bulkiness parameter b, we note that the curve of the bound fraction p versus Γ changes shape under the influence of b, since Γ is considerably affected. In fig. 6.2 we compare the bound fraction measurements for PVP from dioxane as determined by infrared spectroscopy with the theoretically predicted values. The theoretical curve shows a decrease at adsorbed amounts larger than 0.7 monolayers; from the experimental points a similar trend can be concluded. Perhaps, the decrease of p with Γ in the experimental results starts already at a somewhat lower Γ. The striking feature of fig. 6.2 is, however, that at given Γ the theoretical bound fraction exceeds the experimental one by a factor of two or more.
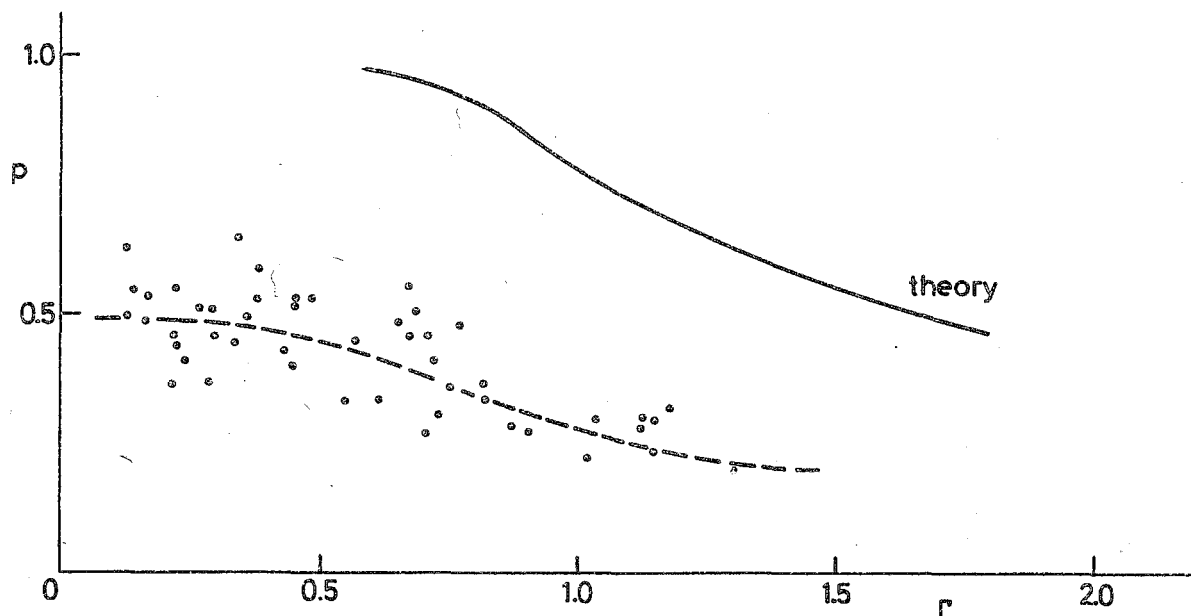
Fig. 6.2. Bound fraction in dioxane calculated from theory (solid curve) and
as inferred from IR spectroscopy (experimental points, dashed line).

The discrepancy can be resolved by assuming that from the monomer units in
train segments maximally only 50% can form a hydrogen bond with the surface.
This may seem a rather drastic restriction. However, by inspection of Stuart
models of the polymer molecule we found that for purely sterical reasons it is
very difficult to bring all carbonyl groups in a train sequence close enough to
the surface to make hydrogen bonding possible. For polymers where the carbonyls
are in the backbone of the chain (e.g. polycarbonates, poly amides) the sterical
restriction would be less. Taking into account the fact that the interaction
occurs almost exclusively with isolated silanol groups (see section 5.3.2) and
that the density of these is low so that they are, on average, rather far apart
we conclude that it is indeed highly probable that only part of the monomer
units in train segments actually form hydrogen bonds with the surface. Hence,
the underestimation of the bound fraction by IR measurements (already discussed
in chapter 5) seems to be very serious, at least in the case of PVP adsorbed on
silica.

The results of *Korn* (1978) for the adsorption of polymers with carbonyl
groups from CCl_4 on silica are also indicative of such an underestimation.
An exception is polycaprolacton, where p measured by IR varies from 0.8 at low
adsorbance to 0.3 at high adsorbance. However, here the carbonyl is part of the

backbone, and the flexibility of the chain is presumably high. Since all polymers used in the study of Korn adsorb through hydrogen bonds (from carbon tetrachloride) we expect them to have rather high segmental adsorption energies (χ_s). Hence, p values would be expected to be high, especially at low adsorbed amounts. Korn finds for those polymers where the carbonyl is in a side chain p-values which, as a rule, are below 0.5, thus corroborating the explanation given above.

It turns out that the infrared technique is useful for qualitative studies concerning the bound fraction. It cannot be employed for quantitative purposes.

Robb et al. (1974) used electron spin resonance to determine bound fractions of PVP adsorbed from water. We compare the theoretical curve for this case with the experimental points, both plotted as p versus Γ (fig. 6.3).
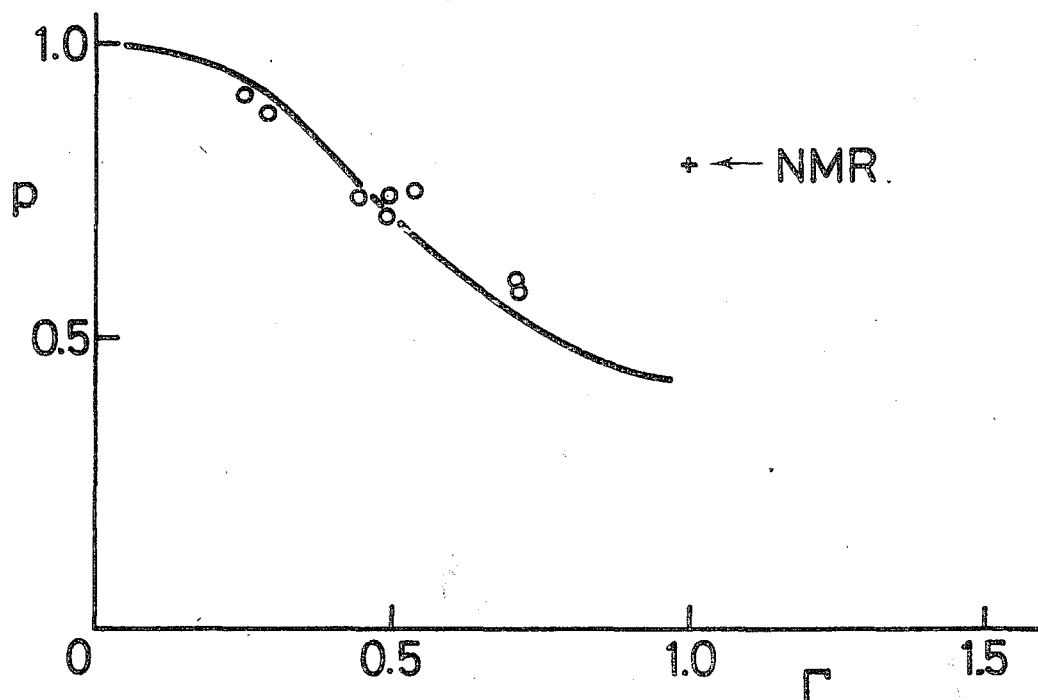
Fig. 6.3. Bound fraction in water, calculated from theory (solid line) and as measured with ESR (experimental points). The NMR result is also indicated.

The agreement is surprisingly good. Overestimation of p, as was regarded a possibility (section 5.2.2) appears negligible. The conclusion must be that ESR is a very good technique for the measurement of bound fractions, at least in the case of PVP.

The NMR result is also indicated in fig. 6.3. Unfortunately, the adsorbed amount is not accurately known; it was estimated as about 1.0 monolayers.

However, the result is undoubtedly higher than the ESR result. Whether this is
due to slight flocculation in the sample or whether NMR inherently overesti-
mates bound fractions cannot be concluded from the present results. In conclu-
sion, ESR seems to be superior to the infrared method. The possibilities of NMR
are not yet fully explored so that an evaluation of this technique cannot be
given as yet.

6.2.3 *Surface occupancy*

In a first approximation, the surface occupancy θ is expected to be propor-
tional to the enthalphy of adsorption, ΔH_{ads} (see e.g. *Killmann et al.*, 1972).
In fig. 6.4 we therefore plotted ΔH_{ads} per unit of surface area against the
total adsorbance Γ for both water and dioxane. As has been discussed in section
5.5.2, the calorimetric measurement is not suitable to measure adsorption
enthalpies for very high molecular weight polymers, because part of these
adsorption processes are too slow to give rise to a measurable heat effect. For
this reason we used only the results obtained with K_{12}, which has a relatively
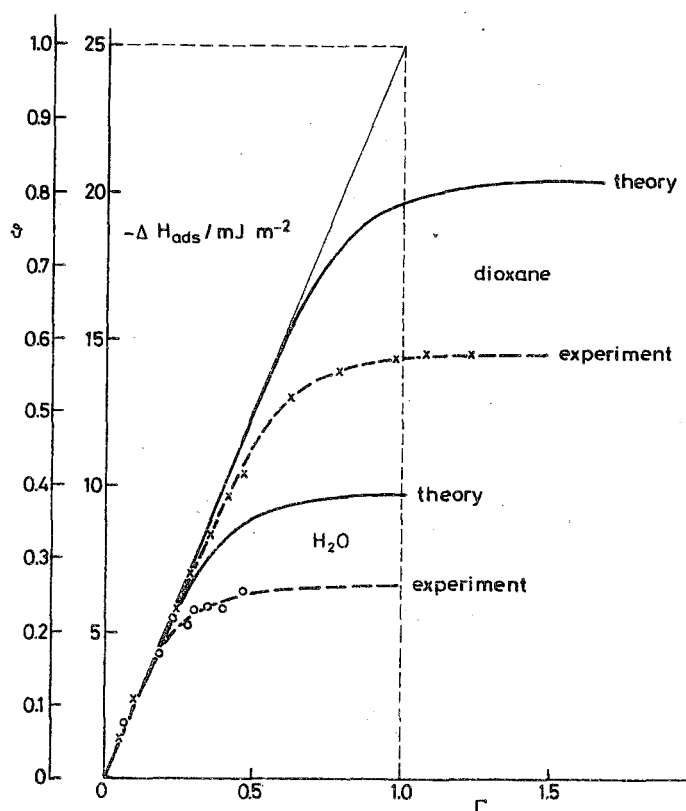low molecular weight.

Fig. 6.4. Surface occupancy θ and adsorption enthalphy ΔH_{ads}, as a function of
adsorbance. Solid curves are theoretically calculated and dashed
curves were drawn through the experimental points. Extrapolation of the
initial slope to $\Gamma = 1$ enabled us to calibrate the ordinate (θ) in
monolayers.

From the theoretical results of *Scheutjens* and *Fleer* (1979) we know that at very low coverage and high χ_s, the (initial) slope of the θ versus Γ curve (which equals p) is almost equal to unity. Since in our case χ_s was estimated as 2.5 and 4, respectively, this must also be so for PVP adsorbed from water and from dioxane onto silica. The important implication is that if we extrapolate the tangent to the initial part of the ΔH versus Γ-plot until it intersects the line $\Gamma = 1$, we find the adsorption enthalphy for which $\theta = 1$. In this way we can calibrate the ΔH-axis in monolayer units.

The curves $\Delta H(\Gamma)$ for water and for dioxane have the same initial slope and, hence, the enthalphy ΔH^{mon} corresponding to $\theta = 1$ is identical in both solvents, namely $\Delta H^{mon} = 25$ mJ m^{-2}. Accordingly, we converted the ΔH-axis into a θ-axis. ΔH^{mon} may be compared to the difference in the enthalpies of wetting between pure polymer (ΔH_{pol}) and pure solvent (ΔH_{sol}). Since a wetting experiment with pure polymer cannot be carried out, we determined the heat of wetting for the analogue of the monomer unit, N-ethyl pyrrolidone (NEP). The latter heat may serve as a reasonable approximation for ΔH_{pol}. Wetting experiments were reported in section 5.5.2. We find a difference of 28 mJ m^{-2} between the wetting enthalpies of NEP and water, and 24 mJ m^{-2} between the heats of wetting of NEP and dioxane. Both values agree within experimental accuracy with the value ΔH^{mon} = 25 mJ m^{-2} derived from the adsorption enthalpies. Hence, both the calibration of θ on the basis of this number and the neglect of mixing enthalpies (ΔH_{mix}) in the initial part of the enthalpy curve seem to be justified. From ΔH^{mon} we calculated the adsorption enthalpy Δh_{tr} per segment, using the contact area $d^2 = 0.61$ nm^2 between a segment and the surface. The result is $\Delta h_{tr} \simeq 4$ kT, which is just the value that was used for χ_s in dioxane. This would mean that in dioxane χ_s is purely enthalpic. However, for water the χ_s-value that seems to describe the adsorption rather well is 2.5, and this leaves a difference of 1.5 kT of entropic origin to be explained. It is difficult to imagine how the entropy is lowered by the exchange of water molecules at the surface with a segment. In view of the many uncertainties in the value of χ_s we do not pursue this point any further.

The calibration described above enabled us to include the theoretical curves $\theta(\Gamma)$ into fig. 6.4. Qualitatively, there is reasonable agreement between these theoretical curves and the experimental points. For dioxane, a high plateau of about 0.8 is calculated, whereas for water the plateau is lower by a factor of 2.1 and amounts to 0.38 monolayers. The experimental ratio of 2.2 for the plateau values is nearly the same. However, in both cases the absolute value of the theoretical plateau in θ is about 45% higher than the experimental one.

We mention a number of possible reasons for this difference. First, ΔH_{ads} may not be strictly proportional to θ. There may be a non-negligible contribution

ΔH_{mix}, arising from polymer-polymer interactions (see section 5.1.4). As was shown, however, the sign of ΔH_{mix} is expected to be different for water and for dioxane, at least for not too concentrated solutions. For dioxane $\Delta H_{mix} < 0$, and an increase above the theoretical plateau rather than a decrease would be expected. So, this explanation seems to fail, unless the heat of mixing reverses sign at high concentrations. A heat of mixing correction could be estimated from eq. (5.10) and the values for κ_1 given in table 5.3. Using $\phi \simeq 0.5$, $\phi' = 10^{-4}$, and, since the volume of the adsorbed layer is negligible small, a dilution volume of about 10 ml m^{-2} we find values of the order of 5 mJ m^{-2} for the heat of mixing. Hence, a correction for the heat of mixing would have the right order of magnitude, provided that the κ_1-values from table 5.3 are still valid for the high volume fractions occurring in an adsorbed layer.

Second, the proportionality may not hold because the silica surface is energetically heterogeneous. The heterogeneity leads to large ΔH_{ads} values at low Γ, because then the sites of highest energy are preferentially occupied. As Γ increases, adsorption occurs on sites of lower energy, leading to a smaller enthalpy change per train segment. Suppose that the distribution of energies among the sites were the same in both water and dioxane. The train segments in dioxane would distribute over all these energies (since θ is high in dioxane) but in water only the sites of high energy would be preferably occupied. Hence the effect of heterogeneity would be more pronounced in water than in dioxane. This is not observed, so that any explanation on the basis of surface heterogeneity must imply different adsorption mechanisms for water and for dioxane.

Third, kinetic factors at high M, as already discussed, may have reduced the expected enthalpy effect; this reduction would probably depend somewhat on the segment density and, hence, on the solvent quality and on χ_s. To avoid it, smaller molecular weights must be used, but then it becomes doubtful whether the full range of θ-values can be covered at low bulk concentrations.

In view of the above discussion we want to stress that straightforward interpretation of adsorption enthalpies in terms of the segment density in the first layer is not possible, because the adsorbing interface may be energetically heterogeneous, enthalpies arising from other interactions than those between the polymer and the surface may contribute to ΔH_{ads}, and kinetic effects may obscure part of the heat effect. In spite of all these problems the theory accounts fairly well for the general shape of the enthalpy curve and for the ratio in plateau values between the curves for dioxane and water. However, the plateau values themselves do not agree wit measured adsorption enthalpies.

6.3 EVALUATION OF THE MODIFIED SCHEUTJENS-FLEER THEORY

In the preceding section we compared the theoretical predictions of the modified Scheutjens-Fleer theory with a variety of experimental data. Looking over these discussions, we arrive at the conclusion that this theory describes the adsorption of the neutral homopolymer polyvinyl pyrrolidone on silica rather well.

Among the parameters, needed for the calculations, only the adsorption energy χ_s is difficult to assess. The uncertainty in the experimental value of this parameter is considerable so that it remains, to some extent, an adjustable quantity. However, with a reasonable choice within the range covered by the experimental values the experimentally determined adsorbed amounts are, within 10 to 20 %, equal to the theoretically predicted values.

Also the conformation, as expressed in p and θ, conforms rather well with the theoretical results. The agreement is best with the ESR results. The bound fraction as inferred from infrared spectroscopy is systematically too low, differing from the theoretical value by a factor of about two. However, the difference can satisfactorily be explained from the structure of the PVP chain and the morphology of the silica surface. The NMR experiment gave a slight overestimation of p, but more data are needed in order to adequately evaluate this technique. For the calorimetric measurements, the slope of the enthalpy curve at low coverage could be correlated with enthalpies of wetting. The theoretical plateau values were too high, but they had the same ratio as the plateau values of the experimental enthalpy curves.

It should be emphasized that such good agreement was not possible with the original Scheutjens-Fleer theory. The introduction, on purely theoretical grounds, of the bulkiness parameter proved to be an essential step towards a complete theory. The large differences found between the adsorption from water and from dioxane could only be satisfactorily explained by the difference in molecular volume between these two solvents.

Since the water molecule is so small, it is to be expected that the pronounced effect of the bulkiness parameter, as found for the adsorption of PVP, will be observed more generally. Thus, homopolymers adsorbing from water will do so in smaller amounts than homopolymers adsorbing from organic solvents, provided that the χ-parameters are not too different. Checking this conjecture would be a worthwile aim for future investigations.

In a number of studies (e.g. *Koopal*, 1978) copolymers are adsorbed. Although copolymers behave like homopolymers in a number of respects, one should not apply the above conclusions to the adsorption of these molecules. E.g., polyvinylalcohol with remaining acetate groups behaves in a rather different way because of preferential adsorption of the more hydrophobic segments.

6.4 THE CONFORMATION OF PVP AT THE SOLID/LIQUID INTERFACE

The Scheutjens-Fleer theory gives a full description of the conformation of adsorbed polymers. Since this theory, after the incorporation of the bulkiness parameter, seems to be well supported by the experimental data gathered in this study, we believe that the theoretically calculated conformations corresponds rather closely to physical reality. It may therefore be useful to present the data calculated for the conformation in more detail. These data are for a PVP molecule adsorbing from a dilute dioxane solution ($c \simeq 800$ mg dm^{-3}).

In fig. 6.5 we have plotted the adsorbed amount Γ as a function of chain length. The obscissa gives, in logaritmic scale, both r and M. We split up Γ into contributions from loops, tails and trains.
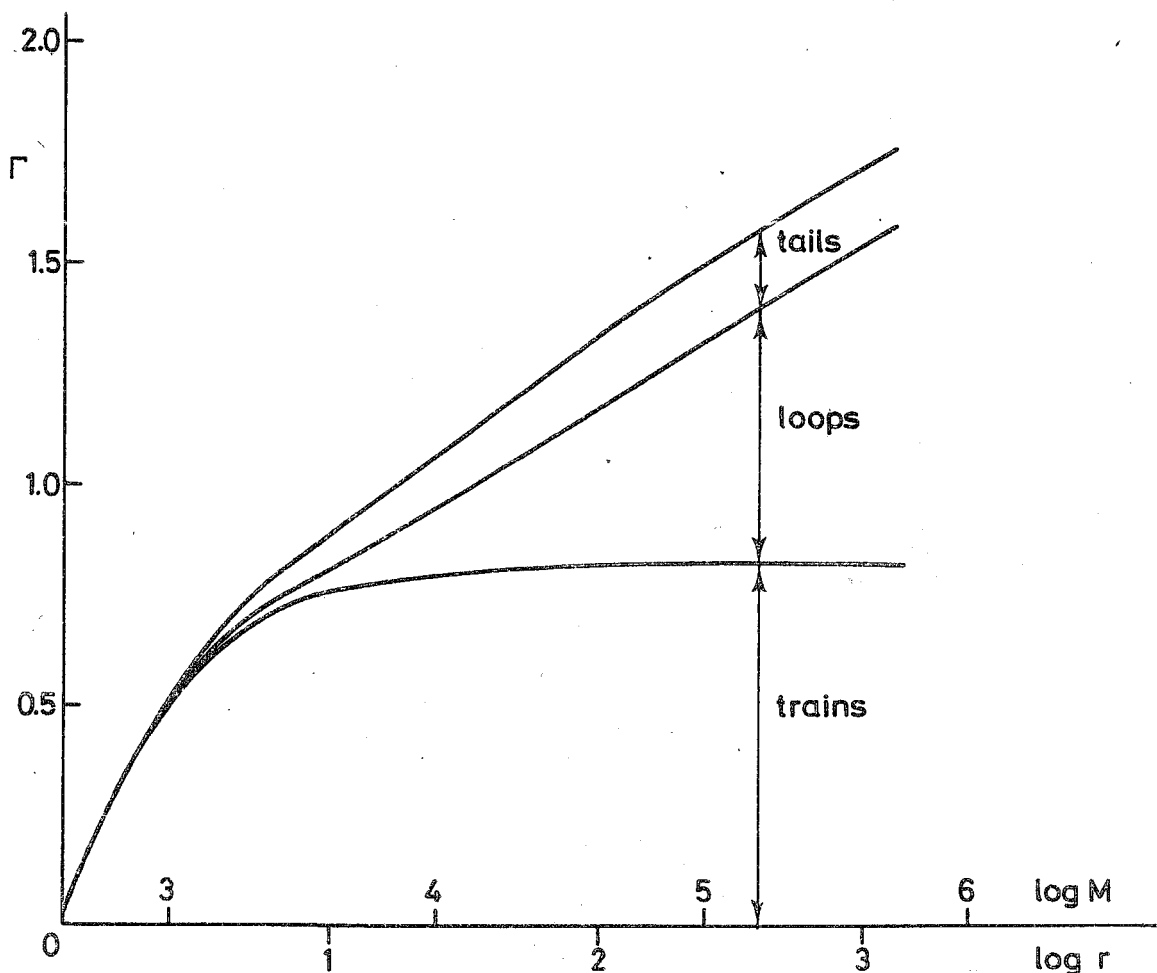
Fig. 6.5. Cumulative representation of the contribution of loops, trains and tails to the adsorbed amount, as a function of chain length. On the obscissa both log r and log M are indicated.

We see that the gradual increase in adsorbed amount is caused by the increase
of the average loop length. Up to chain lengths of about 50 segments (M = 20,000)
the trains give by far the most dominant contribution. For longer chain lengths,
both trains and tails contribute constantly so that the further increase in Γ
is completely due to the increase in the average loop size and the broadening
of the loop size distribution.

Fig. 6.6 gives the fractions of segments in trains, loops and tails,
respectively, in a cumulative representation. The abscissa is the same as in
fig. 6.5. We see that, as the chain length increases, the fraction of loop
segments increases at the expense of the train portion. The tail fraction varies
remarkably little with chain length, having a weak maximum somewhere around a
molecular weight of 30,000.
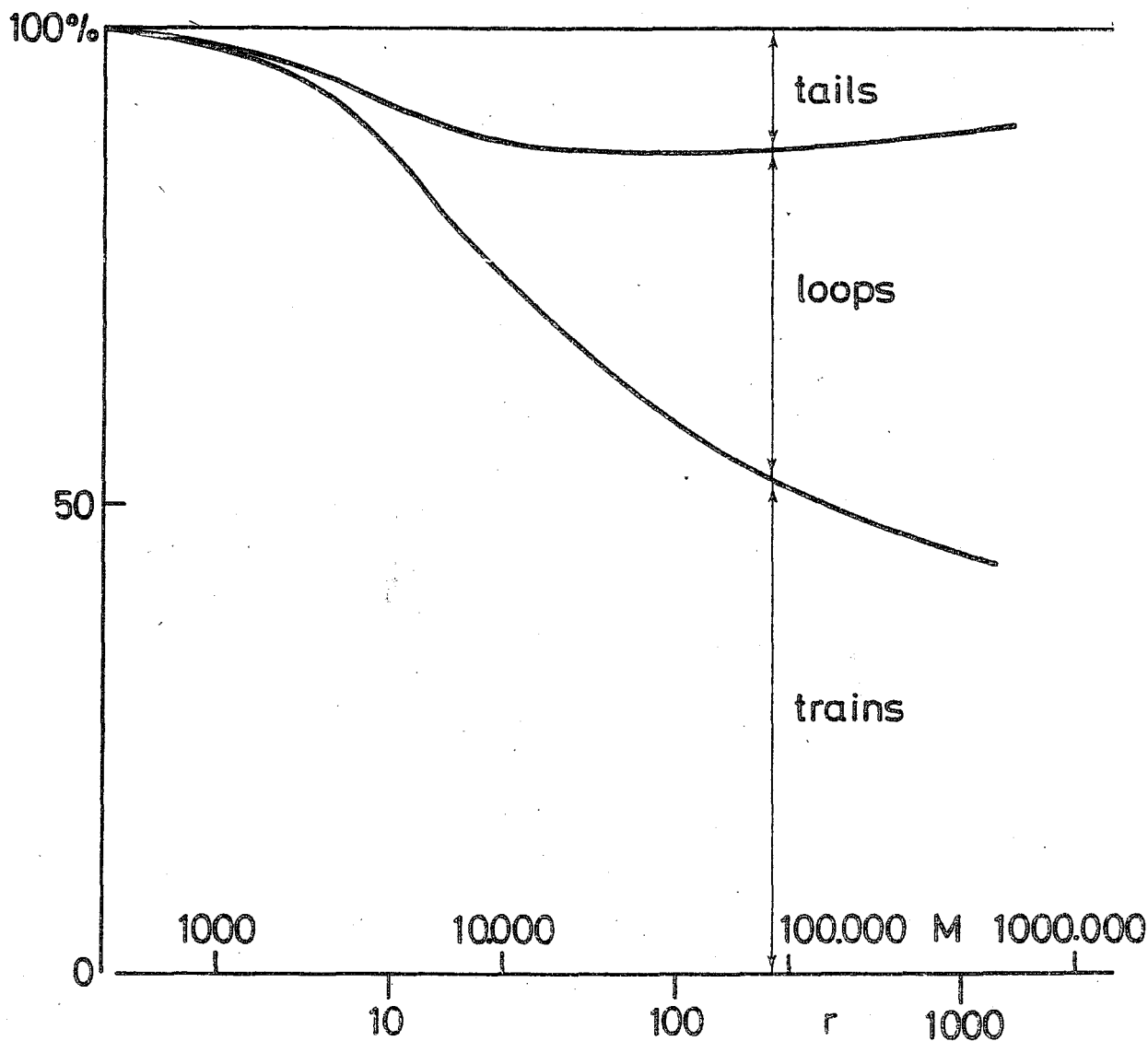
Fig. 6.6. Distribution of segments over tails, loops and trains as a function
of chain length. Both r and M are indicated on logaritmic scales.

A constant tail fraction must imply a drastic increase of tail length with molecular weight, since the number of tails is restricted to two. It turns out that the tail length is approximately proportional to M. This is illustrated in fig. 6.7. Both train and loop length increase only weakly with chain length, in contradistinction with the average tail length. It is rather the large number of small loops and trains per adsorbed chain which is responsible for their high segment fractions.
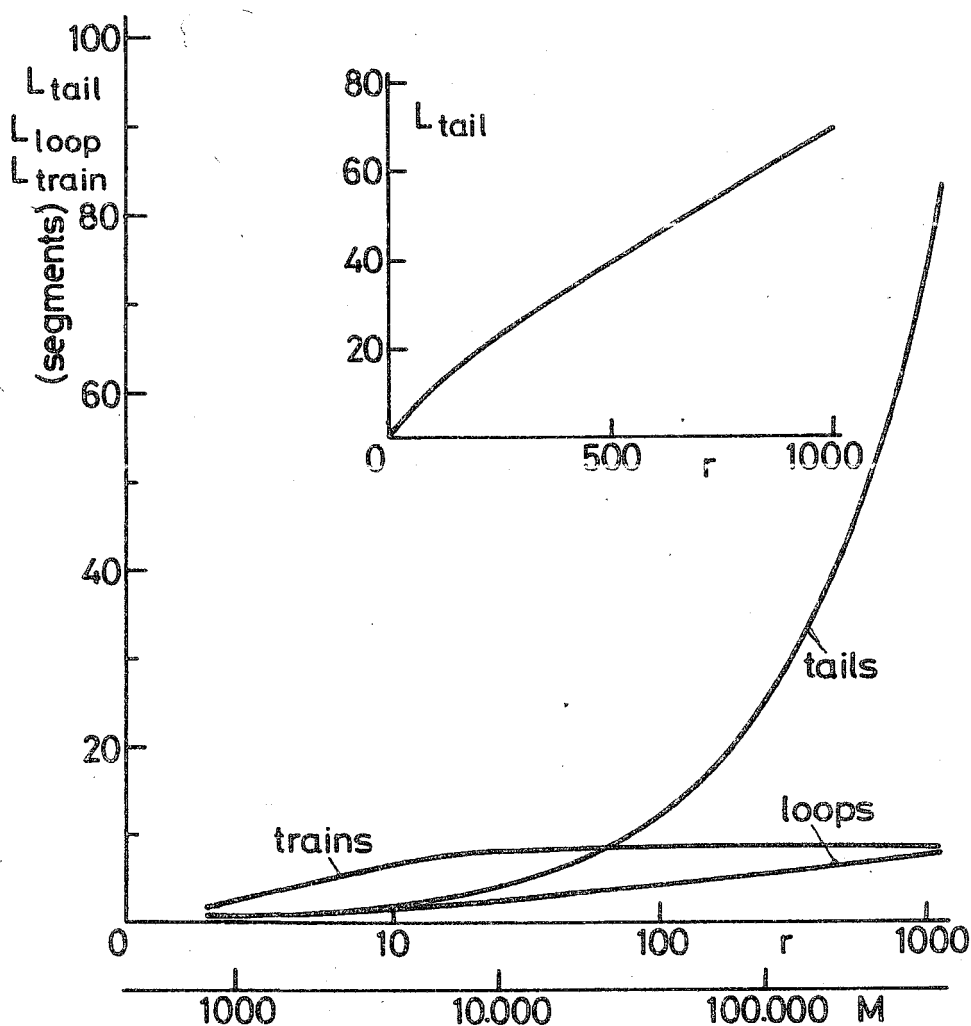
Fig. 6.7. Average length of loops, trains and tails as a function of chain length. Both r and M are indicated on a logaritmic scale.

The typical conformation of a long chain molecule at the solid/liquid interface can thus be pictured as a sequence of many short loops and trains (in alternating order) with a long tail at one or at both ends. As the chain length increases, more and more loops of slightly greater size are formed and the tails become very much longer.

- 136 -

The root mean square layer thickness δ increases also with chain length.
As is seen from fig. 6.8, δ depends linearly on √M. An interesting question
is, how δ is related to an effective hydrodynamic layer thickness. In a recent
paper, *Varoqui* (1977) treats this problem. However, this treatment starts from
the Hoeve theory and, therefore, does not include the effect of long tails.
Probably, the problem needs to be reconsidered on the basis of the results
obtained in this study.
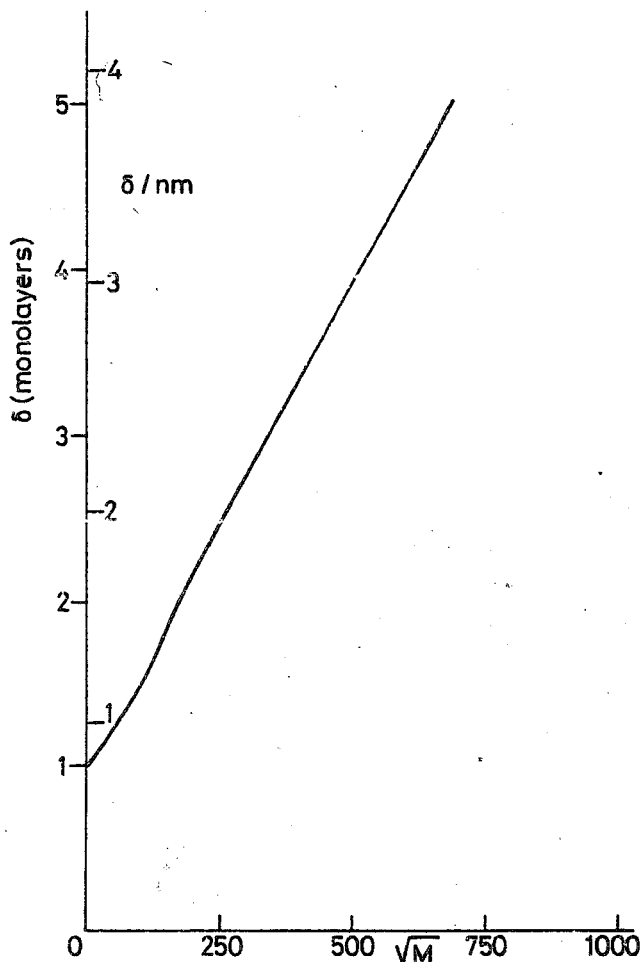
Fig. 6.8. Root mean square layer thickness as a function of √M, δ is given both
in monolayers and in nm.

From the description of the conformations that polymers assume at the solid/
liquid interface we can now sketch what a surface, on which a high polymer is
adsorbed, looks like. From a relatively dense layer of small loops, resembling
a thick carpet, long dangling tails protude here and there into the solution.
Each molecule, when projected on tne surface, occupies on average r/Γ surface
sites, so that the average distance between the centers of gravity of the
molecules is of the order of $\sqrt{r/\Gamma}$ lattice spacings. Since the number of tails
per chain n_{tails} is approximately constant, they must get farther apart with

increasing chain length, the average distance between two tails being $\sqrt{r/\Gamma}\ n_{tails}$. However, the tails also grow in size, and eventually are expected to behave like terminally attached Gaussian coils with a radius of the order of $\sqrt{L_{tail}}$ lattice spacings (L_{tail} is the number of segments per tail).

For a typical molecule of 1000 segments (M = 347,000) we find that L_{tail} = 74, n_{tails} = 1.43 and Γ = 1.7. Thus the tails are, on average, 20 lattice spacings apart and have a radius of about 9 spacings. Although there is a wide distribution of tail sizes, it is not very likely that the tails overlap, since they also tend to repel each other. In other words, they build randomly distributed 'blobs' on the loop-covered surface.

The behaviour of polymers at interfaces is highly relevant to a number of important phenomena, such as, e.g., the stabilization and destabilization of colloidal dispersions. We hope that the above description will be helpful in gaining an understanding of such phenomena. Therefore, we attempted to help imagination, visualizing in fig. 6.9 the layer of polymer molecules at the solid/liquid interface.
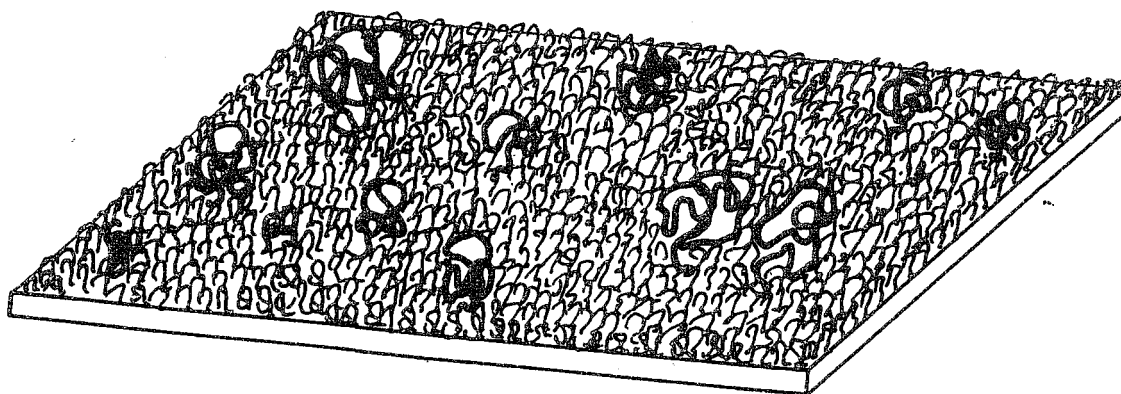

Fig. 6.9. Layer of adsorbed polymer molecules

Summary

We undertook the present study in order to evaluate techniques which are devised to assess the comformations of adsorbed macromolecules. Since recent theories deal with these conformations, we also wanted to investigate to what extent these theories are supported by experimental data.

In chapter 1 we outline the scope of this study and we give reasons for using polyvinyl pyrrolidone / silica as the model system.

Chapter 2 deals with the general aspects of polymer adsorption. Some trends found from experimental work are mentioned, and the four main theories which have treated the problem of interacting chain molecules at a plane interface are briefly discussed. Arguments are presented which lead to the conclusion that, from a theoretical point of view, the best theory available at present is the one recently given by Scheutjens and Fleer (1979). However, it is shown that even this theory fails to take into account both the volume ratio between polymer and solvent and the flexibility of the polymer in a consistent way. We propose a simple way to modify the theory such that these properties are both incorporated; this requires the introduction of a new parameter into the theory: the segment-to-solvent volume ratio or bulkiness parameter b. A few calculations show how the results depend upon b. At the end of chapter 2 we also consider briefly the reversibility of polymer adsorption in connection with polydispersity effects.

Chapter 3 presents a selection of relevant properties of the polymer, the solvents and the adsorbent.

Adsorption experiments are discussed in chapter 4. Adsorbed amounts for two solvents (water and dioxane) are given as a function of chain length, properties of the adsorbent surface and polymer heterodispersity. It is found that PVP adsorbs strongly from both solvents, but in amounts that are substantially higher from dioxane than from water. Chapter 4 also deals with the desorption which occurs if suitable low molecular weight displacers are added to the solution. By means of a simple expression, the amount of displacer needed to just cause complete desorption is related to the strength with which the polymer is bound to the surface. With 5 different displacers an effective adsorption energy is estimated and its meaning is discussed. This type of measurements is entirely new in polymer adsorption studies. Although a detailed interpretation of the results is not straightforward, we obtain reasonable values for the adsorption energy parameter.

Measurements of conformation parameters for adsorbed PVP are described in chapter 5. Bound fractions are determined spectroscopically (infrared, nuclear magnetic resonance) and completed with data from the literature (electron spin resonance). Calorimetry is used as a means to study the surface occupancy. The discrepancies between results from the various methods are considerable, and it is concluded that the techniques do not measure the same property. Nevertheless, the results are useful in gaining a further understanding of the adsorption phenomenon.

In chapter 6 we compare in some detail experimental and theoretical results. The theory used is the aforementioned modification of the Scheutjens-Fleer theory and the experimental data comprise adsorbed amounts, bound fractions and interaction parameters. The adsorbed amounts, which can be fairly accurately measured, agree within 10 tot 20 % with the theoretically calculated values, over the whole molecular weight range. To our knowledge, this is the first time that quantitative agreement is obtained to such an extent. Bound fractions determined with ESR also agree fairly well with the theoretical values, and NMR gives a result in the right range. Infrared data lead to a serious underestimation of the bound fraction, which is easily explained on the basis of the chain structure. To a lesser extent, microcalorimetric results also tend to underestimate the bound fraction, although the results agree surprisingly well with enthalpies of wetting. The dependency on the solvent type is also correctly predicted.

The conclusion is drawn that the introduction of the bulkiness parameter is an essential step towards a complete theory and that the modified Scheutjens-Fleer theory is strongly supported by experiment. Finally, we picture in some detail the conformation of adsorbed PVP, as it emerges from this study.

Samenvatting

Het in dit proefschrift beschreven onderzoek was erop gericht verscheidene technieken waarmee men de conformaties van geadsorbeerde macromoleculen kan bestuderen, aan een evaluatie te onderwerpen. Aangezien deze conformaties door recente theorieën ook berekend kunnen worden, wilden we ook nagaan in hoeverre deze theorieën door de experimenten ondersteund worden.

In hoofdstuk 1 schetsen we de opzet van het onderzoek en we geven aan waarom polyvinyl pyrrolidon / silica als modelsysteem werd gekozen.

Hoofdstuk 2 behandelt algemene aspecten van polymeer-adsorptie. Enkele uit experimenteel werk gevonden trends worden vermeld, en de vier belangrijkste theorieën die het probleem van wisselwerkende ketenmoleculen aan een vlakke fasegrens behandelen worden kort besproken. Op grond van een aantal overwegingen concluderen we dat uit theoretisch oogpunt de recente theorie van Scheutjens en Fleer (1979) op dit moment de best beschikbare is. We tonen echter aan dat het zelfs in deze theorie nog niet mogelijk is zowel de volumeverhouding tussen polymeer en oplosmiddelmolecuul als de flexibiliteit van de polymeerketen op consistente wijze te verdisconteren. We stellen derhalve een eenvoudige wijziging in de theorie voor om dit mogelijk te maken, hetgeen leidt tot de invoering van een nieuwe parameter in de theorie: de volumeverhouding tussen segment en oplosmiddelmolecuul of 'bulkiness parameter' b. Enige berekeningen maken het effect van b op de theoretische resultaten zichtbaar. Aan het eind van hoofdstuk 2 besteden we enige aandacht aan de reversibiliteit van polymeeradsorptie, in samenhang met polydispersiteitseffecten.

In hoofdstuk 3 geven we een aantal relevante eigenschappen van het polymeer, het oplosmiddel en het adsorbens.

Adsorptie-experimenten worden besproken in hoofdstuk 4. Voor twee oplosmiddelen (water en dioxaan) worden de invloeden van ketenlengte, eigenschappen van het adsorbens oppervlak, en de heterodispersiteit van het polymeer bestudeerd. Het blijkt dat PVP sterk adsorbeert vanuit beide oplosmiddelen, maar met dioxaan worden aanzienlijk hogere adsorpties gevonden dan met water. In hoofdstuk 4 komt ook de desorptie aan de orde die optreedt als geschikte laag-moleculaire verdringers toegevoegd worden aan de oplossing. Een eenvoudige uitdrukking geeft het verband tussen de hoeveelheid verdringer waarbij de desorptie juist volledig is en de sterkte van de binding tussen polymeer en oppervlak. Een effectieve adsorptie energie wordt geschat met behulp van 5 verschillende verdringers en de betekenis van het resultaat wordt besproken. In het onderzoek naar de adsorptie van polymeren is dit type metingen volkomen nieuw. Ofschoon een gedetailleerde interpretatie van de resultaten moeilijk is, verkrijgen we redelijke

waarden voor de adsorptie energie-parameter.

Metingen van conformatie parameters voor geadsorbeerd PVP worden beschreven in hoofdstuk 5. Langs spectroscopische weg (infrarood, kernspin resonantie) worden gebonden fracties bepaald; deze worden aangevuld met literatuurgegevens (uit electronspin resonantie). Calorimetrie wordt toegepast om de bedekkingsgraad van het oppervlak te bestuderen. Vergelijking van de resultaten van elk van deze methoden brengt aanzienlijke discrepanties aan het licht; we concluderen dan ook dat we met deze verschillende technieken niet steeds dezelfde eigenschap meten. Niettemin zijn de resultaten van waarde voor het verkrijgen van meer inzicht in het adsorptie verschijnsel.

In hoofdstuk 6 onderwerpen we de experimentele en theoretische resultaten aan een vrij gedetailleerde vergelijking. De gebruikte theorie is de bovengenoemde modificatie van de Scheutjens-Fleer theorie en de experimentele gegevens omvatten geadsorbeerde hoeveelheden, gebonden fracties en wisselwerkingsparameters. De geadsorbeerde hoeveelheden kunnen vrij nauwkeurig gemeten worden en stemmen over het gehele molecuulgewichtsbereik binnen 10 tot 20 % overeen met de theoretisch berekende waarden. Voor zover ons bekend is dit de eerste maal dat kwantitatief zo goede overeenstemming werd verkregen.

Gebonden fracties bepaald met ESR kloppen ook vrij goed met de theoretische resultaten en NMR geeft een resultaat dat in het juiste gebied ligt. De uit infrarood spectroscopie verkregen gebonden fracties liggen beduidend lager dan de theoretische waarden. Dit kan gemakkelijk verklaard worden uit de structuur van de polymeerketen; we concluderen dat infrarood spectroscopie leidt tot een ernstige onderschatting van de gebonden fractie. Dit is, in mindere mate, ook het geval met microcalorimetrie, maar bij lage bedekking stemmen de resultaten hiervan verrassend goed overeen met bevochtigingsenthalpieën, en de invloed van het oplosmiddel wordt eveneens correct voorspeld.

We concluderen tenslotte dat de invoering van de bulkiness parameter een essentiële stap is in de richting van een volledige theorie en dat de aldus gemodificeerde Scheutjens-Fleer theorie door de experimenten goed gesteund wordt. We besluiten met een schets van de conformatie van geadsorbeerd PVP, zoals die uit deze studie naar voren komt.

References

Abe, A., Jernigan, R.L., Flory, P.J. (1966), J. Am. Chem. Soc. 88, 631.
Abendroth, R.P. (1972), J. Phys. Chem. 76, 2547.
Abragam, A. (1961), 'The principles of nuclear magnetism'; Oxford University
    Press, London.
Adamson, A.W. (1967), 'Physical Chemistry of Surfaces', 2nd Ed., Interscience
    Publ., New York.
Armistead, C.G., Tyler, A.J., Hambleton, F.H., Mitchell, S.A., Hockey, J.A.
    (1969), J. Phys. Chem. 73, 3947.
Ash, S.G., Everett, D.H., Findenegg, G.H. (1968), Trans. Faraday Soc. 64, 2645.
Ash, S.G., Everett, D.H., Findenegg, G.H. (1970), Trans. Faraday Soc. 66, 708.
Bartels, T., Tan, Y.Y., Challa, G. (1977), J. Polym. Sci., Polym. Chem. Ed.
    15, 341.
Bianchi, U., Peterlin, A. (1968), J. Polym. Sci. A-2, 60, 1759.
Bode, R., Ferch, H., Fratzscher, H. (1967), Kautschuk u. Gummikunststoffe 20, 578.
Botham, R., Thies, C. (1969), J. Colloid Interface Sci. 31, 1.
Boyer, R.F., Miller, R.L. (1977), Macromolecules 10, 1167.
Brandrup, J., Immergut, E.H. (1975), 'Polymer Handbook', Wiley and Sons, London.
Breitenbach, J.W., Schmidt, A. (1954), Monatshefte Chem. 85, 52.
O'Brien, J., Cashall, E., Wardell, G.H., Mc Brierty, V.J. (1976), Macromolecules 9,
    653.
Burchard, W. (1961), Makromol. Chem. 50, 20.
Burchard, W. (1967), Habilitationsschrift, Freiburg.
Bijsterbosch, B.H. (1974), J. Colloid Interface Sci. 47, 186.
Carrington, A., Mc Lachlan, A.D. (1967), 'Introduction to Magnetic Resonance',
    Harper and Row, New York, and J. Weatherhill, Tokyo.
Cerny, L.C., Helminiak, T.E., Meier, J.F. (1960), J. Polym. Sci. 44, 539.
Chaufer, B., Sebille, B., Quivoron, C. (1975), Eur. Polym. J. 11, 683.
Clark, A.T., Robb, I.D., Smith, R. (1976), J. Chem. Soc., Faraday I 72, 1489.
Cohen Stuart, M.A., Scheutjens, J.M.H.M., Fleer, G.J. (1980), J. Polym. Sci.,
    Polym. Phys. Ed. (in press).
Coll, H., Gilding, D.K. (1970), J. Polym. Sci. A-2, 18, 89.
Curthoys, G., Davidov, V.Y., Kiselev, A.V., Kiselev, S.A., Kuznetsov, B. (1974),
    J. Colloid Interface Sci. 48, 59.
Daoud, M., Cotton, J.P., Farnoux, B., Jannink, G., Sarma, G., Benoit, H.,
    Duplessix, R., Picot, C., de Gennes, P.G. (1975), Macromolecules, 8, 804.
Dawkins, J.V. (1972), Brit. Polym. J. 4, 87.
Dhar, H.B., Conway, B.E., Joshi, K.M. (1973), Electrochim. Acta 18, 789.
Dietz, E. (1976), Makromol. Chem. 177, 2113.
Di Marzio, E.A., Rubin, R.J. (1970), Am. Chem. Soc., Polymer Reprints 11, 1239.
Di Marzio, E.A., Rubin, R.J. (1971), J. Chem. Phys. 55, 4318.
Doi, M. (1975), J. Chem. Soc., Faraday II 71, 1721.
Dole, M., Faller, I.L. (1950), J. Am. Chem. Soc. 72, 414.
Elias, H.G. (1961), Makromol. Chem. 50, 1.
Ellett, J.D. (Jr.), Gibby, M.G., Haeberlen, U., Huber, L.M., Mehning, M.,
    Pines, A., Waugh, J.S. (1971), Advances in Magnetic Resonance 5, 1.
Felter, R.E., Moyer, E.S., Ray, L.M. (1969), J. Polym. Sci. B, 7, 533.
Flory, P.J. (1941), J. Chem. Phys. 9, 660.
Flory, P.J. (1942), J. Chem. Phys. 10, 51.
Flory, P.J., Fox, F.G. (1951), J. Am. Chem. Soc. 73, 1904.
Flory, P.J. (1953), 'Principles of Polymer Chemistry', Cornell Univ. Press,
    Ithaca, New York.
Flory, P.J., Orwoll, R.A., Vrij, A. (1964), J. Am. Chem. Soc. 86, 3057, 3515.
Flory, P.J. (1965), J. Am. Soc. 87, 1833.
Flory, P.J. (1969), 'Statistical Mechanics of Chain Molecules', Wiley and Sons,
    New York, London.

Flory, P.J. (1970), Disc. Faraday Soc. 49, 7.

Frank, H.P., Levy, G.B. (1955), J. Polym. Sci. 17, 247.

Fontana, B., Thomas, J. (1961), J. Phys. Chem. 65, 480.

Fox, K.K., Robb, I.D., Smith, R. (1974), Trans Faraday Soc. 70, 1186.

Gallaugher, A.F., Hibbert, H. (1937), J. Am. Chem. Soc. 59, 2521.

Gargallo, L., Cid, E. (1977), Colloid Polym. Sci. 255, 556.

Glass, J.E. (1968), J. Phys. Chem. 72, 4450.

Goedhart, D.J. (1978), personal communication.

Grant, W.H., Smith, L.E., Stromberg, R.R. (1975), Faraday Disc. Chem. Soc.
    59, 209.

Griot, O., Kitchener, J.A. (1965a), Trans. Faraday Soc. 61, 1026.

Griot, O., Kitchener, J.A. (1965b), Trans. Faraday Soc. 61, 1032.

Hair, M.L. (1977), J. Colloid Interface Sci. 59, 532.

Hansen, R.S. (1951), J. Phys. Chem. 55, 1182.

Helfand, E. (1975), J. Chem. Phys. 63, 2192.

Helfand, E. (1976), Macromolecules 9, 307.

Hertl, W., Hair, M.L. (1968), J. Phys. Chem. 72, 4676.

Herd, J.M., Hopkins, A.J., Howard, G.J. (1971), J. Polym. Sci. C. 34, 211.

Herrle, K. (1965), 'Kunststoffhandbuch', Band 11, ch. 10; Carl Hanser Verlag,
    München.

Hoeve, C.A.J. (1965a), J. Chem. Phys. 42, 2558.

Hoeve, C.A.J. (1965b), J. Chem. Phys. 43, 3007.

Hoeve, C.A.J. (1966), J. Chem. Phys. 44, 1505.

Hoeve, C.A.J. (1970), J. Polym. Sci. C, 30, 361.

Hoeve, C.A.J. (1971), J. Polym. Sci. C, 34, 1.

House, W.A. (1978), J. Colloid Interface Sci. 67, 166.

Huggins, M.L. (1941), J. Chem. Phys. 9, 440.

Huggins, M.L. (1942), J. Phys. Chem. 46, 151.

Huggins, M.L. (1971), J. Phys. Chem. 75, 9.

IUPAC (1972), 'Definitions, Terminology and Symbols in Colloid and Surface
    Chemistry', prepared for publication by D.H. Everett, Pure Appl. Chem.
    31, 579.

Jenkel, E., Rumbach, B. (1951), Z. Elektrochem. 55, 612.

Joppien, G.R. (1975), Makromol. Chem. 176, 1129.

Killmann, E., Strasser, H.J., Winter, K. (1972), VI Intern. Kongress Grenz-
    flächenaktive Stoffe, Zürich; Berichte, Band III, 221.

Killmann, E., Winter, K., (1975), Angew. Makromol. Chem. 43, 53.

Kirkwood, J.G., Riseman, J. (1948), J. Chem. Phys. 16, 565.

Kiselev, A.V., Lygin, V.I. (1975), 'Infrared Spectra of Surface Compounds',
    Halsted Press, Wiley and Sons, New York, Toronto.

Koberstein, E., Voll, M. (1970), Z. Physik. Chemie, Neue Folge, 71, 275.

Koopal, L.K., Lyklema, J. (1975), Faraday Disc. Chem. Soc. 59, 230.

Koopal, L.K. (1978), Thesis, Agricultural University, Wageningen, The Netherlands;
    Meded. Landbouwhogeschool Wageningen 78-12, (1978).

Korn, M. (1978), dissertation, Technische Universität, München.

Kuhn, W. (1934), Kolloid-Z. 68, 2.

Kul'man, R.A. (1970), Colloid J. USSR 32, 465.

Kurata, M., Yamakawa, H. (1958a), J. Chem. Phys. 29, 311.

Kurata, M., Yamakawa, H., Teramoto, E. (1958b), J. Chem. Phys. 28, 785.

Lankveld, J.M.G., Lyklema, J. (1968), Vth Intern. Congr. Surface Activity,
    Barcelona; Proceedings Vol. 2, 633.

Lety-Sistel, C., Chaufer, B., Sebille, B., Quivoron, C. (1975), Eur. Polym. J.
    11, 683.

Lipatov, Yu.S., Sergeeva, L.M. (1974), 'Adsorption of Polymers', J. Wiley and
    Sons, New York, Toronto.

Mc Kenzie, A.P., Rasmussen, D.H. (1971), 161 st Nat. Meeting Am. Chem. Soc.,
    Symp. 'Water Structure at the Water-Polymer Interface', ed. Jellinek,
    1971, 146.

Maron, S.H. (1959), J. Polym. Sci. 38, 329.

Maron, S.H., Nakajima, N. (1959), J. Polym. Sci. 40, 59.

Mills, A.K., Hockey, J.A. (1975), J. Chem. Soc. Faraday I, 71, 2384, 2392, 2398.

Molyneux, P. (1975), 'Water: A Comprehensive Treatise', Ed. F. Franks, Vol. 4, ch. 7, Plenum Press, New York.

Morawetz, H. (1965), 'Macromolecules in Solution', Interscience Publ., New York.

Morrissey, B.W., Stromberg, R.R. (1974), J. Colloid Interface Sci. 46, 152.

Murakami, S., Kimura, F., Fujishiro, R. (1975), Makromol. Chem. 176, 3425.

Myamoto, T., Cantow, H.J. (1972), Makromol. Chem. 162, 43.

Ohno, H., Abe, K., Tsuchida, E. (1978), Makromol. Chem. 179, 755.

Oster, G. (1952), J. Polym. Sci. 9, 553.

Orwoll, R.A. (1977), Rubber Chem. Technol. 50, 451.

Peri, J.B., Hensley, A.L. (jr), (1968), J. Phys. Chem. 72, 2926.

Robb, I.D., Smith, R. (1974), Eur. Pol. J. 10, 1005.

Robb, I.D., (1977a), Personal communication.

Robb, I.D., Smith, R. (1977b), Polymer 18, 500.

Roe, R.J. (1974), J. Chem. Phys. 60, 4192.

Rubio, J., Kitchener, J.A. (1976), J. Colloid Interface Sci. 57, 132.

Sacher, R.S., Harrison, I.D. (1979), J. Colloid Interface Sci. 70, 153.

Saidel, L.J. (1955), J. Phys. Chem. 77, 3892.

Scheutjens, J.M.H.M., Fleer, G.J. (1979), J. Phys. Chem. 83, 1619.

Scheutjens, J.M.H.M., Fleer, G.J. (1980), J. Phys. Chem., in press.

Scholtan, W. (1957), Makromol. Chem. 24, 83.

Schurz, J. (1974), 'Physikalische Chemie der Hochpolymeren', Springer Verlag, Berlin.

Schwartz, A.M., Perry, J.W., Birch, J. (1960), 'Surface Active Substances and Detergents, Interscience Publ., New York.

Shukov, A.I., Kyrysova, I.A., Sidorova, M.P., Fridrichsberg, D.A. (1970), Doklad. Acad. Nauk. VSSR 194, 130.

Silberberg, A. (1962), J. Phys. Chem. 66, 1884.

Silberberg, A. (1967), J. Chem. Phys. 46, 1105.

Silberberg, A. (1968), J. Chem. Phys. 48, 2835.

Silberberg, A. (1970), Am. Chem. Soc. Polymer Reprints 11, 1256.

Silberberg, A. (1971), Pure Appl. Chem. 26, 583.

Stockmayer, W.H., Fixman, M. (1963), J. Polym. Sci. C, 1, 137.

Stillman, J.M. (1924), 'The Story of Early Chemistry', Appleton, New York.

Stromberg, R.R. (1967), 'Treatise on Adhesion and Adhesives', R.S. Patrick Ed., Vol. 1, 69; Marcel Dekker, New York.

Sullivan, R.A., Palermiti, F.M., Annino, R. (1952), Meeting-in-Miniature, New York Section of Am. Chem. Soc., 8th Febr. 1952, New York.

Swinbourne, E.S. (1960), J. Chem. Soc. 2, 2371.

Tadros, Th.F. (1978), J. Colloid Interface Sci. 64, 36.

Tadokoro, Y., Okazaki, S., Yamamura, H. (1965), J. Sci. Hiroshima Univ., Ser. A-II, 29, 89.

Takagishi, T., Naoi, Y., Kuroki, N. (1977), J. Polym. Sci., Polym. Chem. Ed. 15, 2789.

Thies, C., Peyser, P., Ullman, R. (1967), IVth Congr. Surface Active Compounds, Brussel; Proceedings, 1041.

Trienekens, C.G. (1976), Doctoraalscriptie Landbouwhogeschool, Wageningen.

Vander Linden, C. (1976), Thesis, Université Libre de Bruxelles, Brussel,

Vander Linden, C., Van Leemput, R. (1978a), J. Colloid Interface Sci. 67, 48.

Vander Linden, C., Van Leemput, R. (1978b), J. Colloid Interface Sic. 67, 63.

Varoqui, R., Dejardin, P. (1977), J. Chem. Phys. 66, 4395.

Vink, H. (1971), Eur. Pol. J. 7, 1411.

Wadsö, I. (1968), Acta Chem. Scand. 22, 927.

Wartmann, H.J. (1958), Dissertation, ETH Zürich.

Weldring, J.A.G., Wolters, J., Van den Berg, C. (1975), Meded. Landbouwhoge-
      school Wageningen 75 - 18, 1.
Wilson, C.W., Pake, G.F. (1957), J. Chem. Phys. 27, 115.
Winter, K. (1973), dissertation Technische Universität, München.
Yamakawa, H., Kurata, M. (1958), J. Phys. Soc. Japan 13, 94.
Yamakawa, H. (1971), 'Modern theory of Polymer Solutions', Harper and Row,
      New York.
Young, G.J. (1958), J. Colloid Interface Sci. 13, 67.
Zimm, B.H., Stockmayer, W.H., Fixman, M. (1953), J. Chem. Phys. 21, 1716.

Glossary of symbols

DMSO dimethylsulfoxide

NEM N-ethylmorpholine

NEP N-ethylpyrrolidone

NMP N-methylpyrrolidine

PVP polyvinyl pyrrolidone

PYR pyridine

A (A_{tr}, A_l, A_t)	Adsorbed amount (in trains, in loops, in tails)
A_{ex}	Excess adsorbed amount
A^{mon}	Monolayer capacity
A_{*}	Amount (of polymer) excluded from the surface
A^{tot}	The sum of A and A_{*}
a	Mark Houwink exponent
a_H	Distance between protons in the water molecule
B_2	Second virial coefficient
b	Bulkiness parameter
C	Characteristic ratio for the mean square end-to-end distance
C_M	Viscosity constant
c	Concentration of polymer in solution
c_A	Concentration of adsorbed polymer (in a dispersion)
c_H	Flexibility parameter in Hoeve's theory
d	Thickness of polymer chain (thickness of monolayer)
d_g	Distance from center of gravity in polymer coil
E (E_o, E_A)	Infrared absorbance (of reference, of bound carbonyls)
E_j	Energy of state j
F	(Helmholtz) free energy
ΔF^{ca}, ΔF^m	Free energy for conformation and adsorption, for mixing
f	Conversion factor for adsorption energy parameter
ΔG_m (ΔG_m^R)	Gibbs free enthalpy (residual free enthalpy)
g_N	Nuclear g-factor
H_o (H_1)	Magnetic field strength of static field (of rotating field)
ΔH_{ads} (ΔH_{tr}, ΔH_{mix})	Enthalpy of adsorption (due to trains, due to concentration effects)
Δh_{tr}	enthalpy of adsorption of one train segment

$\langle h^2 \rangle$ $(\langle h_o^2 \rangle)$	Mean square end-to-end distance (unperturbed)
h	Planck's constant
i	Layer number in lattice model (also index)
K (K_o)	Mark-Houwink constant (under theta conditions)
K_H, K_{cal}, K_x	Hydrodynamic constants
k	Boltzmann's constant
k_H	Huggins' constant
L	Contour length of a polymer chain
L_{tail}, L_{loop}, L_{train}	Average number of segments in a tail, a loop, a train
L_w	Number of sites in a lattice layer
l	Bond length between atoms in a polymer chain backbone
l_s	Length of a statistical (Kuhn) segment
l_l	Length of a step in a lattice
M (M_{cal}, M_x)	Molecular weight (specified molecular weight)
M_n, M_w, M_v)	Number-, weight-, viscosity averaged molecular weight
M_o, M_D	Molecular weight of the monomer unit, of a displacer
m	Number of carbon atoms in polymer backbone
m_τ	Number of trains of length τ (Hoeve's theory)
N_{AV}	Avogadro's number
n (n_c)	Number of polymer molecules (in conformation c)
n^o	Number of solvent molecules
n_i	Number of polymer segments in layer i
n_i^o	Number of solvent molecules in layer i
$\{n_c\}$	Specified conformation set
n_{tr}	Number of segment-surface contacts
n_λ	Number of loops of length λ (Hoeve's theory)
n_{tail}	Number of tails per polymer molecule
n_+^o	Number of moles of solvent added in a dilution experiment
n_m	Number of maxima in an infrared interference pattern
P	Degree of polymerization
P_s (P_o)	Vapour pressure over a solution (pure solvent)
p	Bound fraction
$p_1, \ldots, p_i$	Weighting factor for layer 1, ..., i
$p_{1,cr}$	Critical value for p_1
Q (Q^{ca})	Canonical partition function (for conformation and adsorption in Hoeve's theory)
R	Gas constant
r	Number of statistical segments per chain

S	Available surface area
S_{sp}	Specific surface area
ΔS_m	(Ideal) entropy of mixing
$\langle s^2 \rangle$ $(\langle s_o^2 \rangle)$	Radius of gyration (unperturbed)
T (T_o, T_1, T_2)	Absolute temperature (specified temperatures)
T_I, T_{II}	Longitudinal, transverse relaxation time
Tr (Tr_o, Tr_A)	Infrared transmission (of reference, of bound carbonyls)
t_p	Duration of radiofrequency pulse
t_i	Time interval between pulses
V	Volume
V_H	Hydrodynamic volume of a polymer coil
V_2	(Partial) specific volume of polymer
v_2	Volume of a solute molecule
v_1	Volume of a solvent molecule
v_{mon}	Volume of a monomer unit
v_{seg}	Volume of a statistical segment
$\underline{v}^o$	Molar volume of solvent
$\bar{v}$	Molar volume of polymer
W	Number of lattice layers in the adsorption models of Roe and Scheutjens/Fleer
X_{in}	Mole fraction of adsorbate at the initial part of a low molecular weight adsorption isotherm
Z (Z^*, Z_{tr})	Coordination number (in bulk, at the surface)
Z_p	Effective coordination number for a given polymer chain
z (chapter 2)	Distance along a direction perpendicular to the adsorbing wall
z (z_o) (chapter 3)	Excluded volume parameter (limiting value at infinite temperature)
α $(\alpha_h, \alpha_s, \alpha_\eta)$	Linear expansion factor (for the end-to-end distance, the radius of gyration, the hydrodynamic radius)
β_N	Nuclear magneton
Γ, Γ_{ex}	Adsorbance, excess adsorbance
Γ_{in}	Adsorbance in the initial part of a (low molecular weight) isotherm
γ	Magnetogyric ratio
γ_1, γ_{tr}	End effect parameters (Silberberg's theory)
Δ	Optical path length
δ	Root-mean square adsorbed layer thickness
$\delta_{i,1}$	Kronecker delta function

ε_o (ε_A)	Infrared absorption coefficient for free (bound) carbonyls
η	Viscosity
η_{sp}	Specific viscosity
$[\eta]$	Intrinsic viscosity
Θ	Theta temperature
θ	Surface occupancy
κ_1, κ_2	Heat of dilution constants
λ	Loop length
ν_o, ν_1, ν_2	Infrared wavenumbers
ν_τ	Partition function for trains
$\mu_1 - \mu_o$	Excess chemical potential of solvent in a (polymer) solution
σ_H	Partition function for train segments (Hoeve's theory)
τ	Train length
τ_c	Correlation time for molecular motion
Φ_o	Viscosity constant
ϕ	Volume fraction of polymer
ϕ	Volume fraction of polymer after dilution
ϕ_l, ϕ_{tr}, ϕ_t	Volume fraction of polymer in loops, trains, tails
ϕ_1, ..., ϕ_i, ...	Volume fraction of polymer in layer 1, ..., i, ...
$<\phi_i>$	Weighted average of ϕ_i over layers i-1, i and i+1
ϕ^o	Volume fraction of solvent
ϕ_1^o, ..., ϕ_i^o, ...	Volume fraction of solvent in layer 1, ..., i, ...
ϕ_*	Volume fraction of polymer in bulk solution
ϕ_*^o	Volume fraction of solvent in bulk solution
ϕ_1^D, ϕ_*^D	Volume fraction of displacer in layer 1, in the bulk solution
$\phi_{*,cr}^D$	Critical displacer volume fraction
χ	Polymer-solvent interaction parameter
χ_s $(\chi_{s,cr})$	Polymer adsorption energy parameter (critical value of χ_s)
$\Delta\chi_s$	Residual adsorption energy parameter $(\chi_s - \chi_{s,cr})$
χ_s^D	Displacer adsorption energy parameter
χ_S	Entropic part of χ
χ_H	Enthalpic part of χ
Ω_j	Multiplicity of state j
Ω^c	Conformational partition function of a polymer chain

- 150 -

Ω_n^c Scheutjens/Fleer partition function (configurational part)

ω_λ partition function of a loop (Hoeve's theory)

ω_c Conformation factor (Scheutjens-Fleer theory)

ω_o NMR Larmor frequency

Curriculum vitae

Ik werd op 25 april 1948 geboren te Haarlem en groeide op in 's Gravenhage, waar ik in 1966 het einddiploma gymnasium B behaalde. Daarna volgde de schei-kunde studie aan de Rijksuniversiteit te Groningen, met als hoofdvak polymeer-chemie (prof. G. Challa) en als bijvak fysische chemie (prof. J. Kommandeur). In mei 1973 sloot ik de studie af met het doctoraalexamen. In de erop volgende twee jaren vervulde ik de vervangende dienstplicht in het Klinisch Chemisch Laboratorium te Leeuwarden. Sinds 1 oktober 1975 ben ik als medewerker van de vakgroep fysische en kolloidchemie in dienst van de Landbouwhogeschool. Het in dit proefschrift beschreven onderzoek werd hier onder leiding van dr. G.J. Fleer uitgevoerd; mevr. P. Bosman-van Dulm en J. Nuysink waren er nauw bij betrokken.